# Calibration Report of the EFW Measurements in the Cluster Active Archive (CAA)

prepared by

Yuri Khotyaintsev

# 1 Introduction

This document describes calibration results and procedures of the CSA products from the EFW instrument.

# 2 Instrument Description

A detailed description of the EFW instrument is provided in *Gustafsson et al*. (1997). We first briefly describe the raw quantities measured by the instrument, which correspond to Level 1 products in the CSA. The detector of the instrument consists of four spherical sensors numbered 1 to 4 deployed orthogonally on 44-meter-long wire booms in the spin plane of the spacecraft, as illustrated in Figure 1. The potential drop between two sensors, separated by

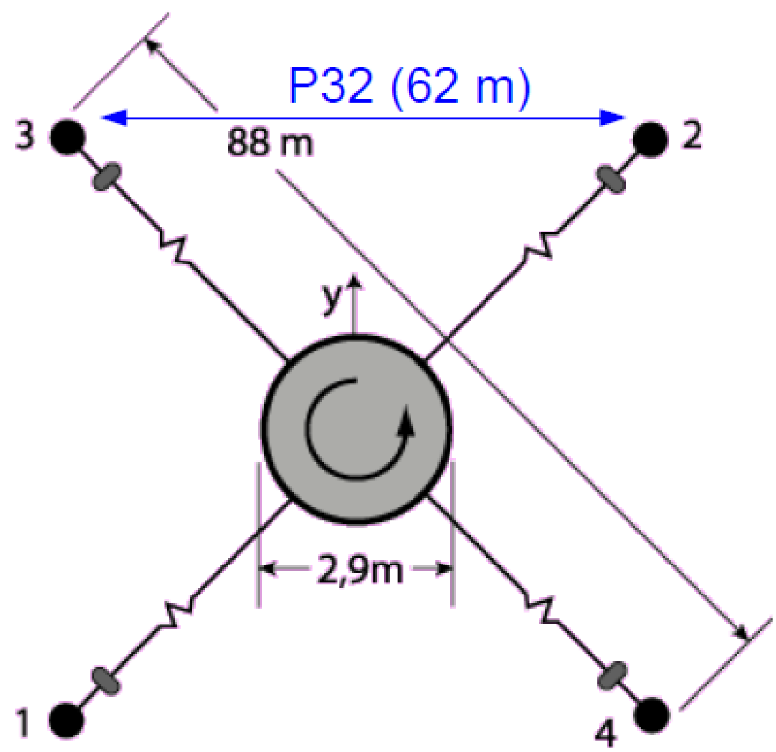


*Figure 1: The EFW experiment*

88 m tip-to-tip (62 m for P32), is measured to provide an electric field measurement (CSA dataset L1_E). The probe difference signals are normally routed through 10 Hz low-pass filters if sampled at 25 $s^{-1}$, and through 180 Hz low-pass filters when sampled at 450 $s^{-1}$ (see "EFW non-standard operations dataset" in Section 4.1 for the exceptions). The potential

difference between each sensor and the spacecraft (CSA dataset L1_P1) is measured separately with a sampling frequency of 5 $s^{-1}$ after routing through low-pass filters with a cut-off frequency of 10 Hz.

The EFW instrument measures the electric field only in the spacecraft spin plane; therefore, a spin-plane-oriented coordinate system is best suited for scientific studies involving the electric field. The **ISR2** (Inverted Spin Reference) system, also known as **DSI** (Despun System Inverted), is such a system. The X and Y axes are in the spin plane, with X pointing as near sunward as possible and Y perpendicular to the sunward direction, positive towards dusk. The Z-axis is along the (negative) spacecraft spin axis, pointing towards the north ecliptic pole. The coordinate system is called "Inverted" because the actual spin axis of Cluster is pointing towards the south ecliptic. The difference between ISR2 (DSI) and the GSE (Geocentric Solar Ecliptic) is a tilt of 2 to 7 degrees of the Z-axis performed in order to avoid shading of the EFW probes by the spacecraft. The exception is the May 2008 "tilt campaign", when the tilt angle on C3 can be up to 45 degrees.

# 3 Measurement Calibration Procedures

Spacecraft potential data (probe-to-spacecraft, not the plasma-to-spacecraft potential; see *Cully et al., 2007*) in the CSA do not require any special calibration. L2_P is usually computed as the average of all four probes; if one or two probes are missing, it is calculated as the average of two opposing probes, or if the probes are non-opposing, it is set to the value of one of the probes. If only one probe is available, L2_P is set to that probe's potential. In case of probe saturation due to high bias current (see "*Detection of saturation due to high bias current in dense plasmas"* in Section 4), we switch from averaging to using the maximum of all available probes, which gives the best estimate of the spacecraft potential.

Here, we describe the processing chain of the electric field data. At the initial stage of production, we remove intervals with bad data caused by electronic issues, probe saturation due to low plasma density, and non-optimal bias current settings. Usually, only a few minutes of data are removed from each orbit for these reasons. However, large data gaps may occasionally occur. If the spacecraft is in the solar wind, we attempt to correct for the wakes usually present in the raw data (see "Cleaning wakes in the solar wind").

## 3.1 Spin fitting

In the presence of a constant ambient electric field, the raw data signal (probe potential difference) is a sine wave, with its amplitude and phase determining the magnitude and direction of the electric field. A *least-squares fit* to the raw data of the form

$$y = \boldsymbol{A} + \boldsymbol{B} \sin(\omega t) + \boldsymbol{C} \cos(\omega t) + \boldsymbol{D} \sin(2\omega t) + \boldsymbol{E} \cos(2\omega t) + \ldots \qquad (1)$$

is done once every 4 seconds ($2\pi/\omega \approx 4$ sec is the spacecraft spin period), and gives the following output:

- The sine and cosine terms, ***B*** and ***C*** (L3_SFIT dataset), are used to compute the 4-sec-resolution electric field in ISR2.
- The *raw data DC offset*, ***A***. Ideally, the raw data DC level should be zero, but small differences between the probe surfaces and the electronics create a DC offset. If not corrected, it shows up as a signal at the spin frequency in the despun electric field. The DER dataset is based on ***A*** (see section 3.2).
- The standard deviation of the raw data from the fitted sine wave (L3_E dataset).
- Higher-order terms, ***D***, ***E***, ..., may be used to diagnose data quality (not delivered to the CSA).

The electric field (computed from ***B*** and ***C*** for one of the probe pairs) and the standard deviation are available in the CSA as Level 3 E.

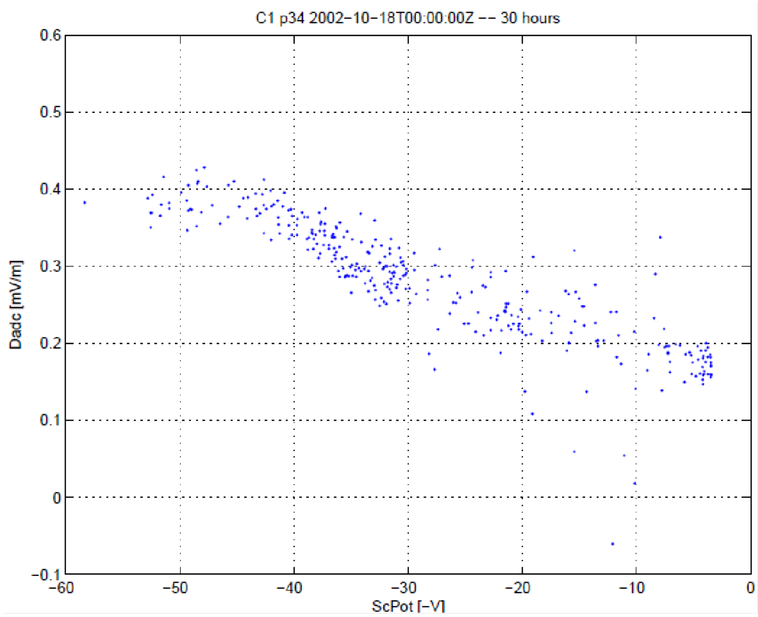


*Figure 2: Raw data DC offset vs spacecraft potential*

## *3.2 Raw data DC offset*

The raw data DC offset (***A***) from both probe pairs is used for processing the full-resolution (L2) data. It is applied to P12/P32 and P34 prior to despinning and is available in the CSA as the L3_DER product. Variations in the electric field cause small changes in the DC offset. DC offset also depends on the surrounding plasma environment, as illustrated in Figure 2. Therefore, we want a smoothed value and, at the same time, to track changes in the plasma environment, which is why the DC offset is smoothed using a weighted average over 7 spins using weights [.07 .15 .18 .2 .18 .15 .07] (see the EFW ICD). The smoothed offset is delivered to the CSA as the DER dataset. Intervals containing WHISPER pulses are blanked prior to despinning.

### 3.3 Delta offset

Another offset applied during despinning is the so-called Delta offset, which is based on the difference between the electric fields in ISR2 obtained from the least-squares fit procedure for the individual probe pairs P12/P32 and P34. This offset arises from differences in probe characteristics that evolve over time. Evolution of delta offsets for Cluster 2 for 2001-2005 is shown in Figure 3. The spikes in the plot are usually due to one of the probe pairs being partially saturated (removed during the offset computation). To remove these spikes and account for the very slow evolution of the offset, we use a median over a 6-day period, corresponding to approximately 3 orbits (shown in green). The blue curve shows the offset values computed over 90-min (NM) or 30-min (BM1) intervals.  On rare occasions when the delta offset changes rapidly, as for example after some of the maneouvres, we use manually

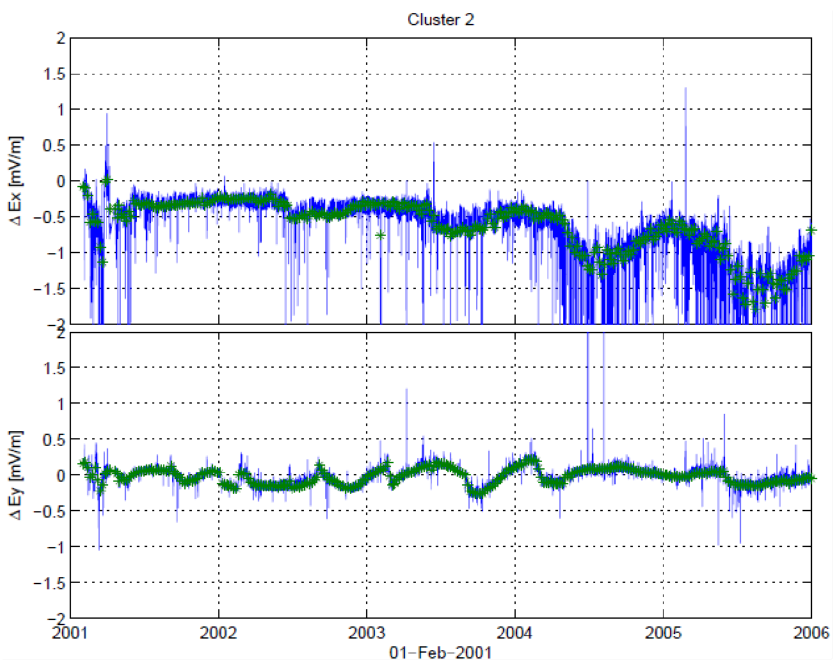


*Figure 3: Delta offsets for Cluster 2*

verified tabulated values. The delta offset is applied during the despin when L2_E is produced. The delta offset is always corrected on P12/32. The value applied is given in FILE_CAVEATS section of the CEF file:

```
ENTRY       =   "2007-12-02T00:00:00.000Z/2007-12-02T01:09:00.000Z
p12 offset (ISR2): dEx=0.21 dEy=-0.05"
```

## 3.4 Amplitude correction

At this stage, both the full-resolution (L2, from despinning) and 4-sec (L3, from least-squares fit) electric fields contain systematic errors, namely an amplitude factor and a DC offset, which need to be corrected for.

The ambient electric field is "short-circuited" by the presence of the spacecraft and wire booms. This is caused by the spacecraft's potential, which is also the potential of the wire booms extending out to a large distance from the spacecraft. On the basis of simulations and comparisons with other Cluster instruments, it has been determined that the measured electric field magnitude needs to be multiplied by a factor of 1.1 (see "ISR2 offsets and Amplitude correction factor" in Section 6.1 for more detail) to get the real electric field (see also *Cully et al., 2007*). However, this factor depends on the plasma environment and, in some cases, may deviate from the value used. In the case of Cluster, it can range from 1.0 to ~1.2, but is usually 1.1.

## 3.5 ISR2 DC offset

The spacecraft, wire booms, and probes emit photoelectrons, which create an excess of negative charge on the sunward side. This will be measured by the EFW instrument as a spurious sunward electric field, generally referred to as the sunward DC offset. Most of the time, the offset varies slowly with time and plasma conditions around the spacecraft and is slightly different for each spacecraft. However, rapid changes can also occur, for example, due to fast crossings of plasma boundaries or rapidly varying solar UV flux, which can both alter the satellite photoelectron cloud.

The magnitude of the offset is determined by comparisons with other measurements from the Electron Drift Instrument (EDI) and the Cluster Ion Spectrometry experiment (CIS). The values of the offsets that have been subtracted from the data in the CSA are given in the FILE_CAVEATS section of the CEF files. The photoelectron asymmetry responsible for the sunward DC offset, by definition, gives an offset in the sunward direction only. However, results of comparisons with other instruments have at times shown an offset of a fraction of mV/m also in the duskward direction, which is not yet well understood. In most cases, the duskward offset is negligible.

Prior to delivery to the CSA, we attempt to identify and mark intervals with suspected spurious fields in various magnetospheric regions (see "Detection of spurious electric fields in the plasmasphere" and "Detection of cold ion flow wakes" in Section 4.6).

# 4 Measurement Processing Procedures

## *4.1 Issues due to electronics & instrument saturations*

In this chapter, we describe the procedure we use to identify bad data caused by electronic issues. These include instrument misconfiguration, malfunction, digital saturation, etc. Data during such intervals cannot be recovered.

First, we remove all data within the 1-minute interval prior to the EFW reset (exact timing unknown) and the 3-minute interval after the EFW reset. Following the reset, EFW boots into default mode, which has non-optimal bias current settings. These settings are usually reprogrammed to nominal 2-3 minutes after a reset.

After that, we check the actual bias current measurements and disregard all data with non-nominal settings. Nominal bias current settings for all years of operation are in the "EFW User Guide", and actual bias current settings are included in the HK dataset.

Then we check for probe saturations. First, we look for probes and probe pairs "getting stuck," which is identified by a non-changing measurement for four consecutive points. Then we check for measurements being saturated due to low density when the probes reach the maximum digital value of 68 V.

Some additional intervals may be manually disregarded based on the "EFW non-standard operations database" (see caveats dataset C[1-4]_CQ_EFW_INST). These usually include maneuvres, bad telemetry packets, unusual sampling modes, and instrument settings. These intervals are marked in the quality information supplied with the electric field data: bits 0-6 set in the E_bitmask (see EFW User Guide). For such intervals, the data will typically contain the fill value or a data gap.

## 4.2 Detection of saturation due to high bias current in dense plasmas

Due to long-term evolution in probe characteristics, the nominal bias current setting of 140 nA began to cause saturation in the dense magnetosheath plasmas in spring 2004. The problem became more prominent in 2005, and the nominal setting was lowered to 100 nA. See the EFW User Guide for more details. The saturated time intervals usually contain very large electric field spikes in every spin, with amplitudes sometimes reaching the digital saturation level. We have developed an algorithm that detects such saturations based on spike amplitude, shape, and other features. The algorithm is, in many ways, similar to the one used for detecting solar wind wakes. Figure 4 illustrates the algorithm in action. The time intervals during which saturation was observed are marked by a red/green envelope. The saturated time intervals are blanked in the CSA because they typically contain useless measurements. These intervals are marked in the quality information supplied with the electric field data: bit 14 set in the E_bitmask (see the EFW User Guide).

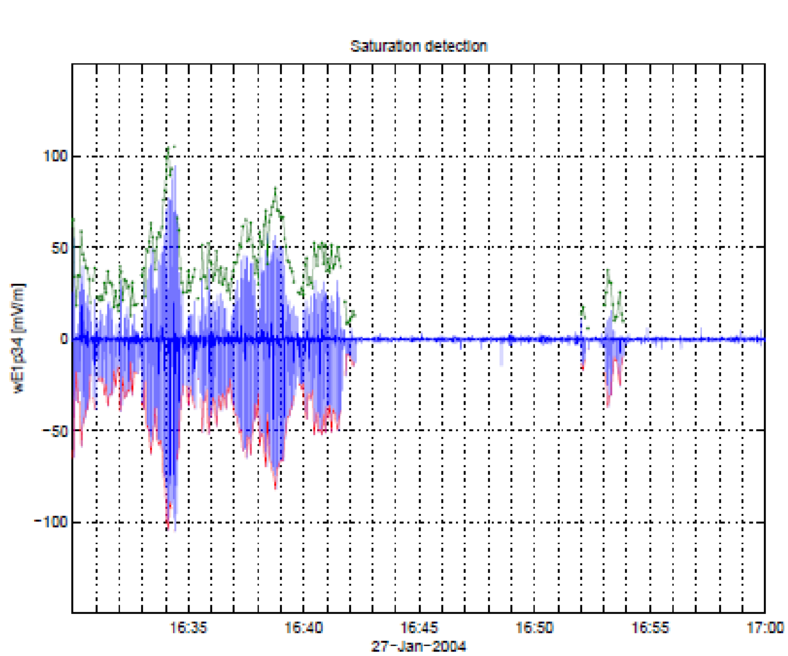


*Figure 4: Detection of saturated intervals due to high bias current.*

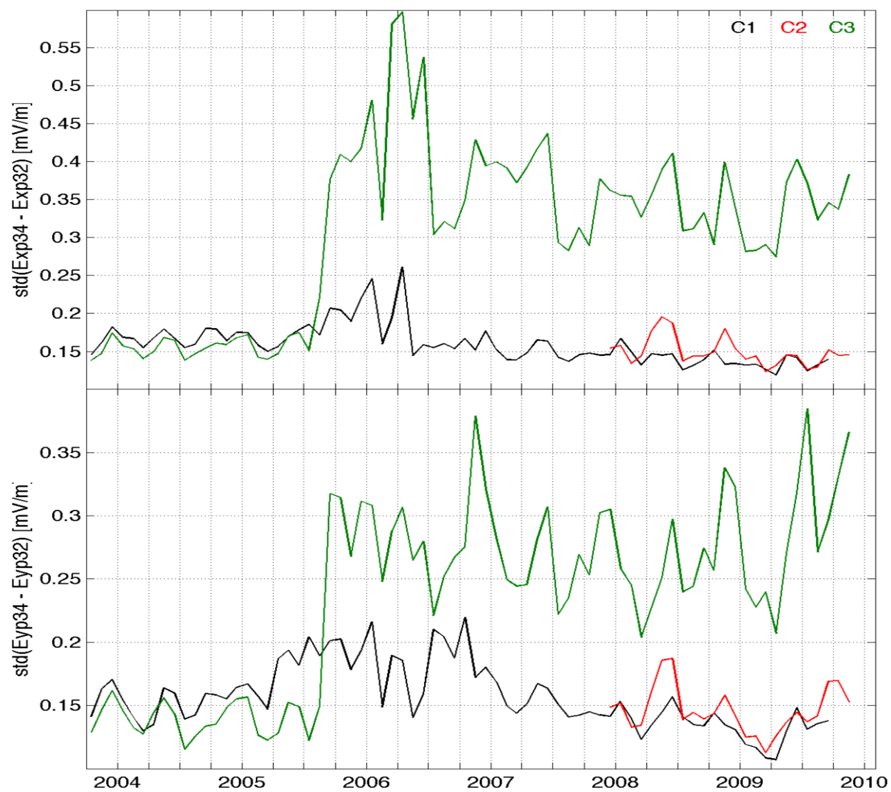


*Figure 5: Difference between the spin fits from the long (p34 – 88m) and short asymmetric (p32 – 62m) probe pairs.*

## 4.3 Measurements with an asymmetric probe configuration

To measure full-resolution electric fields with EFW, two probe pairs are required. The optimal situation is when the probe pairs are equally long, orthogonal, and symmetric with respect to the spacecraft. The spacecraft on which probe 1 failed after some period of operations (for exact times see caveats dataset C[1-4]_CQ_EFW_INST) are normally run in so-called "asymmetric mode", e.g., the difference between probe pairs 2 and 3 is measured in addition to p34. Then p12 can be computed (on ground) from a combination of p32 and p34, and the normal processing procedure can be used.

However, this measurement has lower quality than "normal" p12 because p32 is shorter (62 m instead of 88 m) and is not symmetric with respect to the spacecraft. The spin-fit data is practically unaffected by this problem. Figure 5 shows the standard deviation of the difference between the spin-resolution electric fields obtained from the long p34 and the short p32 probe pairs. Here we have included data only from spacecraft spins with relatively quiet electric activity, i.e., when the standard deviation of the spin fit is below 0.3. One can see that the statistical difference between the spin fits for the long and short probe pairs is small, typically about 0.15 mV/m for C1 and C2 and about 0.3-0.4 mV/m for C3 before September 2005. Since September 2005, something has happened to C3, resulting in reduced data quality.

For the full-resolution electric field, using the short probe pair results in modulation at 2 times the spin frequency in the raw data, yielding signals at 1 and 3 times the spin frequency (about 0.25 and 0.75 Hz) in the despun data (see the upper panel in Figure 6). This

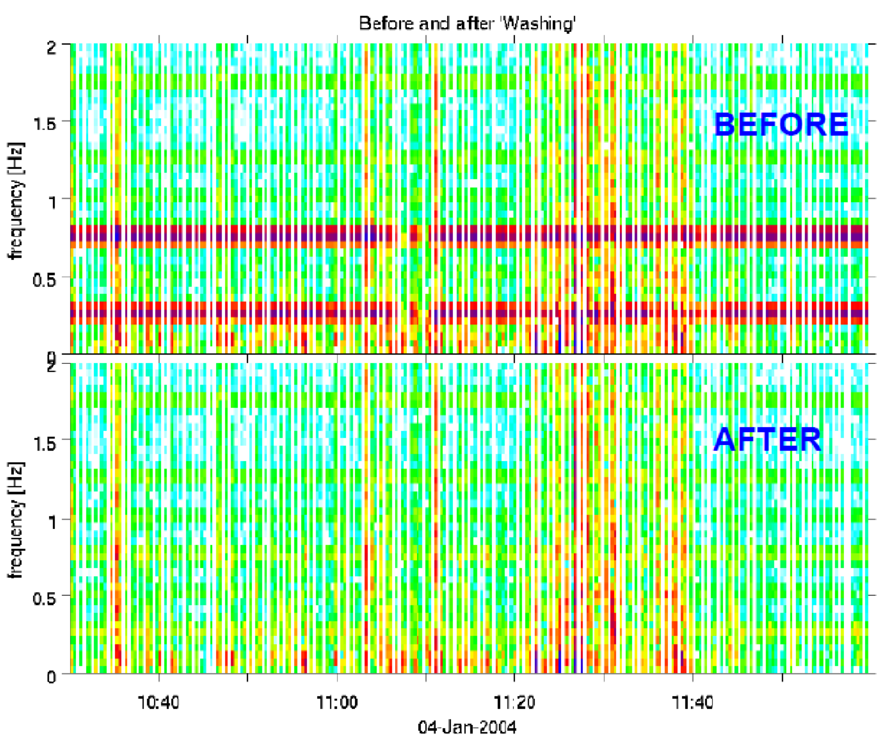


*Figure 6: Original and "washed" data in the asymmetric configuration*

modulation becomes apparent when electric fields become small.

We have tried two algorithms for cleaning (we use the term "washing") this modulation in the data. The first algorithm, referred to as "old", computed the FFT of the p32 data, removed the peak at 2 times the spin frequency by interpolating the spectrum, and then computed the inverse FFT. The results from this method were good but not satisfactory; they caused

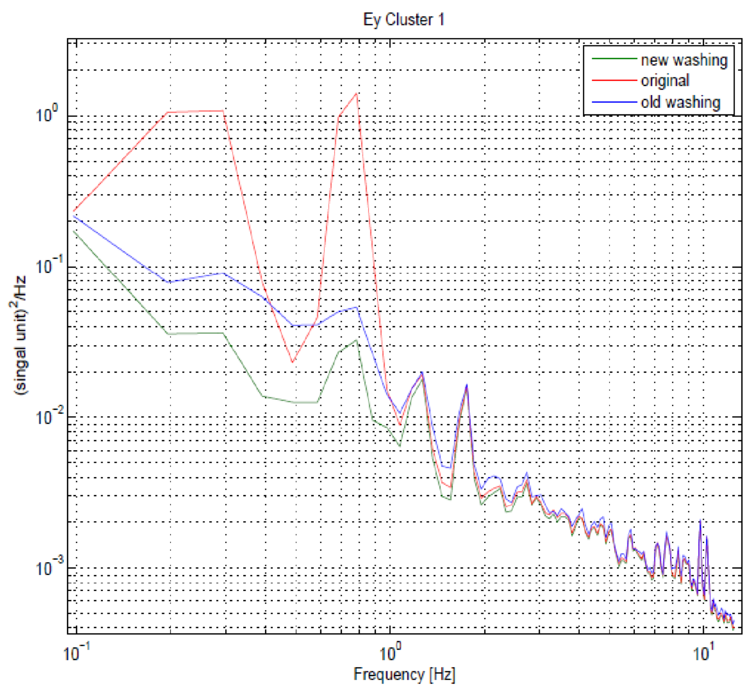


*Figure 7: E spectrum before and after washing. The spacecraft spin frequency is ~0.25 Hz.*

problems at the edges of the FFT window. That is why we developed a new algorithm, referred to as "new", which simply removes the signal at 2 times the spin frequency obtained from spin fitting (terms ***D*** and ***E*** in Equation 1). Figures 7 and 8 show the spectra and time series produced by these two algorithms.

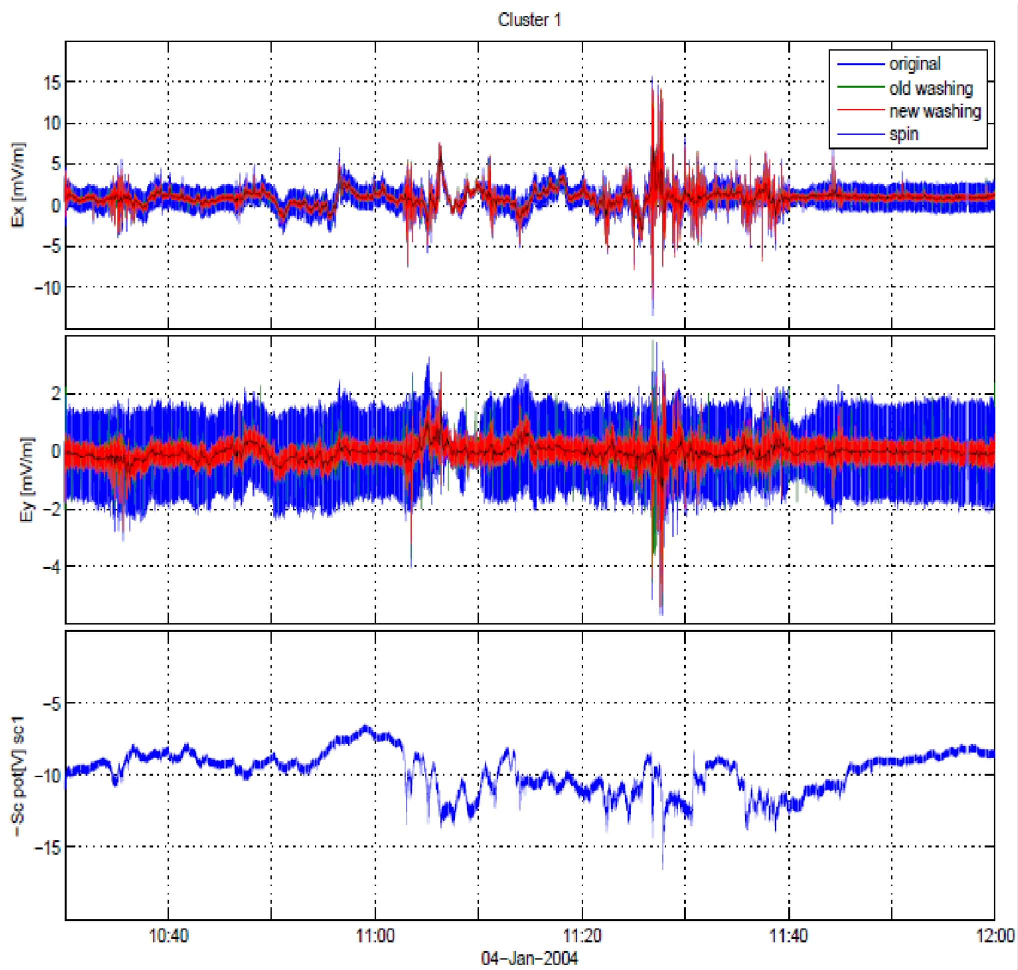


*Figure 8: Timeseries of the despun electric field resulting from raw and washed data.*

### 4.4 Cleaning wakes in the solar wind

In the solar wind, we remove wakes. A detailed description of the procedure can be found in *Eriksson et al. (2007)*. Wakes are routinely removed in the solar wind, and the affected spins have bit 10 set in the E_bitmask for the electric field datasets (see the EFW User Guide). This is done before the spin fitting procedure.

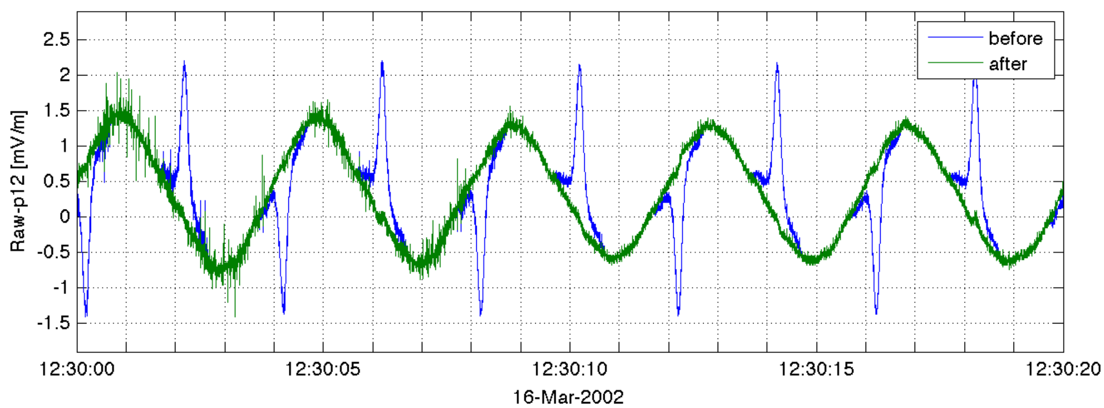


*Figure 9: Solar wind wake removal.*

### 4.5 Detection of spurious electric fields in the plasmasphere

During comparisons of electric field measurements made by EFW and EDI in the inner magnetosphere, it was found that EFW sometimes measures a spurious field of the order of 1-2 mV/m, mostly in the sunward direction (Figure 10, see also Figure 1c in *Puhl-Quinn et al. 2008*). The raw data signal is often non-sinusoidal (top panel). This problem is not quantitatively understood, but apparently depends on simultaneously acting phenomena:

(a) The plasmaspheric plasma density can sometimes be so high as to give a random electron current to the probes almost as large as the applied bias current, driving the probe away from its vacuum potential with respect to the plasma;

(b) The wake created by the spacecraft makes the random current and the resulting error dependent on the spin phase and hence gives an apparent DC field in a non-spinning reference frame; and

(c) Small differences in probe surfaces and bias circuitry will make this effect slightly different between the probes, further complicating the result.

A first principles error treatment is therefore complex. Nevertheless, an empirical algorithm has been developed to detect the bad data. We have developed an algorithm to detect such spurious fields by comparing the electric field measured by EFW to the corotation electric field. If the 1-minute averaged measured field deviates from corotation by more than 1 mV/m, such an interval will be marked as "plasmaspheric wake" in the quality information supplied with electric field data. This Algorithm is applied only for altitudes below 6 $R_E$ and when the negative of the spacecraft potential exceeds -1.5 V, e.g., really only in very dense

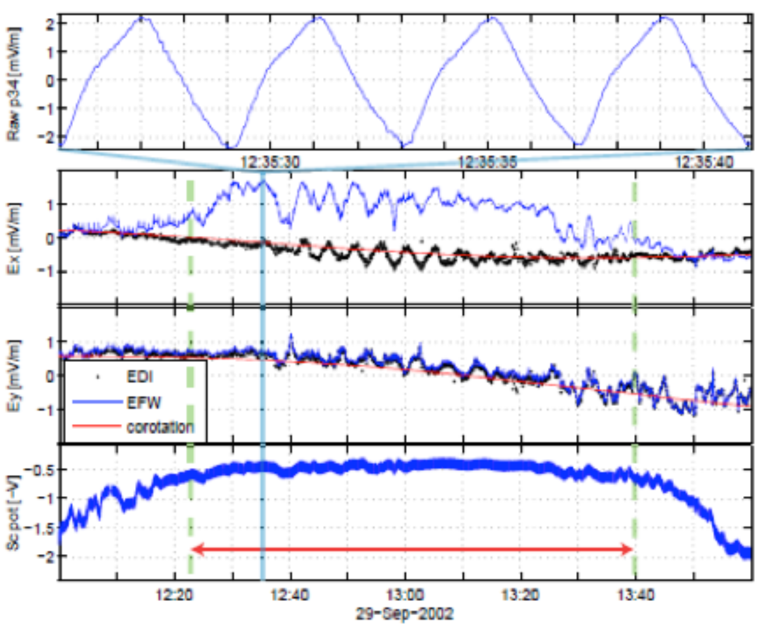


*Figure 10: Spurious fields in the plasmasphere*

corotating plasmasphere. We need to compare to corotation because the EDI measurements are not always available and never on C4. The algorithm in action is illustrated in Figure 10. The panels show the ISR2 components of electric fields measured by EFW and EDI, as well as the corotation fields. The upper panel shows a large deviation of EFW Ex from both the corotation and EDI measurements, and this data interval will be marked as "wake" in the quality data, with bit 12 set in the E_bitmask for the electric field datasets (see the EFW User Guide). Note that the spurious field may also appear in the ISR2 Y direction.

### 4.6 Detection of cold ion flow wakes

One of the most problematic regions for measuring electric fields with double probe instruments (such as EFW) is regions with low plasma density and flowing cold plasmas. In the low-density plasma encountered, for example, in the tail lobes, above the polar caps, and

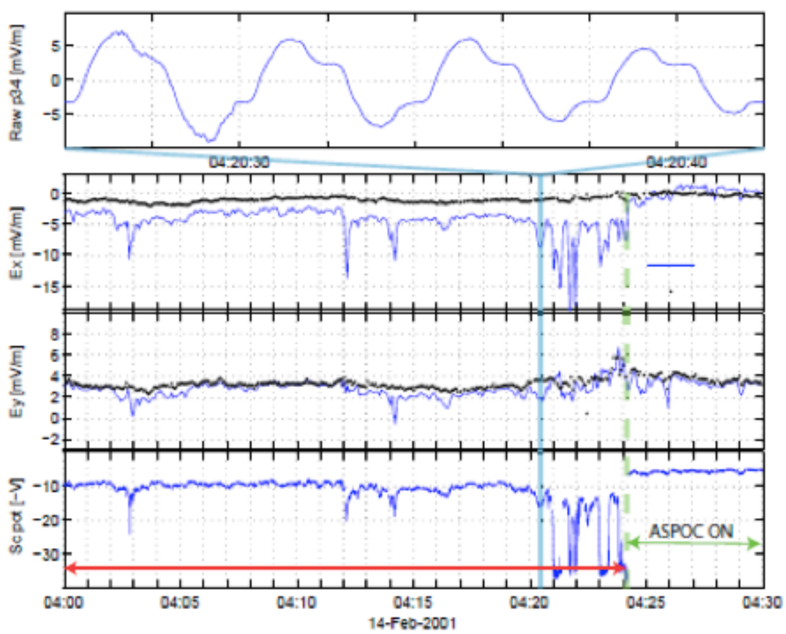


*Figure 11: Wake detection in low density plasmas (EFW-blue, EDI-black).*

in the low latitude dayside magnetosphere, the spacecraft potential is usually of the order of several tens of volts. A cold ion population flowing in such plasma environments will see effectively much thicker booms (several meters instead of a few mm), creating a large negatively charged wake behind the booms in the direction of flow (*Eriksson et al. 2006, Engwall et al. 2006*).

Figure 11 shows an example of such a wake, defined by a large deviation of $E_x$ measured by the EFW and EDI. When ASPOC is operating, the spacecraft potential is kept much lower, and the problem of wakes caused by cold ion drift is much less severe. In comparison to the solar wind wake, the ion drift wake is broader and more diffuse. For a relatively small wake, the raw data are non-sinusoidal (see top panel in Figure 11). For a large wake, they can become sinusoidal again and look very similar to those created by a real ambient electric field.

The CSA production software attempts to detect such ion wakes by analyzing a combination of parameters, including spacecraft potential, magnetic field direction, and relationships among electric field components. For small magnetic field elevations (B direction within 15 degrees of the spin plane), we check the ratio of the components of E along the projection of B into the spin plane and perpendicular to it. For larger elevations, we consider the ratio of the measured (spin-plane) and unmeasured (perpendicular to the spin plane) components of $E_\perp$, where $E_\perp$ is computed assuming zero parallel electric field, $\mathbf{E}\cdot\mathbf{B} = 0$. Higher ratios indicate a greater likelihood that the wake is present in the data. Currently, no algorithm corrects the data, and the bad intervals are marked in the quality information supplied with Level 2 and Level 3 data: bit 11 is set in the E_bitmask (see the EFW User Guide). Since it can sometimes be difficult to distinguish these wakes from a real electric field, analysis of the electric field should be done with caution in regions with possible cold-ion drifts.

# 5 Results of Calibration Activities

Major calibration activities include determining the Raw Data Offset (L3_DER product) and Delta Offsets, as described in the previous section.

## *5.1 EFW noise and sensitivity*

Here, we describe the expected sensitivity and noise characteristics of the EFW data. Figure 12 shows a typical spectrum of Ey ISR2 measured by EFW in the solar wind; in this example, the E-field is sampled at 450 Hz (BM1) and then low-pass filtered at 180 Hz. In the solar wind, the electric field has one of the lowest signal levels compared to all the regions encountered by Cluster, and the EFW sensitivity level is often reached at frequencies above several Hz. We choose to study the Ey ISR2 component on C4, which is one of the cleanest EFW signals available on Cluster. The expected spectrum has a power-law shape, corresponding to a straight line on a log-log plot. The measured spectrum is approximately a power law at low frequencies and begins to flatten at several Hz, reaching the sensitivity floor of ~5×10^-6 $(mV/m)^2/Hz$ above 20 Hz.

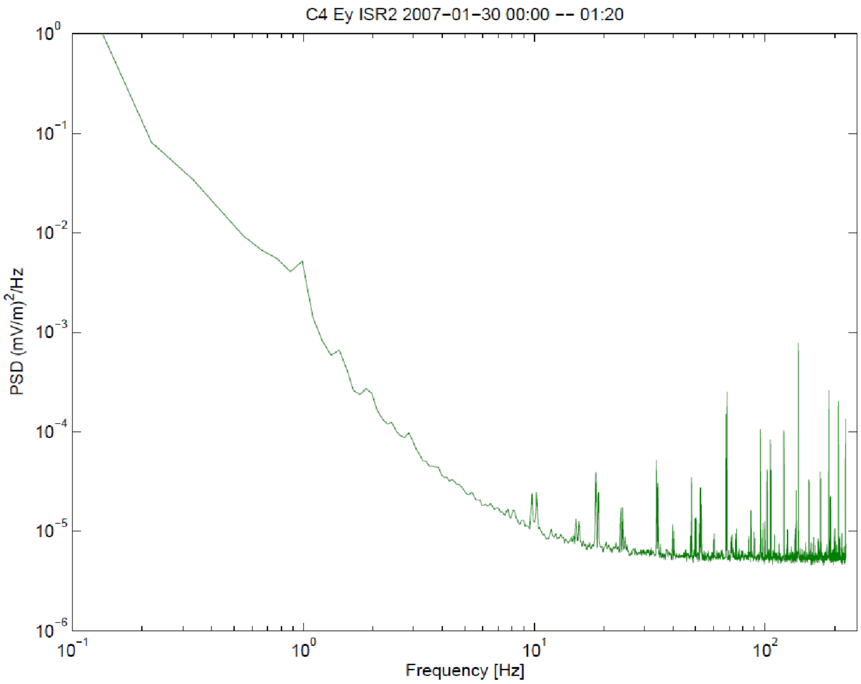


*Figure 12: Ey spectrum in the solar wind.*

Another striking feature in Figure 12 is the presence of sharp peaks at frequencies above 10 Hz. These peaks are due to a high-frequency signal within the EFW electronics, aliased down and unaffected by the 180 Hz low-pass filter.

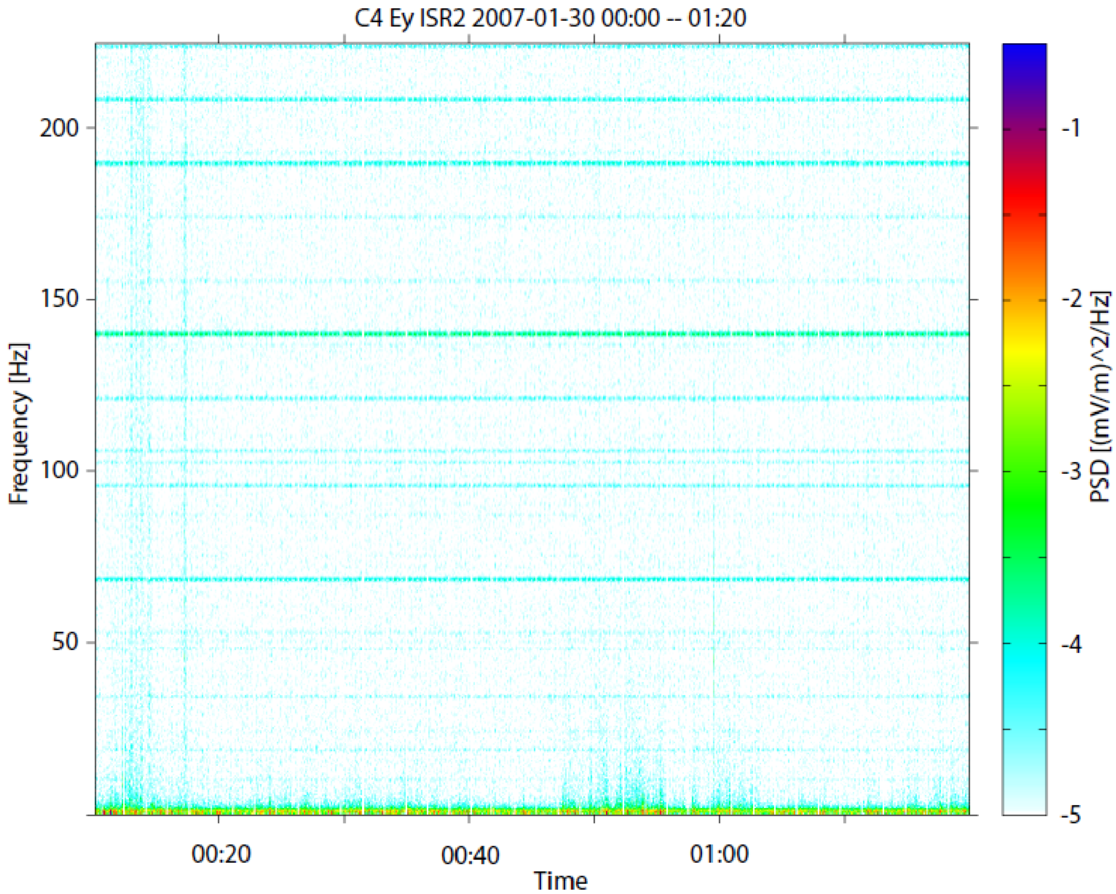


*Figure 13: Time-frequency spectrogram of Ey in the SW*

Figure 13 shows a time-frequency spectrogram of the same data, and one can clearly see that the peaks in the spectrum correspond to the narrow spectral lines. In some cases, a small frequency drift in these lines can be observed, possibly due to heating/cooling of the electronic components as the spacecraft enters a plasma region with different properties. These lines could, in principle, be removed from the data, but it does not make much sense, since the actual signal level is significantly below the sensitivity level in this case.

We have studied the sensitivity of EFW by examining the frequency range from 70 to 180 Hz. The BM1 EFW data for 2001-2008 were split into 30-minute intervals; a spectrum was computed every 4 seconds, spikes were removed, and the mean was computed in the 70-180 Hz range. Then we selected the lowest value in the 30-minute interval. The results for probe pair 12/32 across all spacecraft are plotted in Figure 14. One can see that the sensitivity level is ~2×10^-6 $(mV/m)^2/Hz$ at the beginning of the mission. Then it increases by a factor of 10-20 after probe 1 gets broken on C1, C3, and C2.

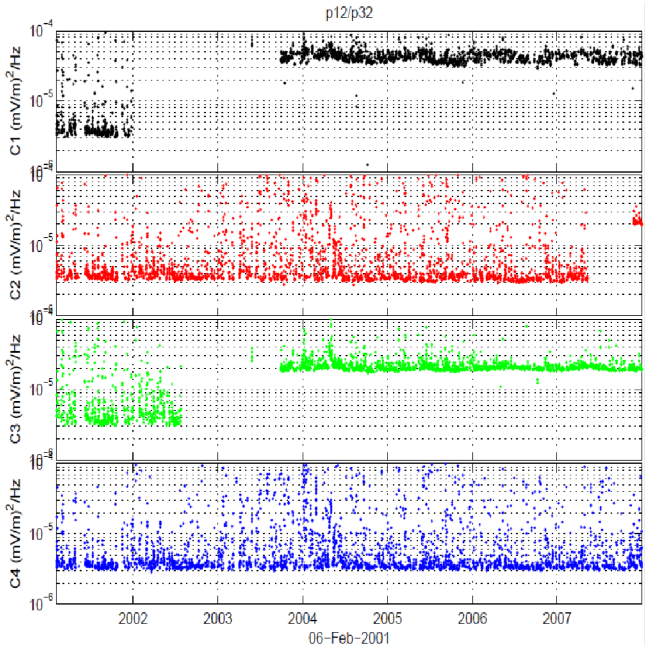


*Figure 14: Evolution of sensitivity level on p12/p32*

The results for probe pair 34 are shown in Figure 15. Here, the initial level is about 5 times higher than for p12. The level rises slightly with the introduction of the EFW flight software version 2.4 (FSW 2.4) at the end of 2003, when the analog difference is replaced by a digital value to compute p32.

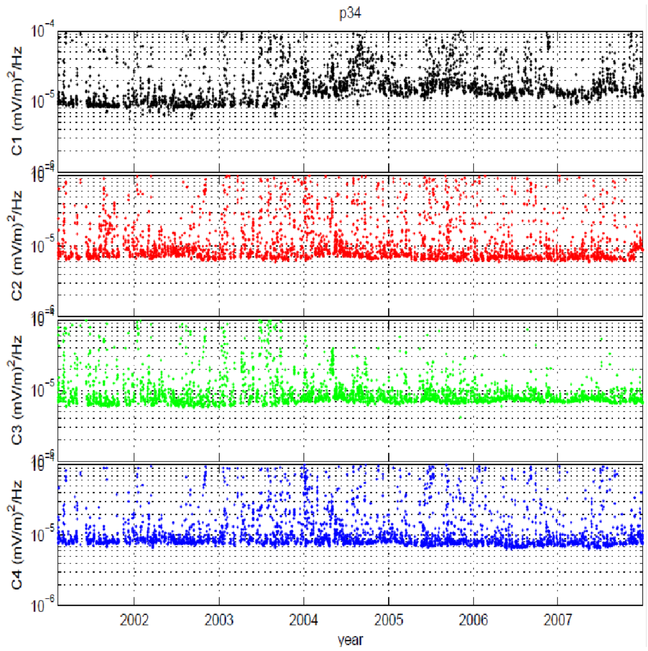


*Figure 15: Evolution of sensitivity level on p34*

# 6 Results of Cross-Calibration Activities

Cross-calibration was mainly used to determine the amplitude correction factor for the electric field data and offsets in ISR2.

We also performed a large "Cross-calibration study" to evaluate the quality of electric fields measured by different instruments.

## *6.1 ISR2 offsets and Amplitude correction factor*

Our main assumption in the study of ISR2 offsets is that the offsets depend on the instrument configuration, spacecraft attitude and that the dependence on surrounding plasma parameters is weak, i.e. being in the same kind of plasma environment (for example plasmasheet) and having the same instrument settings and probe properties for two different time intervals, the difference for between ISR2 offsets for the two intervals must be within the uncertainty of the offset determination (several tenth of mV/m). As the offsets still depend on the plasma environment, we decided to split the dataset into two groups: "solar wind/magnetosheath" and "magnetosphere", corresponding to "cold and dense" and "hot and rarefied” plasmas, respectively. To split every orbit into these two groups, we have used the Shue magnetopause model (*Shue et al. 1997*) with realistic solar wind parameters measured by ACE.

### 6.1.1 Offsets in the solar wind and magnetosheath

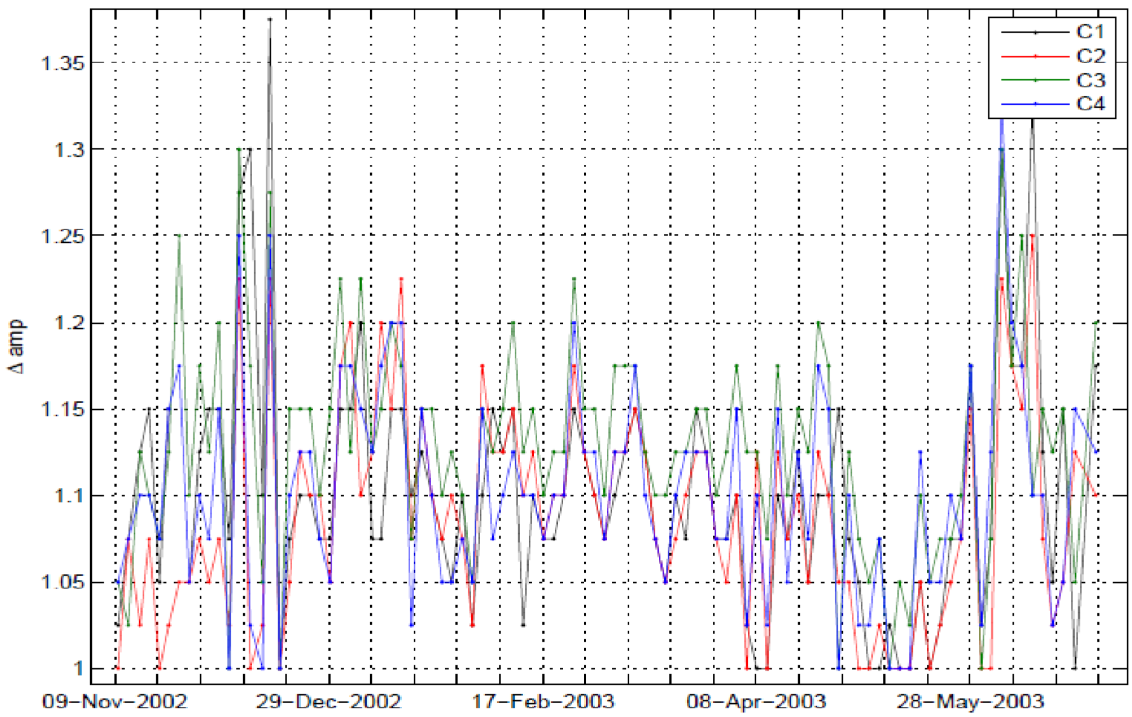


*Figure 16: Amplitude correction factor in fall 2002 - spring 2003*

#### *6.1.1.1 Amplitude correction factor*

First, we studied the amplitude correction factor (see Section 3.4 , i.e., the factor by which the measured electric field amplitude needs to be increased to obtain the actual electric field present in plasmas. The ambient electric field is “*short-circuited*” by the presence of the spacecraft and wire booms. This is caused by the spacecraft’s potential, which is also the potential of the wire booms extending out to a large distance from the spacecraft.

We have used the ISR2 Y components of the electric field to determine the amplitude correction factor. This component of E is generally free of offsets, and thus, by comparing Ey from EFW and CIS-HIA, we can deduce the amplitude correction factor. Results of such computations are shown in Figure 16: Amplitude correction factor in fall 2002 - spring 2003. Every point in the plot corresponds to one orbit of data. We note that the variations observed in the data are not due to changes in the factor, but rather to bad data and insufficient data coverage.

Based on simulations and comparisons with other Cluster instruments, it has been determined that the measured electric field magnitude must be multiplied by 1.1. We use this constant value throughout the entire mission. It is given as a dAmp parameter in the FILE_CAVEATS section in the CEF files for the electric field data.

#### *6.1.1.2 ISR2 offsets*

Once we know the amplitude correction factor, we can determine the ISR2 offsets, which are simply the differences between the spin-plane electric fields measured by EFW and CIS-HIA (VxB).

First, we perform the inter-spacecraft calibration under the assumption that all the spacecraft observe the same large-scale electric field, which is usually the case in the solar wind. Then, using CIS-HIA from C1 and/or C3 as reference data, we determine the ISR2 offsets for EFW for each spacecraft. We get one offset value per orbit.

The procedure can be controlled visually using the plot shown in Figure 17. The two upper panels show all the available EFW and CIS-HIA data (Ex and Ey in ISR2). Then we construct the *reference E-field* from the available CIS-HIA by averaging. This is possible because the difference between the spacecraft in the SW/MSH is small. Then we compute the difference between the EFW Ex on all spacecraft and the reference E-field, and plot it in the third panel. The average of the difference over the entire interval gives the local ISR2 offset. This offset is then applied to the EFW on different spacecraft. The resultant corrected and reference E-fields are plotted in the two bottom panels.

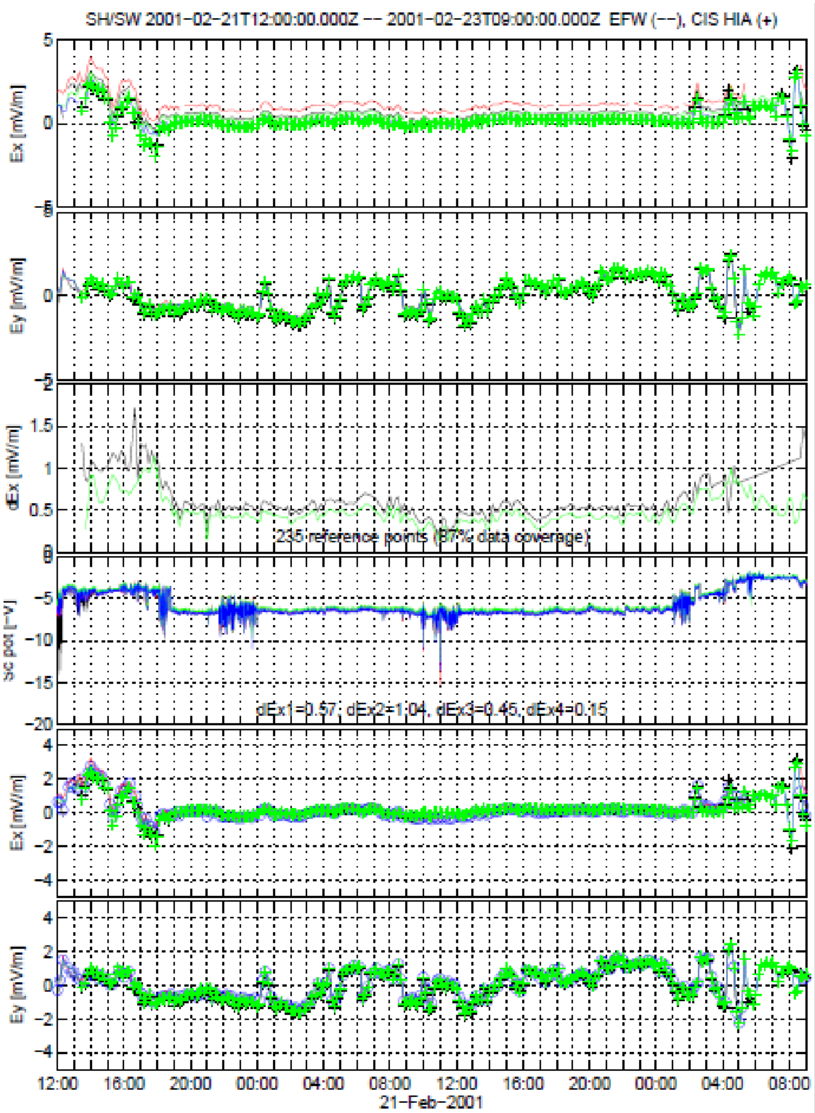


*Figure 17: ISR2 offsets in the SW/MSH. The two lower panels show the electric field data to which the local offsets determined for this orbit have been applied.*

We have conducted this analysis on all available solar wind and magnetosheath data, grouping the data into “solar wind periods” from November to June. The resulting ISR2 offsets for EFW on all Cluster spacecraft for 2003 are shown in Figure 18. It is evident that the distribution of offsets is quite centered around the mean. The scatter mainly results from poor data quality and limited data coverage.

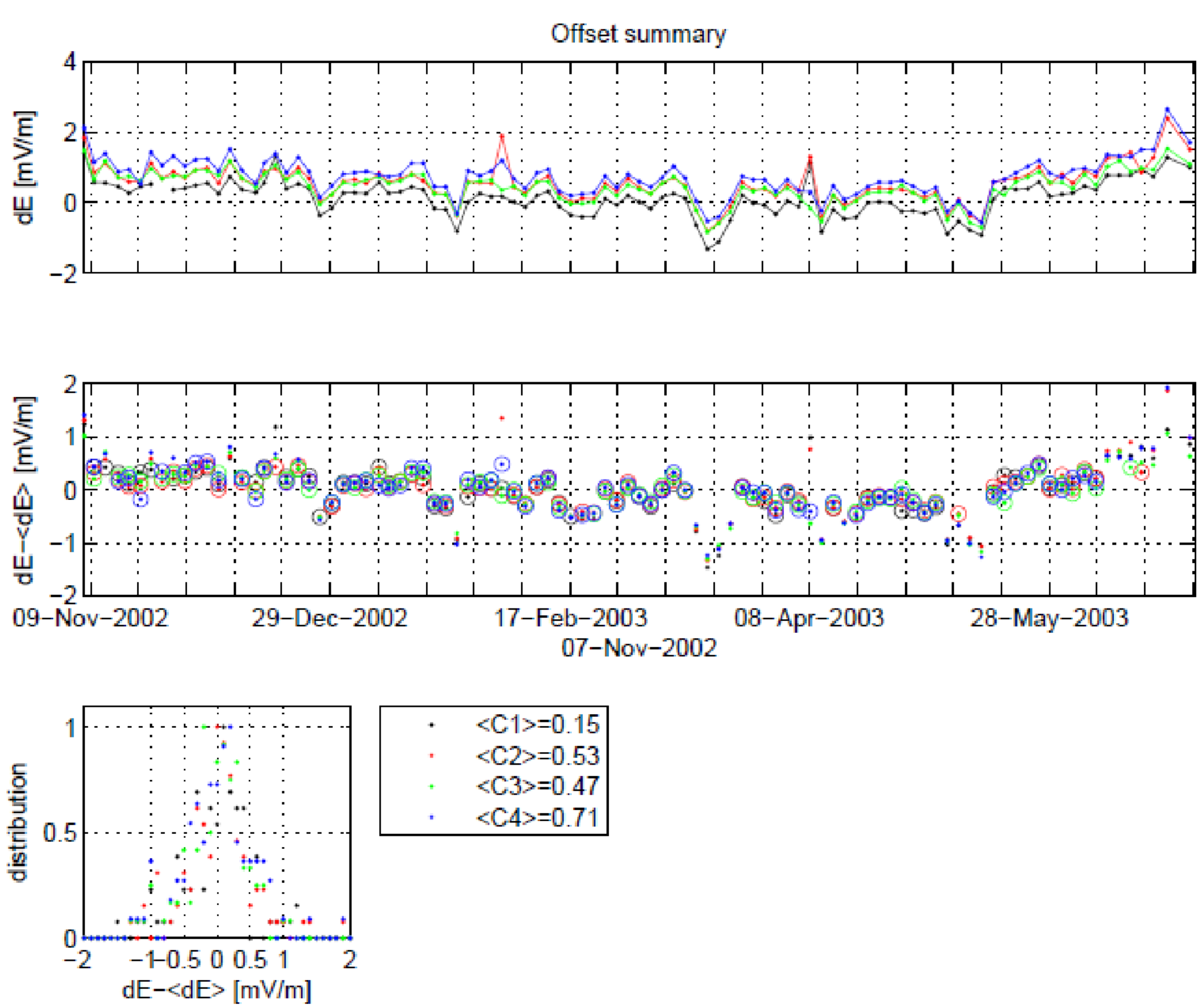


*Figure 18: ISR2 offset summary (Ex) in the SW/MSH for spring 2003. The top panel shows the instantaneous offsets determined for each orbit. The middle panel shows the difference between the instantaneous offsets and the average "seasonal" offset, which is used in the CSA production (<C1>..<C4> in the panel below), and which is computed on the basis of the encircled points. The distribution of the difference is shown in the bottom-left panel.*

Later, the offset values obtained by this automatic procedure are manually verified and, if necessary, corrected; the values applied are given in the FILE_CAVEATS section in the CEF files for the electric field data, for example:

```
ENTRY       =   "2007-12-02T00:00:00.000Z/2007-12-02T01:09:00.000Z
ISR2 offsets: dEx=0.85 dEy=0.00, dAmp=1.10"
```

gives the values of the ISR2 offsets and correction factor applied between 00:00 and 01:09.

### 6.1.2 Offsets in the magnetosphere

Determining offsets in the magnetosphere is significantly more complicated than in the solar wind/magnetosheath. Data from the other instruments, which could have been used as a reference, are of very low quality in large areas of the magnetosphere due to low counts or low magnetic fields (see "Cross-Calibration study"). Also, the EFW data are subject to frequent problems, such as electrostatic wakes.

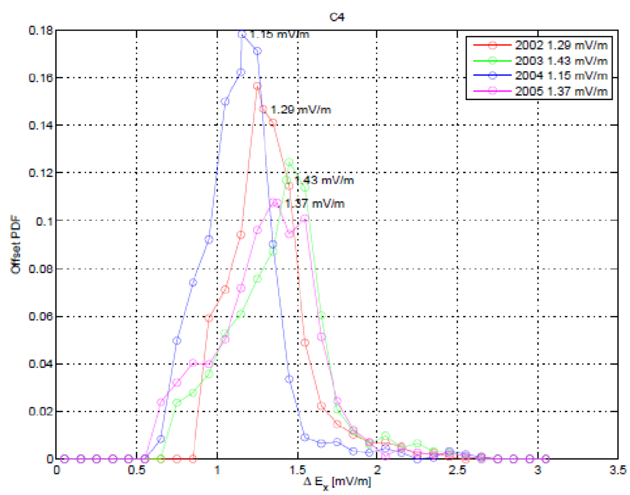


*Figure 19: Example of statistical distributions of ISR2 X offsets for Cluster 4 in the magnetosphere.*

In the ISR2 offset determination procedure, we decided not to use any reference data, but rather use a condition of zero electric field $\langle E_x \rangle = 0$, as most of the times the electric fields are really very weak in the magnetotail (X_GSE < 0 and R > 5 $R_E$), and averaged over a tail season this should give a rather good estimate for the ISR2 X offset.

Results for Cluster 4 are summarized in Figure 19. One can see a prominent peak around 1.3 mV/m in all years; a group of points also shows broadening towards lower offset values. The nature of this broadening can be understood by plotting the ISR2 X offset against the spacecraft potential (see Figure 20). We can see a clear cluster of points around 1.3 mV/m corresponding to the primary peak of the distribution. The main cause of broadening is due to data with ASPOC on, which can be easily identified as a cluster of points at the spacecraft potential of -7 V.

In the production of the magnetospheric data we use two sets of offsets: in the dense plasma (SC potentials above -8 V), we use the “solar wind/magnetosheath” offsets, and in low-density plasmas, we use the “magnetospheric” offsets. The values of the offsets applied

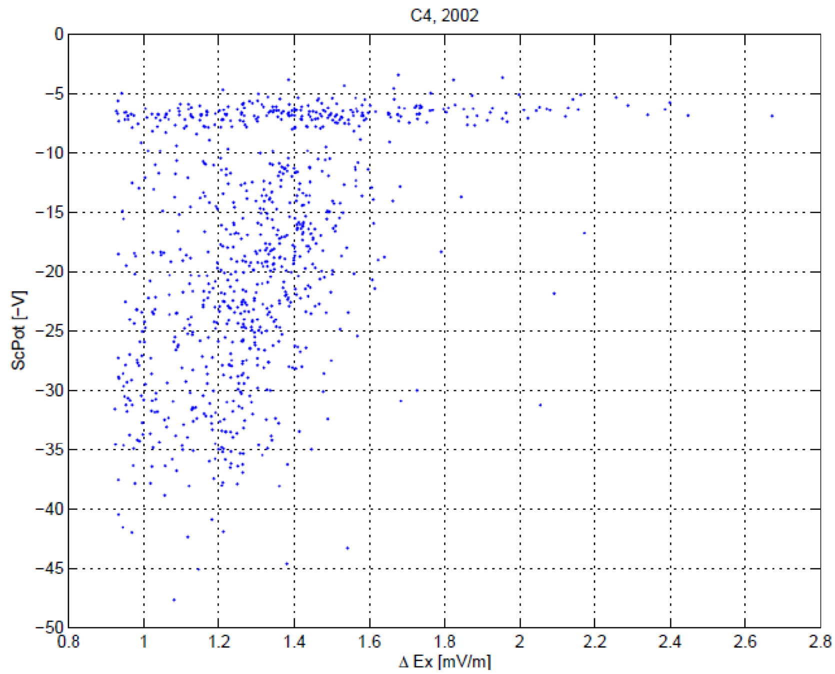


*Figure 20: Sunward offset vs spacecraft potential (Cluster 4, June-November 2002).*

together with corresponding time intervals are given in the FILE_CAVEATS section in the CEF files for the electric field data. The offsets are typically updated every several months following the spacecraft maneuvres, etc.

## 6.2 Comparison of E measured by EFW vs other instruments

Here, we present a summary of a study comparing electric field data in the CSA measured by the EFW with EDI, CIS-HIA, CIS-CODIF, and PEACE to evaluate the data quality resulting from the current production procedure used by the EFW team. We used 20 events covering different regions along the Cluster orbit and present the electric field and convection velocity components measured by different instruments in a standard format. We conclude that EFW, as expected, provides the highest quality electric field measurements in the spacecraft spin plane.

### 6.2.1 Methodology and dataset

We compare the CSA Cluster EFW measurements with those of EDI (CX_CP_EDI_MP), CIS-HIA (CX_PP_CIS), CIS-CODIF (CX_CP_CIS-CODIF_HS_H1_MOMENTS, CX_CP_CIS-CODIF_LS_H1_MOMENTS) and PEACE (CX_CP_PEA_MOMENTS). For each event, there is at

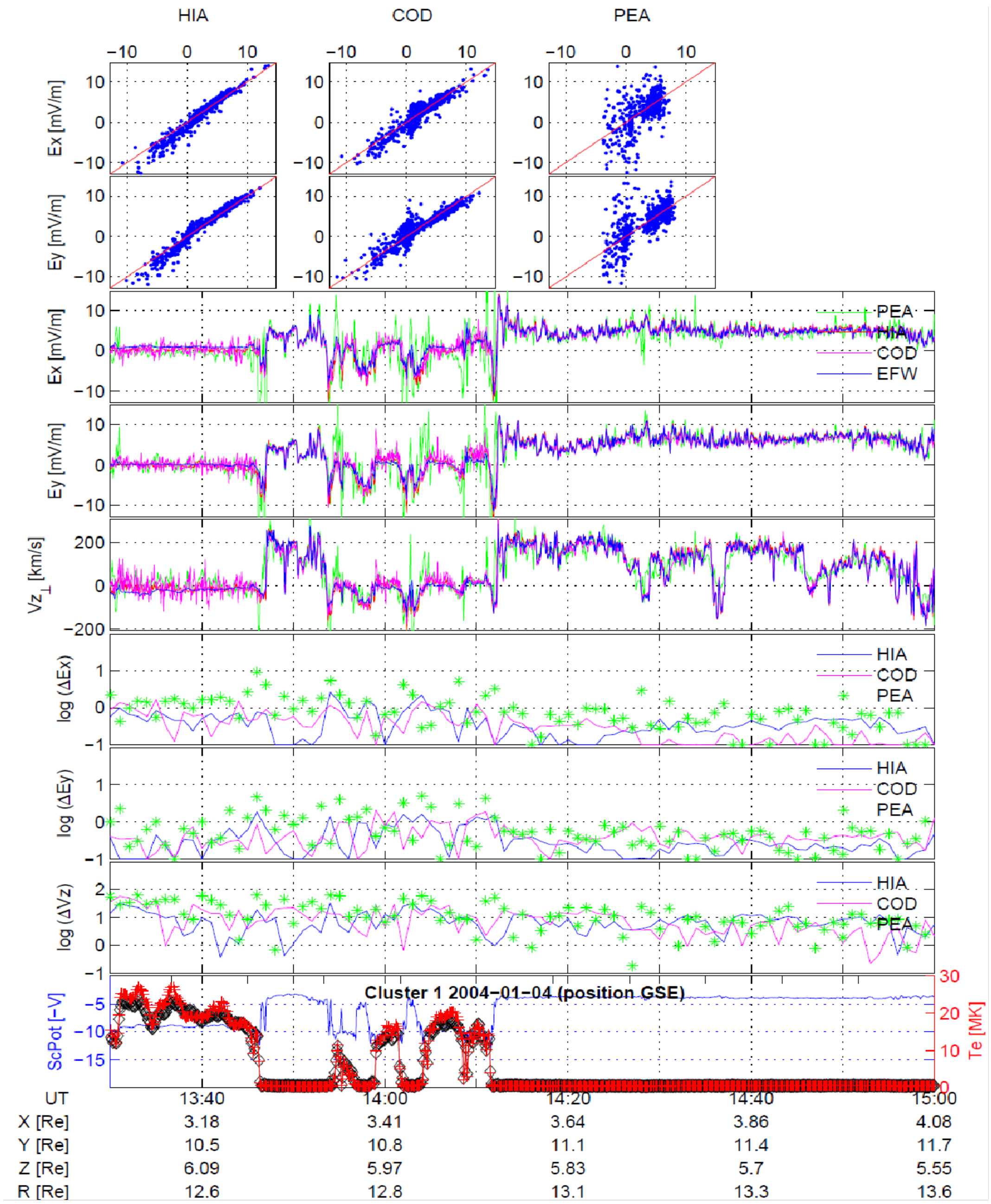


*Figure 21: Cluster 1 at the magnetopause. EFW vs HIA, CODIF and PEACE.*

least one “standard” plot of the above-described data for each available instrument. For most events, there are plots for both C1 and C3. C2 was not included since CIS is not operational, and C4 was not included since EDI and CIS-HIA are not operational. It should be mentioned that EFW data is routinely cross-calibrated between the spacecraft, and it is sufficient to show only C1 and C3.

For many events, there are also “fine” plots, where one or more relevant instruments have been selected to highlight good or bad agreement. On these plots, the top three line plot panels may have a somewhat different format. Data from instruments other than EFW may be plotted as Max and Min instead of a line plot. This Max-Min envelope of the particle instruments may be plotted in two ways: either as two lines indicating the maximum and minimum envelope of the data, or as a shaded area showing the same. The color coding is given in the top panel. The envelope of the data has been calculated at 1-minute time resolution for EDI, HIA, and COD, and at 4-minute time resolution for PEA.

### 6.2.2 Plot format

The plots contain up to 8 panels: at the top, scatter plots of data vs data; followed by 7 plots of data vs time. An example plot for a magnetopause crossing is shown in Figure 21.

The scatter plots at the top show EFW on the x-axis vs. another instrument (EDI, HIA, COD, or PEA) on the y-axis. The EFW data have been resampled to the time resolution of the other instrument. The top panel is Ex, and the bottom panel is Ey. A red line through the origin with slope 1 has been included for reference.

The next three panels show line plots of Ex, Ey, and Vzperp (= ExB/B2) for all available instruments. The color coding is given in the top panel. EFW, HIA, COD, and PEA are plotted as lines, while EDI is plotted as points. Each instrument is plotted with its own time resolution.

The next three panels show plots of the time-averaged (1-minute) difference between EFW and the other instruments on a logarithmic scale. For example, the blue line shows the difference between EFW and HIA, computed as `log(abs(time_average(Ex[EFW]-Ex[HIA])))`. Ex and Ey are measured in mV/m, and Vz is measured in km/s. The scale is 0.1-100 mV/m for E and 0.1-1000 km/s for V. The EFW data are resampled to the particle data time resolution before computing the differences. EFW-HIA and EFW-COD are plotted as lines, while EFW-PEA and EFW-EDI are plotted as points.

The bottom panel contains, for reference, the spacecraft potential measured by EFW (blue) together with the electron temperature measured by PEACE (red = perpendicular, black = parallel). The spacecraft number and date are given in the bottom panel. The spacecraft coordinates below the plot are in GSE.

### 6.2.3 Conclusions

We compared the CSA EFW electric field with EDI, CIS-HIA, CIS-CODIF, and PEACE. We conclude that EFW generally provides the best-quality electric-field measurement. Normally, the statistical difference between the electric fields measured by EFW and other instruments lies within 1 mV/m, provided the measurements by other instruments are reasonable at all.

The observed differences between EFW and the other instruments are usually due to higher noise and offsets in the EDI and particle instruments. However, in some cases, the difference may be caused by spurious fields measured by EFW, which cannot be corrected by applying offsets to the data.

EFW generally agrees best with CIS-HIA. CIS-CODIF has a much larger noise level and Z-direction offset than CIS-HIA (especially CIS-CODIF on C3). On the other hand, we find that in some cases CIS-HIA does not follow the large electric field variations observed by EFW, PEACE, and CODIF. We also found cases when HIA and CODIF data differ by a constant factor.

We find that PEACE moments have very limited use inside the magnetosphere. However, there is good agreement between EFW and PEACE in the magnetosheath, especially when the SC is in the burst mode.

EFW-EDI comparisons, in some cases, show remarkable agreement down to 0.1 mV/m in quiet fields. However, in more active regions, EDI shows much greater scatter, as expected. In general, the agreement between EFW and EDI is very good.

Finally, we conclude that we see the expected picture: the quality of the electric field measured by the different instruments strongly depends on the plasma environment. We usually find a statistical agreement between EFW and at least one of the other instruments within 1 mV/m. Provided that the measured field is real, EFW generally provides the best measurement of the electric field. The EFW team's data production process results in high data quality.

More information about this study can be found in “Cross-Calibration study”; see Annex 1.

# 7 Summary

Processing EFW data for the CSA is a complex procedure that requires several calibration and cross-calibration steps, during which different offsets are determined.

## *7.1 Raw data and calibration parameters*

The calibration parameters determined during data processing, along with some instrument setting values and raw data signals, are available as ancillary datasets (for details, see the EFW ICD).

| **Sampling rate** | **CSA Dataset name** | **Description** |
|---|---|---|
| 5 $s^{-1}$ | C[n]_CP_EFW_L1_P1 | Potential, Probe 1 to spacecraft (raw data) |
| | C[n]_CP_EFW_L1_P2 | Potential, Probe 2 to spacecraft (raw data) |
| | C[n]_CP_EFW_L1_P3 | Potential, Probe 3 to spacecraft (raw data) |
| | C[n]_CP_EFW_L1_P4 | Potential, Probe 4 to spacecraft (raw data) |
| 25 $s^{-1}$ or 450 $s^{-1}$ | C[n]_CP_EFW_L1_P12 | Potential, Probe 1 to Probe 2 (raw data) |
| | C[n]_CP_EFW_L1_P32 | Potential, Probe 3 to Probe 2 (raw data) |
| | C[n]_CP_EFW_L1_P34 | Potential, Probe 3 to Probe 4 (raw data) |
| 0.25 $s^{-1}$ | C[n]_CP_EFW_L3_DER | Electric Field offsets (4 second resolution) |
| 0.25 $s^{-1}$ | C[n]_CP_EFW_L3_SFIT | Spinfits of the electric field from the individual probe pairs |
| 1/32 s-1 | C[n]_CP_EFW_L2_HK | Instrument settings |

The Level 1 datasets (first 7 rows above) are the ***raw data*** from the instrument, decommutated and converted to physical units. **P1**, **P2**, **P3**, and **P4** are the potentials of the four individual probes, measured relative to the spacecraft. **P12**, **P34,** and **P32** are potential differences between probes. Notice that the spacecraft attitude and orbit parameters, as well as the sun reference pulse, all needed for the interpretation of the raw signal, are given in the CSA spacecraft auxiliary datasets (see Laakso, 2011).

**C[n]_CP_EFW_L3_DER** is the DC offset in the raw data. See section 6.1 for more information. DER is a vector with 2 components and, depending on which probes are available for E-field measurements, contains either the offsets in p12 and p34 or the offsets in p32 and p34.

## 7.2 Long-term evolution of offsets

Figure 22 shows the evolution of Delta offsets (difference between ISR2 E measured by probe pairs 12/32 and 34). Several factors cause variations in the offset. First is the solar cycle. The offset is small and steady at the beginning of the mission, then grows as the solar minimum approaches, reaching its maximum in spring 2006. This behavior was caused by non-optimal bias current settings, and it improved significantly after the bias current was lowered in June

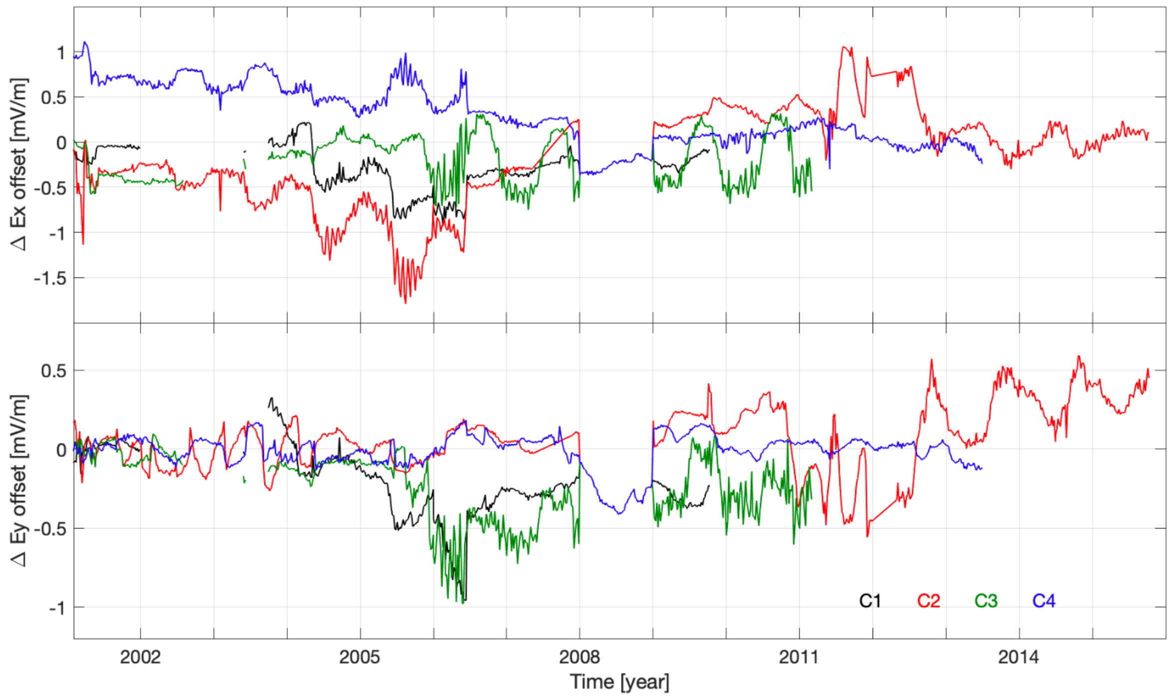


*Figure 22: Evolution of delta offsets*

2006. The second cause is the probe failures, which forced the use of P32 instead of P12. P32 is of lower quality because it is not symmetric with respect to the spacecraft. Note that Delta offsets are available as long as there are two functioning probe pairs.

Figure 23 shows the evolution of ISR2 (DSI) offsets in the solar wind and magnetosheath over the mission lifetime. One can see that the offsets are rather steady and slowly decreasing as the solar minimum (~2009) approaches. The sudden increase in the C3 offset in 2005 remains unexplained. The large increase in the C2 offsets since 2012 is attributed to the drastic reduction in the probe photoemission caused by atomic oxygen contamination.

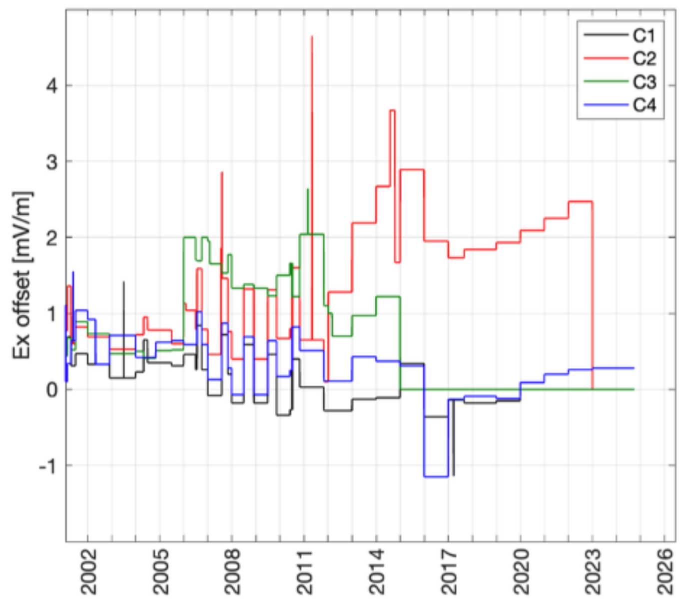


*Figure 23: Evolution of ISR2 (DSI) offsets in the SW/MSH*

Evolution of ISR2 offsets in the magnetosphere over the mission lifetime is shown in Figure 24. The offsets are steady and slowly decreasing as the solar minimum approaches.

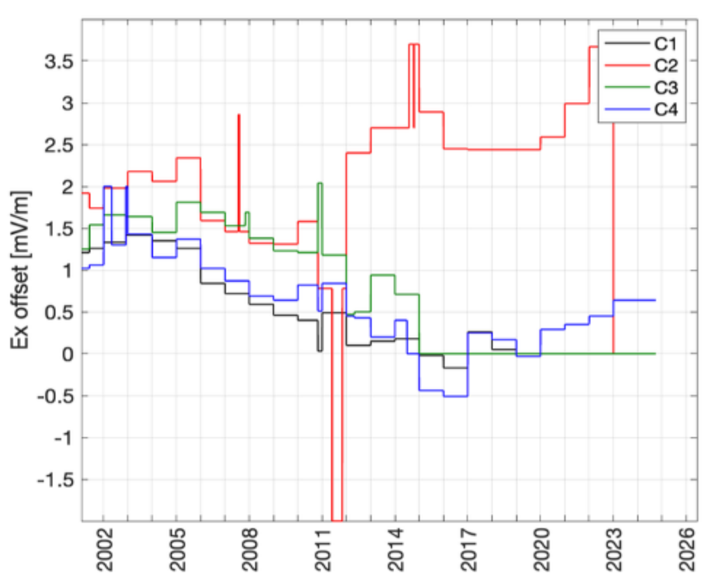


*Figure 24: Evolution of ISR2 (DSI) offsets in the magnetosphere*

# 8 References

EFW “non-standard operations” database (caveat dataset C[1-4]_CQ_EFW_INST).

Cully C. M., R. E. Ergun, and A. I. Eriksson, Electrostatic structure around spacecraft in tenuous plasmas, J. Geophys. Res. 112, A09211, doi:10.1029/2007JA012269, 2007.

Gustafsson, G., R. Boström, B. Holback, G. Holmgren, A. Lundgren, K. Stasiewicz, L. Åhlén, F. S. Mozer, D. Pankow, P. Harvey, P. Berg, R. Ulrich, A. Pedersen, R. Schmidt, A. Butler, A. W. C. Fransen, D. Klinge, M. Thomsen, C.-G. Fälthammar, P.-A. Lindqvist, S. Christenson, J. Holtet, B. Lybekk, T. A. Sten, P. Tanskanen, K. Lappalainen, and J. Wygant, The Electric Field and Wave Experiment for the Cluster Mission, Space Sci. Rev. 79, 137-156, doi:10.1023/A:1004975108657, 1997.

Engwall, E., A. I. Eriksson, and J. Forest, Wake formation behind positively charged spacecraft in flowing tenuous plasmas, Phys. Plasmas 13, 062904, doi:10.1063/1.2199207, 2006.

Eriksson, A. I., M. André, B. Klecker, H. Laakso, P.-A. Lindqvist, F. Mozer, G. Paschmann, A. Pedersen, J. Quinn, R. Torbert, K. Torkar, and H. Vaith, Electric field measurements on Cluster: comparing the double-probe and electron drift techniques, Ann. Geophys. 24, 275-289, doi:10.5194/angeo-24-275-2006, 2006.

Eriksson, A. I., Y. Khotyaintsev, and P.-A. Lindqvist, Spacecraft wakes in the solar wind, In Proceedings of the 10th Spacecraft Charging Technology Conference (SCTC-10), doi:10.48550/arXiv.2603.12860, 2007.

Laakso, H. Cluster Active Archive – User Guide, CAA-EST-UG-0001, 2011.

Lindqvist, P.-A. and Y. Khotyaintsev, Cluster Active Archive: Interface control document for EFW, ESA document CAA-EFW-ICD-0001, doi:10.5270/esa-rp1zebe, 2026.

Lindqvist, P.-A., C. M. Cully and Y. Khotyaintsev, User Guide to the EFW measurements in the Cluster Active Archive (CAA), ESA document CAA-EST-UG-EFW, doi:10.5270/esa-rp1zebe 2026.

Puhl-Quinn, P. A., H. Matsui, V. K. Jordanova, Y. Khotyaintsev, and P.-A. Lindqvist, An effort to derive a convection electric field model in the inner-magnetosphere: Merging Cluster EDI and EFW data, J. Atmosph. Solar-Terr. Phys., 70, 564-573, doi:10.1016/j.jastp.2007.08.069, 2008.

Shue, J.-H., J. K. Chao, H. C. Fu, C. T. Russell, P. Song, K. K. Khurana, and H. J. Singer, A new functional form to study the solar wind control of the magnetopause size and shape, J.

Geophys. Res., 102, 9497-9512, doi:10.1029/97JA00196, 1997.

# 9 Annex 1: Cross-calibration study

Included below.

# Cross-calibration study: Comparing EFW to EDI, HIA, CODIF and PEACE

by Yuri Khotyaintsev, Per-Arne Lindqvist and Anders Eriksson

2008-04-30

Archived from: https://www.cluster.irfu.se/efw/efw_vs_others/

Here we present a study comparing electric field data in the CAA measured by the EFW to EDI, CIS-HIA, CIS-CODIF and PEACE in order to evaluate the data quality resulting from the current production procedure used by the EFW team. We use 20 events covering different regions along the Cluster orbit and present electric field and convection velocity components measured by different instruments in a standard format. We conclude that EFW, as expected, provides the highest quality electric field measurements in the spacecraft spin plane.

# Methodology and dataset

We compare the CAA Cluster EFW measurements with those of EDI, CIS-HIA, CIS-CODIF and PEACE. For each event there is at least one “standard” plot with the above described data, for as many instruments as are available. For most events there are plots for both C1 and C3. C2 was not included since CIS is not operational, and C4 was not included since EDI and CIS-HIA are not operational. It should be mentioned that EFW data is routinely cross calibrated between the spacecraft and it is sufficient to show only C1 and C3.

For many events there are also “fine” plots, where one or more relevant instruments have been selected to highlight good or bad agreement. On these plots, the top three line plot panels may have a somewhat different format. The data from other instruments than EFW may be plotted as Max and Min instead of just a line plot. This Max-Min envelope of the particle instruments may be plotted in two ways, either as two lines indicating the maximum and minimum envelope of the data, or as a shaded area indicating the same thing. The color coding is given in the top panel. The envelope of the data has been calculated at 1 minute time resolution for EDI, HIA and COD, and at 4 minute time resolution for PEA.

### *Plot format*

The plots contain up to 8 panels with scatter plots of data vs data at the top, followed by 7 plots of data vs time.

The scatter plots at the top are plots of EFW on the x-axis vs another instrument (EDI, HIA, COD or PEA) on the y-axis. The EFW data have been resampled to the time resolution of the other instrument. The top panel is Ex and the bottom panel is Ey. A red line through the origin with slope 1 has been included for reference.

The next three panels are line plots of Ex, Ey and vz⊥ (= $ExB/B^2$) for all instruments available. The color coding is given in the top panel. EFW, HIA, COD and PEA are plotted as lines, while EDI is plotted as points. Each instrument is plotted with their own time resolution.

The next three panels are plots of the time-averaged (1 minute) difference between EFW and the other instruments, on a logarithmic scale. For example, the blue line shows the difference between EFW and HIA, computed as log(abs(time_average(Ex[EFW]-Ex[HIA]))). Ex and Ey are measured in mV/m, vz is measured in km/s. The scale is 0.1-100 mV/m for E and 0.1-1000 km/s for v. The EFW data are resampled to the particle data time resolution before computing the differences. EFW-HIA and EFW-COD are plotted as lines, while EFW-PEA and EFW-EDI are plotted as points.

The bottom panel contains for reference the spacecraft potential measured by EFW (blue) together with the electron temperature measured by PEACE (red = perpendicular, black = parallel). The spacecraft number and date is given in the bottom panel. The spacecraft coordinates below the plot are in GSE.

## Solar wind

## Event 1: Solar wind

2003-03-04 08:00 - 11:00 | CAA quicklook

**Standard plots:**

030304_C1_SW.pdf

030304_C3_SW.pdf

This event shows agreement to within 1 mV/m between all the instruments providing data: EFW, HIA, CODIF and PEACE. During one period, 10:00-10:30, EFW Ex consistently deviates from the consensus value from the three other instruments, but not by more than by 1 mV/m, on SC1 as well as on SC3. A consistent deviation can be seen also in the Ex scatter plots, where the bullet swarms stay above the diagonal unit line. Another consistent behaviour is that CODIF and HIA moments differ by a constant factor, as is obvious from the different slopes in the scatter plots.

This event demonstrates agreement to within 1 mV/m for most instruments, with CODIF differing by some factor to the others.

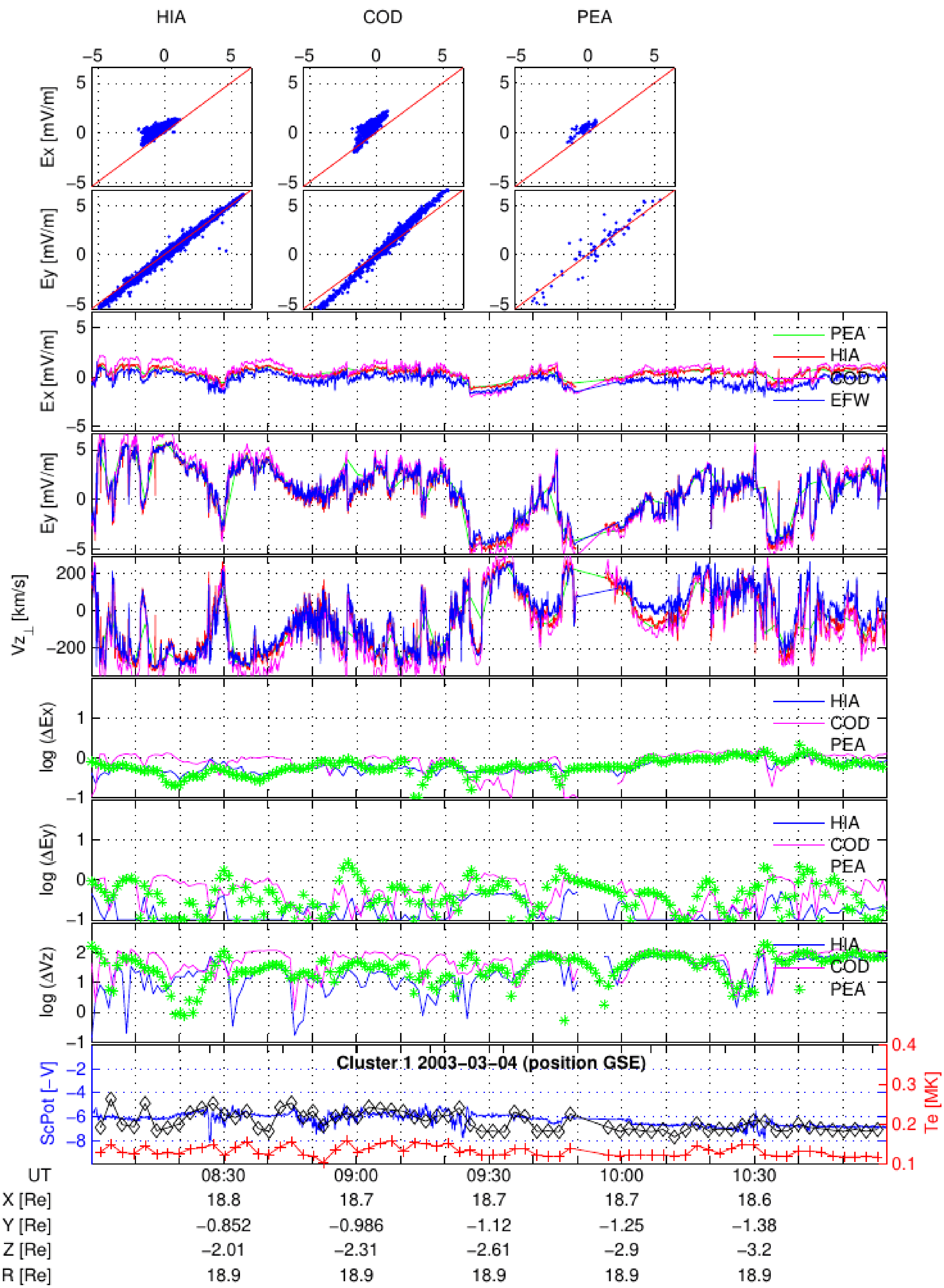

HIA
COD
PEA
Ex [mV/m]
Ey [mV/m]
PEA
HIA
COD
EFW
Vz⊥ [km/s]
log (ΔEx)
log (ΔEy)
log (ΔVz)
Cluster 1 2003-03-04 (position GSE)
ScPot [−V]
Te [MK]
UT 08:30 09:00 09:30 10:00 10:30
X [Re] 18.8 18.7 18.7 18.7 18.6
Y [Re] −0.852 −0.986 −1.12 −1.25 −1.38
Z [Re] −2.01 −2.31 −2.61 −2.9 −3.2
R [Re] 18.9 18.9 18.9 18.9 18.9

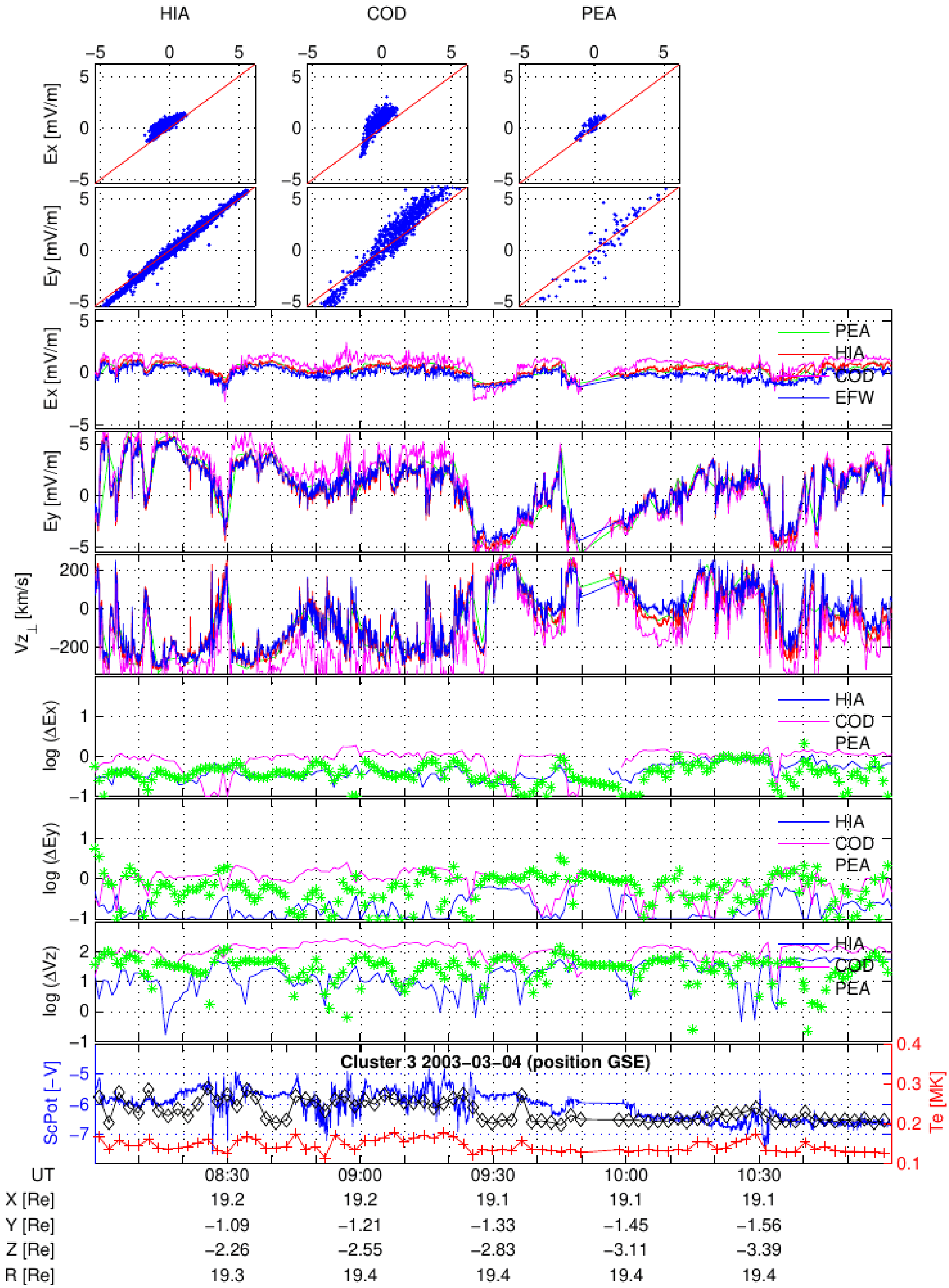
HIA
COD
PEA
Ex [mV/m]
Ey [mV/m]
PEA
HIA
COD
EFW
Ex [mV/m]
Ey [mV/m]
Vz⊥ [km/s]
log (ΔEx)
log (ΔEy)
log (ΔVz)
Cluster 3 2003−03−04 (position GSE)
ScPot [−V]
Te [MK]
UT 08:30 09:00 09:30 10:00 10:30
X [Re] 19.2 19.2 19.1 19.1 19.1
Y [Re] −1.09 −1.21 −1.33 −1.45 −1.56
Z [Re] −2.26 −2.55 −2.83 −3.11 −3.39
R [Re] 19.3 19.4 19.4 19.4 19.4

## Magnetopause

## Event 2: Magnetopause

2002-02-20 12:00 - 15:00 | CAA quicklook

**Standard plots:**

`020220_C1_MP.pdf`

`020220_C3_MP.pdf`

In the second half of the interval, showing magnetosheath data, EFW, HIA and CODIF give excellent agreement, as usual with the highest noise level in CODIF and lower noise in HIA. PEACE also agrees qualitatively, though noise and offsets can be large at times. EDI data shows reasonable agreement at the start of the interval, but for some reason fails to pick up a lot of the E-fields in the magnetosheath after 14:00. The difference EFW-CIS is below 1 mV/m except in active areas at the start of the plot, where CIS moments may be difficult.

This interval demonstrates good agreement between most instruments, to the extent that the noise levels in the moments from the particle instruments allow comparison. The only odd feature is the strange EDI magnetosheath data.

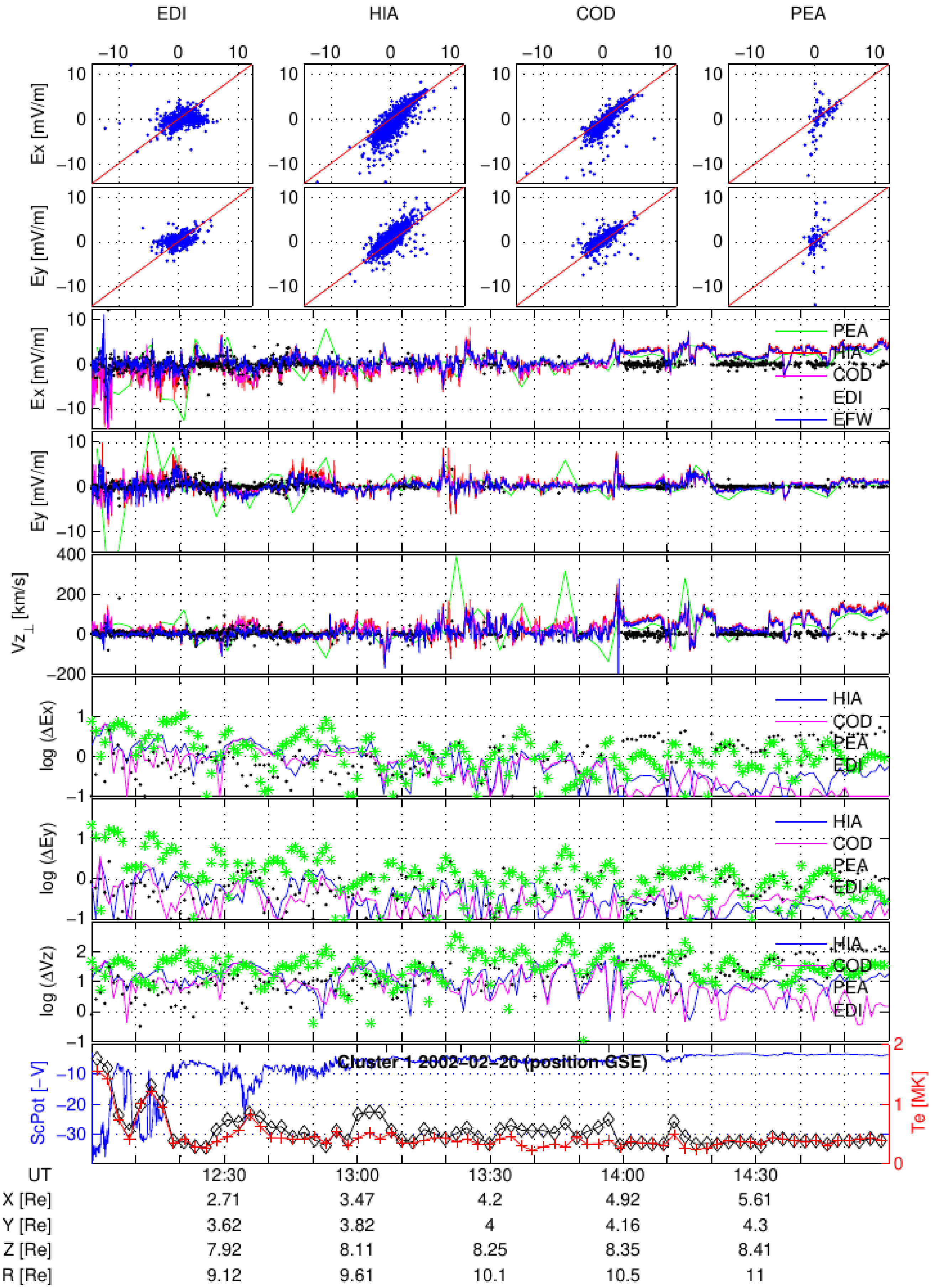
EDI
HIA
COD
PEA
Ex [mV/m]
Ey [mV/m]
PEA
HIA
COD
EDI
EFW
Vz⊥ [km/s]
log (ΔEx)
log (ΔEy)
log (ΔVz)
HIA
COD
PEA
EDI
Cluster 1 2002-02-20 (position GSE)
ScPot [−V]
Te [MK]
UT
12:30
13:00
13:30
14:00
14:30
X [Re] 2.71 3.47 4.2 4.92 5.61
Y [Re] 3.62 3.82 4 4.16 4.3
Z [Re] 7.92 8.11 8.25 8.35 8.41
R [Re] 9.12 9.61 10.1 10.5 11

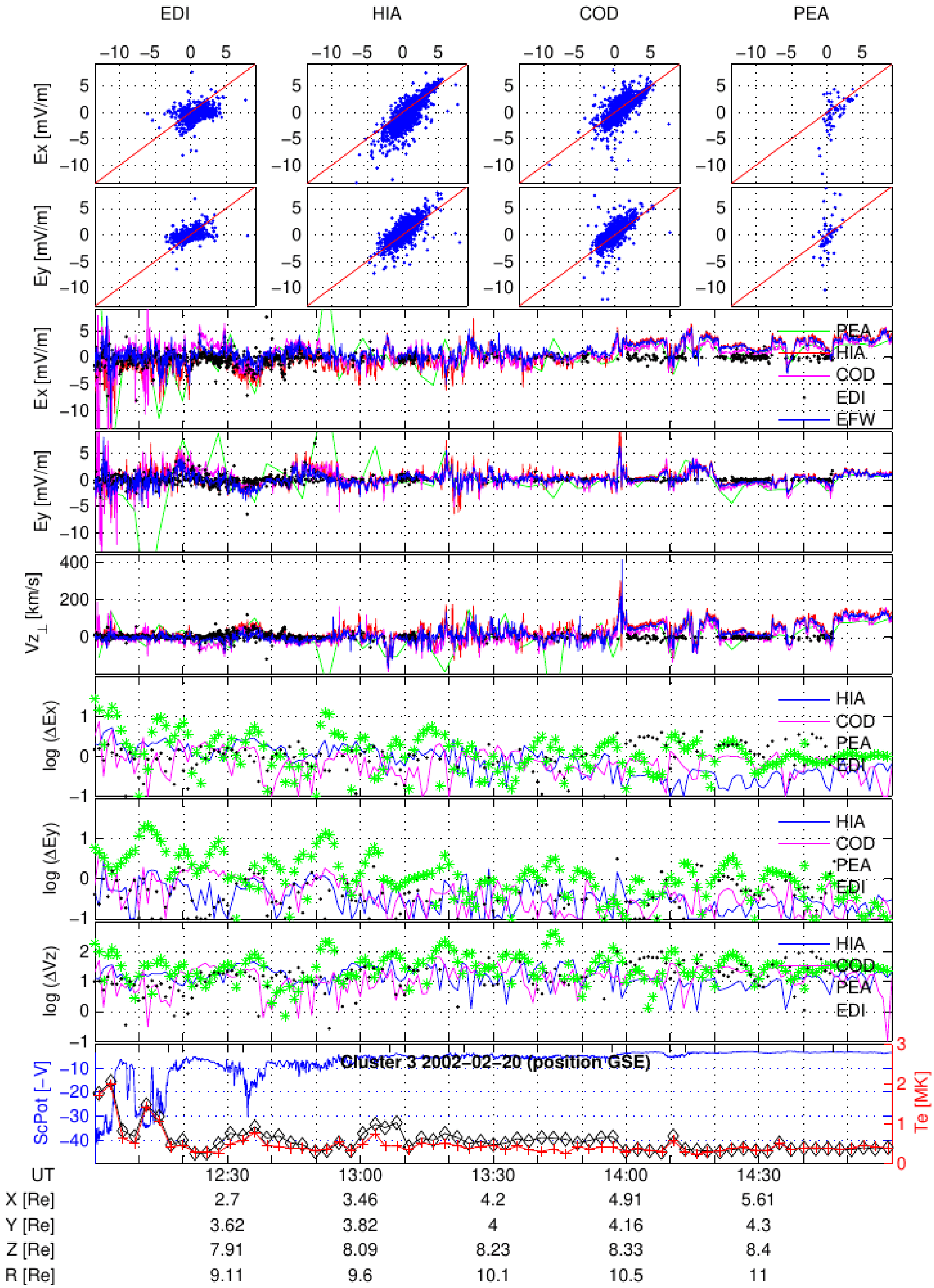

EDI
HIA
COD
PEA
Ex [mV/m]
Ey [mV/m]
PEA
HIA
COD
EDI
EFW
Vz⊥ [km/s]
log (ΔEx)
log (ΔEy)
log (ΔVz)
Cluster 3 2002−02−20 (position GSE)
ScPot [−V]
Te [MK]
UT
12:30
13:00
13:30
14:00
14:30
X [Re]
2.7
3.46
4.2
4.91
5.61
Y [Re]
3.62
3.82
4
4.16
4.3
Z [Re]
7.91
8.09
8.23
8.33
8.4
R [Re]
9.11
9.6
10.1
10.5
11

## Event 3: Magnetopause

2004-01-04 13:30 - 15:00 | CAA quicklook

**Standard plots:**

`040104_C1_MP.pdf`

`040104_C3_MP.pdf`

No EDI data are available, but the agreement on SC1 between EFW, HIA and CODIF is excellent, with good agreement also with PEACE. SC3 lacks PEACE data, and there is clearly something wrong with both HIA and CODIF data, so here EFW is the only instrument able to measure the electric field. It is striking how well the SC1 data agree both inside the magnetosphere, in the magnetosheath and throughout magnetopause crossings, as seen by the crossings between 13:45 and 14:12. The differences are generally much better than 1 mV/m, and often below 0.1 mV/m.

This event demonstrates nicely that EFW is in excellent agreement with HIA and CODIF across the magnetopause boundary, with different plasma on the magnetosphere and magnetosheath sides of the boundary.

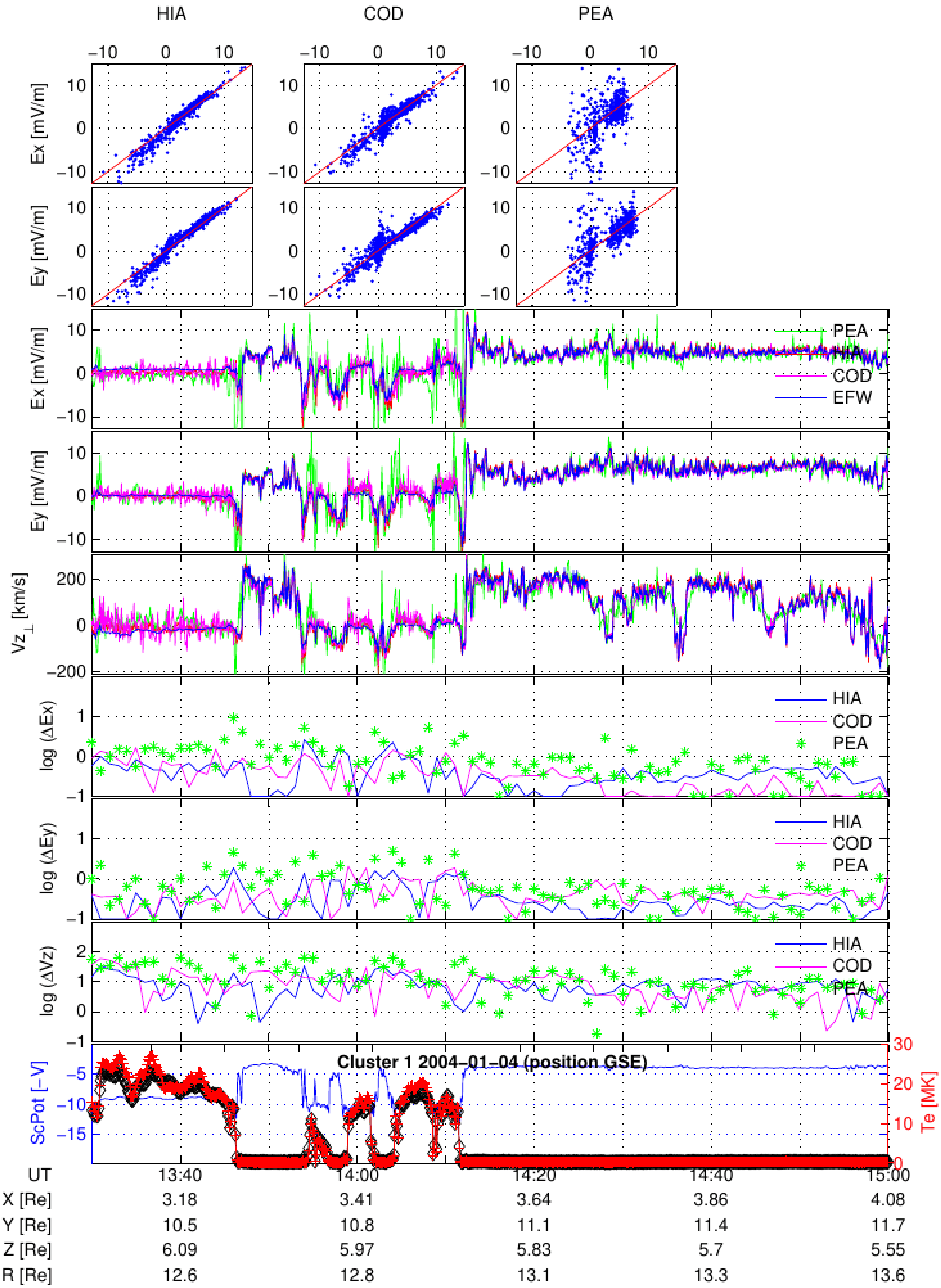
HIA
COD
PEA
Ex [mV/m]
Ey [mV/m]
PEA
HIA
COD
EFW
Vz⊥ [km/s]
log (ΔEx)
log (ΔEy)
log (ΔVz)
Cluster 1 2004–01–04 (position GSE)
ScPot [–V]
Te [MK]
UT
X [Re]
Y [Re]
Z [Re]
R [Re]
13:40
14:00
14:20
14:40
15:00
3.18
3.41
3.64
3.86
4.08
10.5
10.8
11.1
11.4
11.7
6.09
5.97
5.83
5.7
5.55
12.6
12.8
13.1
13.3
13.6

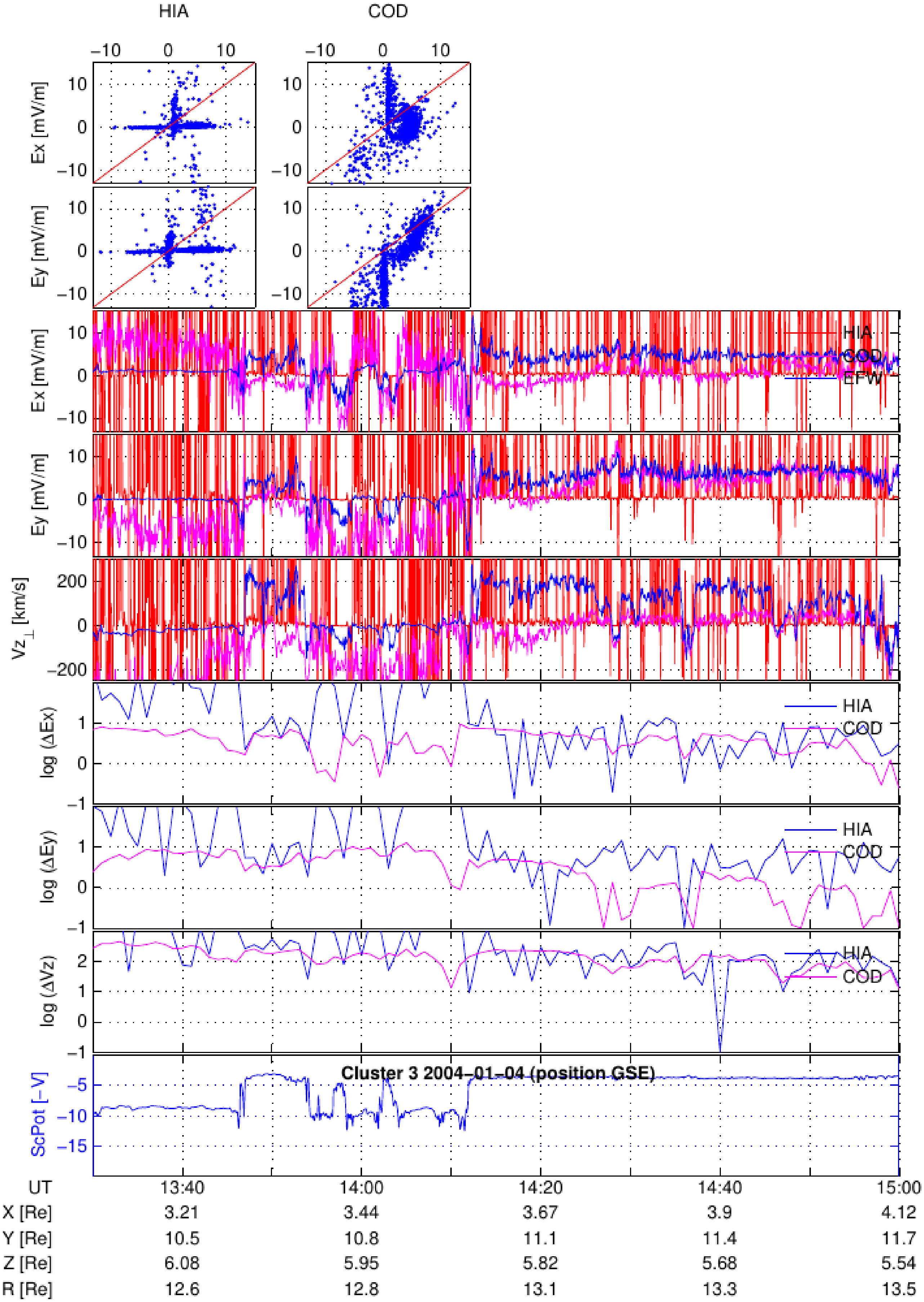
HIA
COD
Ex [mV/m]
Ey [mV/m]
HIA
COD
EFW
Vz⊥ [km/s]
log (ΔEx)
log (ΔEy)
log (ΔVz)
Cluster 3 2004–01–04 (position GSE)
ScPot [–V]
UT 13:40 14:00 14:20 14:40 15:00
X [Re] 3.21 3.44 3.67 3.9 4.12
Y [Re] 10.5 10.8 11.1 11.4 11.7
Z [Re] 6.08 5.95 5.82 5.68 5.54
R [Re] 12.6 12.8 13.1 13.3 13.5

## Event 4: High latitude cusp/Magnetopause

2002-03-04 07:00 - 11:00 | CAA quicklook

**Standard plots:**

`020304_C1_Cusp.pdf`

`020304_C3_Cusp.pdf`

For the second half of the plotted interval, where the density is higher, there is good agreement between all instruments. PEACE shows the highest noise level, followed by CODIF. Also EDI shows quite a number of noise and outlier points, making a detailed comparison between EDI and EFW not meaningful. HIA and EFW generally agrees well, and so do EDI and EFW when EDI data is not so much contaminated by outliers.

For greater clarity, these show EFW and HIA data only, as HIA is the least noisy of the other instruments in this case. The agreement between EFW and HIA is excellent, to the extent that the HIA noise allows a comparison, with EFW staying within the HIA envelope except at some instances of very rapid variation. The average difference EFW-HIA stays below 1 mV/m except where variations are strong, in which circumstances HIA moments naturally becomes more problematic. One may note gaps in the EFW data in some parts of the lowest density region around 08:00. These are intervals removed by the wake detection algorithm.

This event demostrates good agreement between HIA and EFW, to the extent allowed by the higher HIA noise level. This noise decreases in the denser plasmas at the second half of the interval, where agreement still is good.

**Fine plots:**

`020304_C1_Cusp_fine.pdf`

`020304_C3_Cusp_fine.pdf`

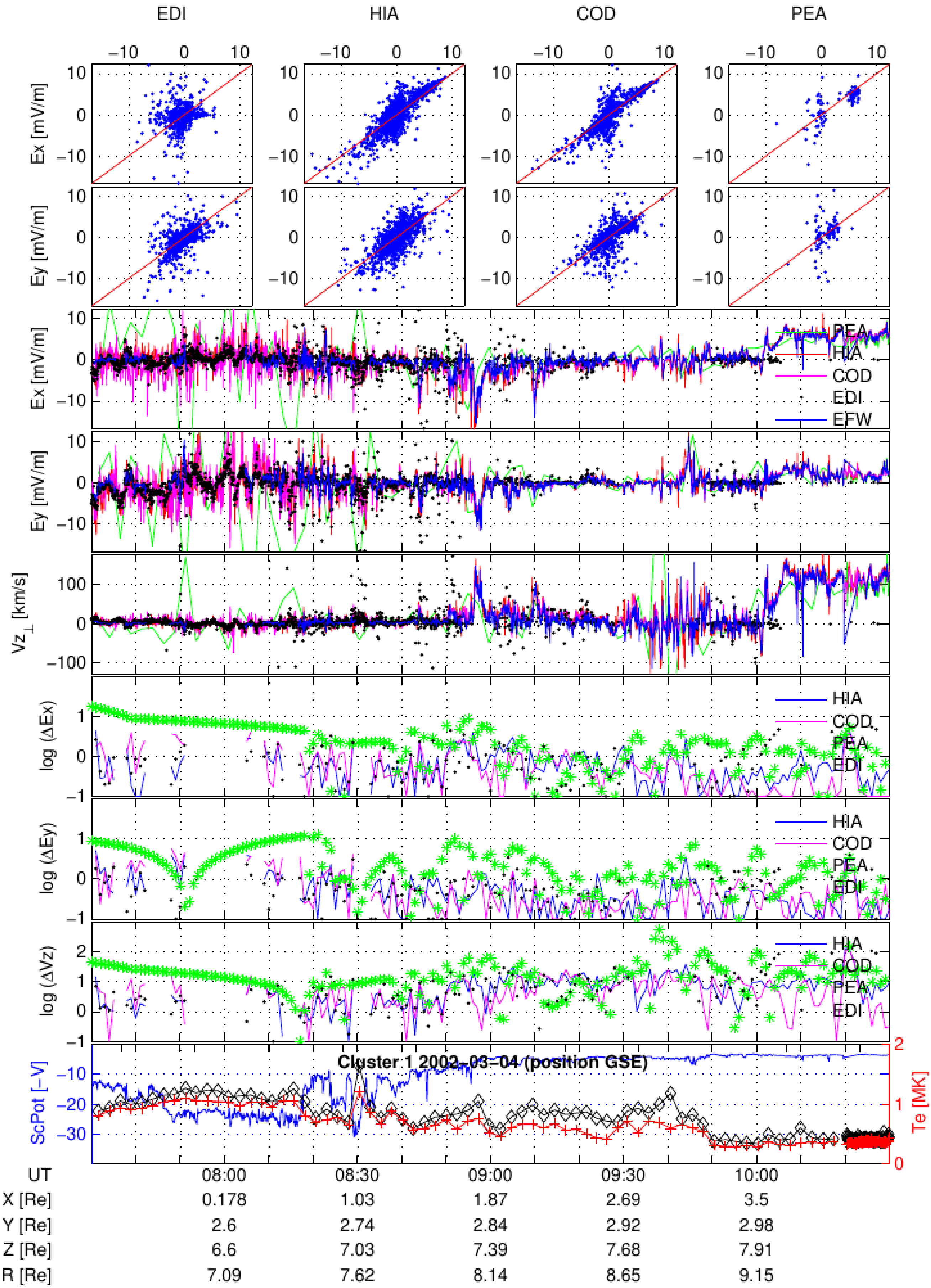
EDI
HIA
COD
PEA
Ex [mV/m]
Ey [mV/m]
Vz⊥ [km/s]
log (ΔEx)
log (ΔEy)
log (ΔVz)
PEA
HIA
COD
EDI
EFW
Cluster 1 2002–03–04 (position GSE)
ScPot [–V]
Te [MK]
UT 08:00 08:30 09:00 09:30 10:00
X [Re] 0.178 1.03 1.87 2.69 3.5
Y [Re] 2.6 2.74 2.84 2.92 2.98
Z [Re] 6.6 7.03 7.39 7.68 7.91
R [Re] 7.09 7.62 8.14 8.65 9.15

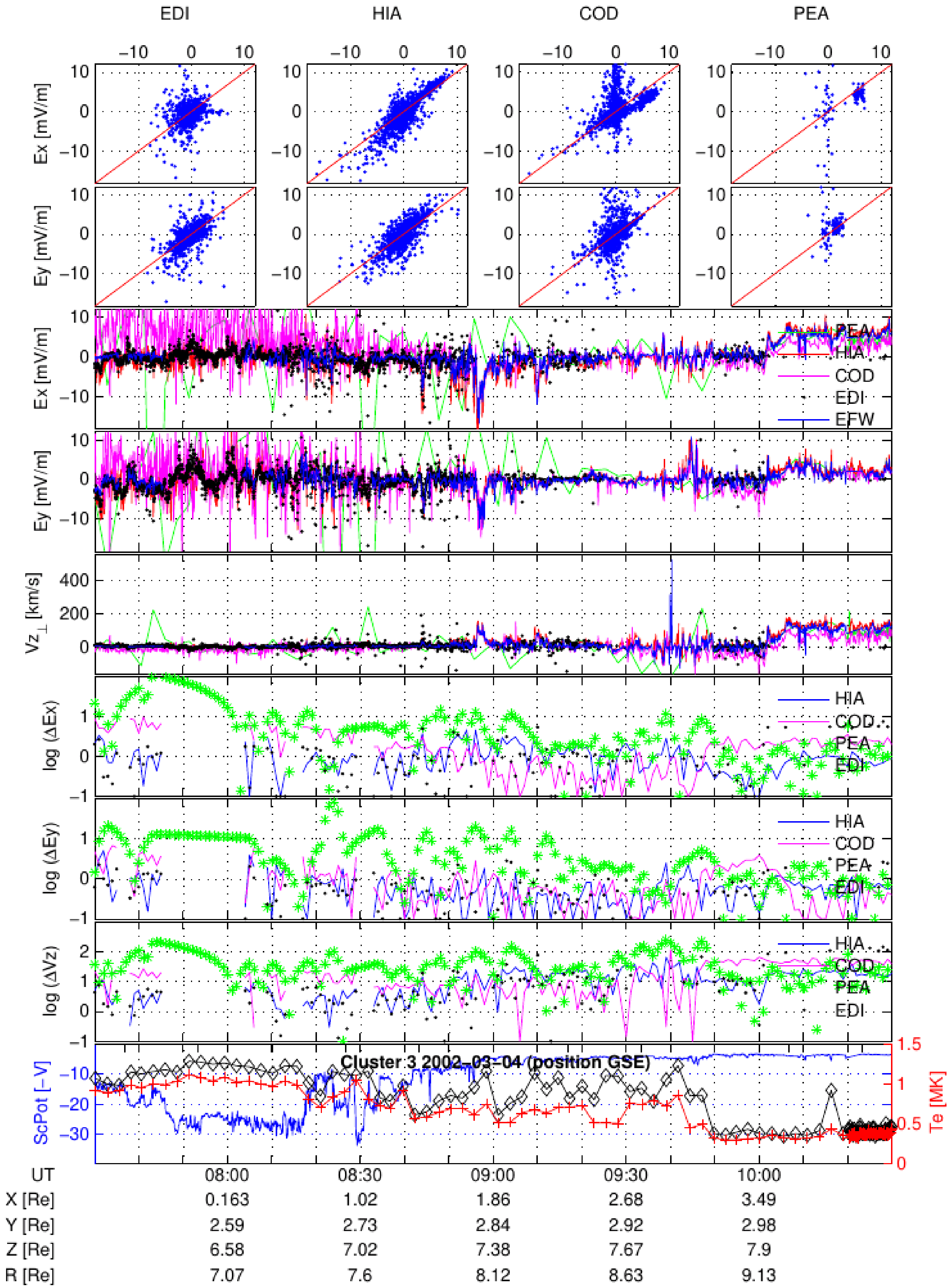
EDI
HIA
COD
PEA
Ex [mV/m]
Ey [mV/m]
PEA
HIA
COD
EDI
EFW
Vz⊥ [km/s]
log (ΔEx)
log (ΔEy)
log (ΔVz)
Cluster 3 2002–03–04 (position GSE)
ScPot [–V]
Te [MK]
UT
08:00
08:30
09:00
09:30
10:00
X [Re]
0.163
1.02
1.86
2.68
3.49
Y [Re]
2.59
2.73
2.84
2.92
2.98
Z [Re]
6.58
7.02
7.38
7.67
7.9
R [Re]
7.07
7.6
8.12
8.63
9.13

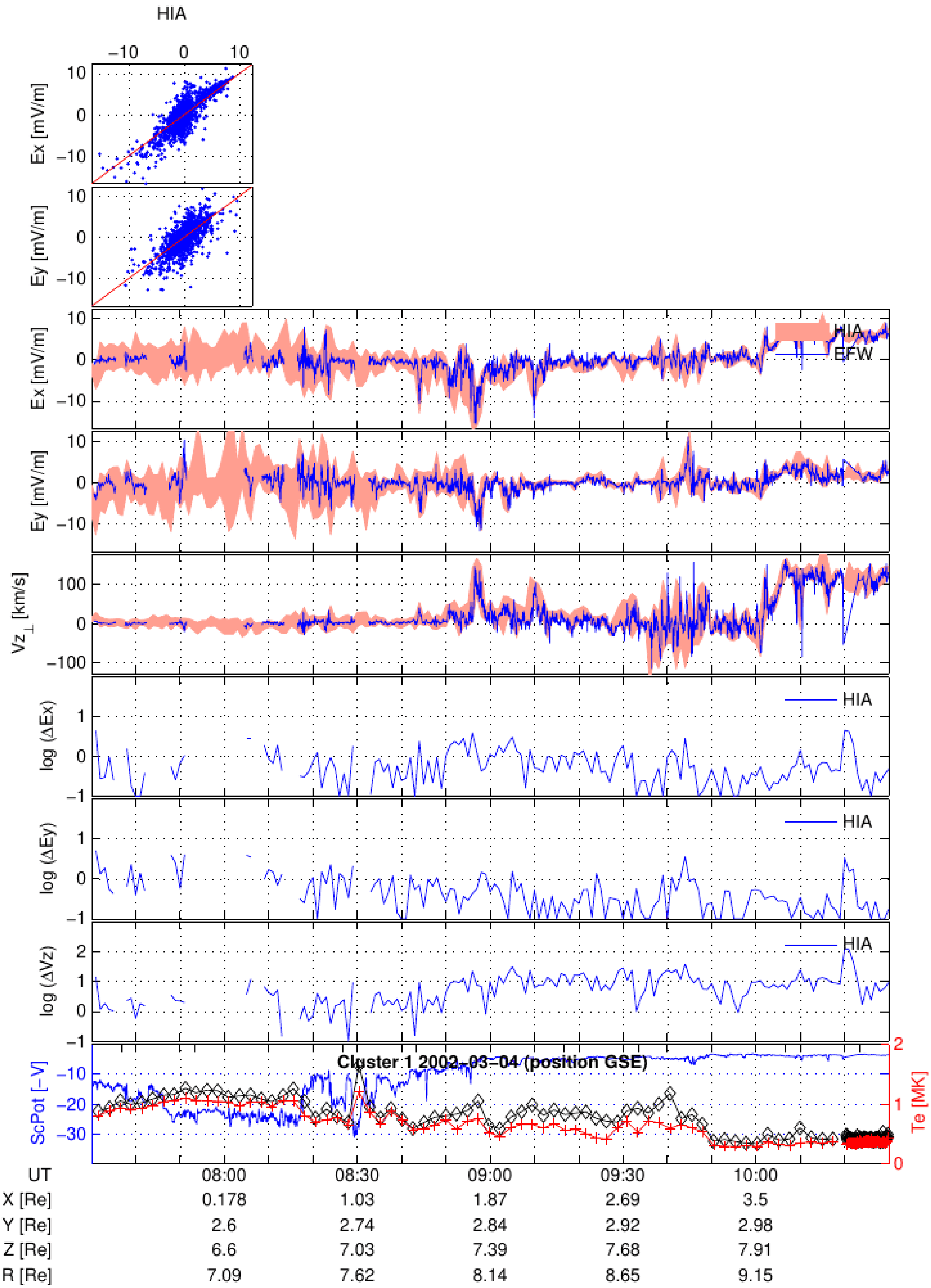
HIA
−10
0
10
Ex [mV/m]
Ey [mV/m]
HIA
EFW
Vz⊥ [km/s]
100
0
−100
log (ΔEx)
log (ΔEy)
log (ΔVz)
Cluster 1 2002−03−04 (position GSE)
ScPot [−V]
Te [MK]
UT
08:00
08:30
09:00
09:30
10:00
X [Re]
0.178
1.03
1.87
2.69
3.5
Y [Re]
2.6
2.74
2.84
2.92
2.98
Z [Re]
6.6
7.03
7.39
7.68
7.91
R [Re]
7.09
7.62
8.14
8.65
9.15

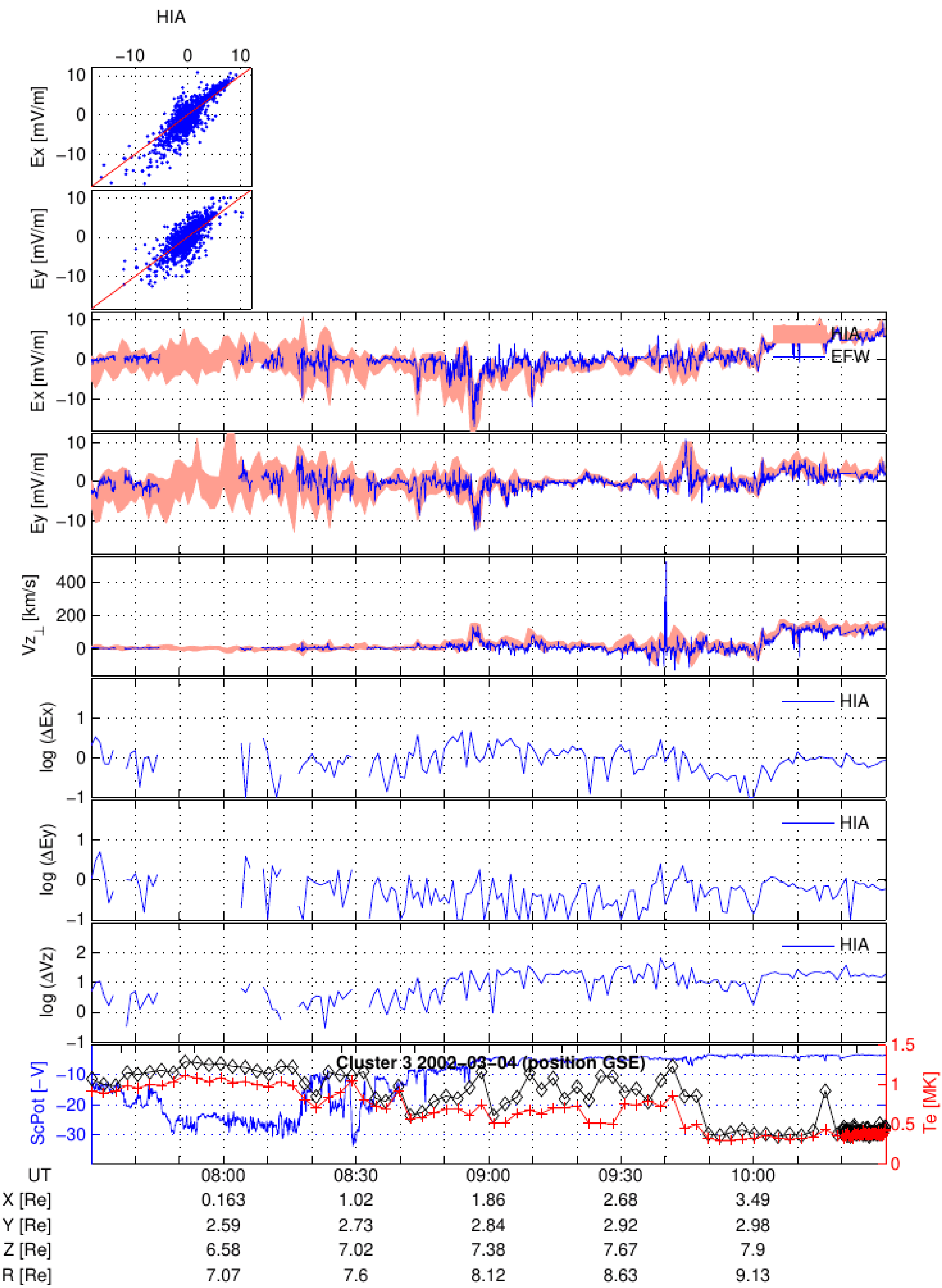
HIA
−10
0
10
Ex [mV/m]
Ey [mV/m]
HIA
EFW
Vz⊥ [km/s]
400
200
log (ΔEx)
log (ΔEy)
log (ΔVz)
Cluster 3 2002-03-04 (position GSE)
ScPot [−V]
Te [MK]
1.5
1
0.5
UT
08:00
08:30
09:00
09:30
10:00
X [Re]
0.163
1.02
1.86
2.68
3.49
Y [Re]
2.59
2.73
2.84
2.92
2.98
Z [Re]
6.58
7.02
7.38
7.67
7.9
R [Re]
7.07
7.6
8.12
8.63
9.13

## Event 5: Magnetopause

2005-02-22 11:00 - 14:00 | CAA quicklook

**Standard plots:**

050222_C1_MP.pdf

050222_C3_MP.pdf

This event shows data from high-latitude magnetopause crossings between 12:00 and 13:00 on SC1 and around 13:00 on SC3. Only HIA and PEACE data are available. The PEACE data are useful only in the magnetosheath and have large scatter in the magnetosphere. The comparison between EFW and HIA is highlighted in the fine plots, where the envelope of the HIA variations are shown as a shaded band. EFW for the most part lies well within the HIA variations, and the averaged difference between EFW and HIA is generally between 0.1 and 1 mV/m. Note in particular the very good EFW-HIA agreement on SC3, where the Ey difference is below about 0.1 mV/m for the entire magnetosheath period. The slight disagreement in Ex between EFW and HIA on SC1 at 12:10 - 12:20 is not unexpected, since a perfect agreement between field and particle measurements is not to be expected at the actual magnetopause crossing.

This event demonstrates good agreement between EFW and HIA at and around a magnetopause crossing at high latitude.

**Fine plots:**

050222_C1_MP_fine.pdf

050222_C3_MP_fine.pdf

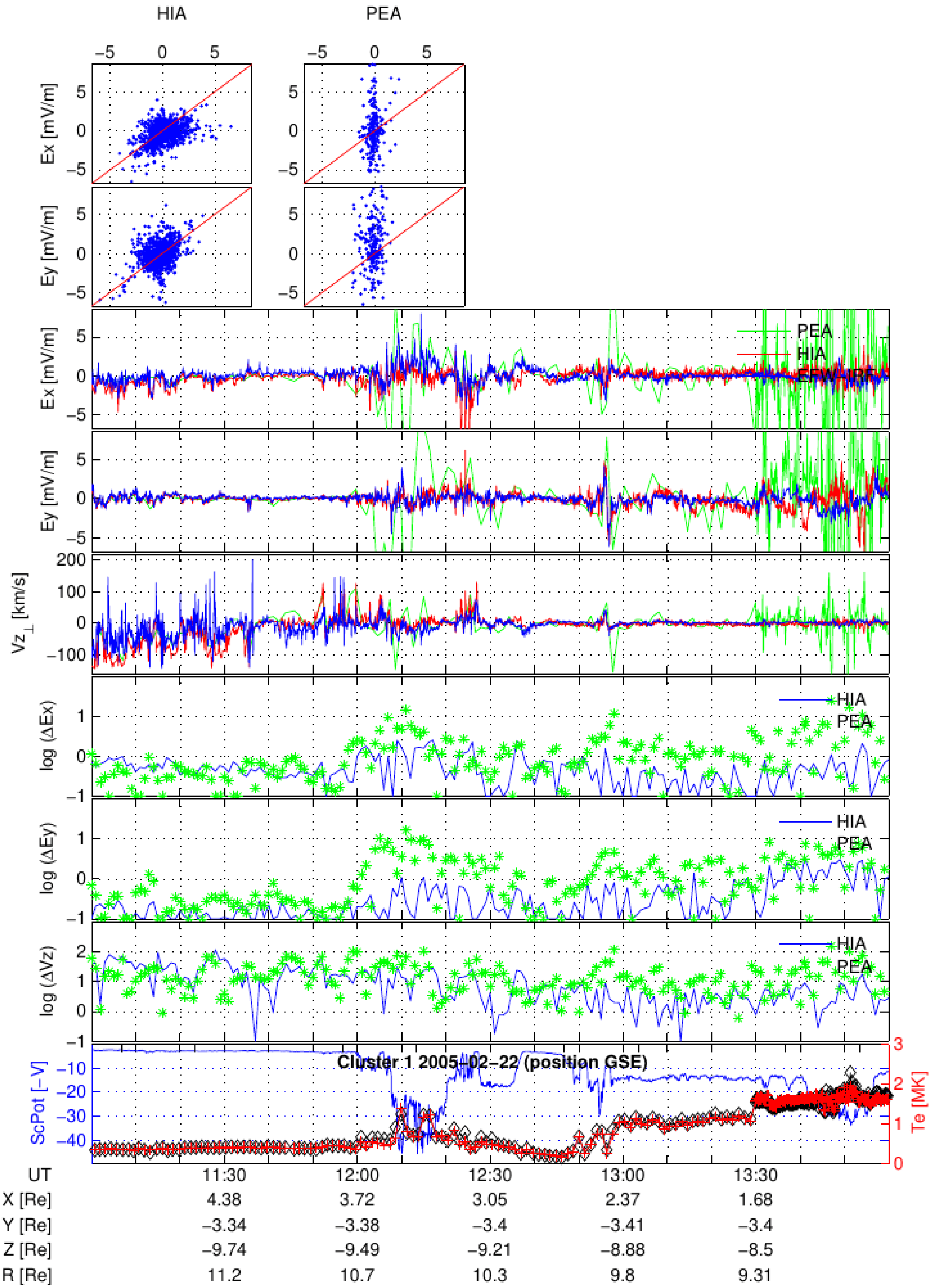
HIA
PEA
Ex [mV/m]
Ey [mV/m]
PEA
HIA
EFW-IRF
Vz⊥ [km/s]
log (ΔEx)
log (ΔEy)
log (ΔVz)
HIA
PEA
Cluster 1 2005-02-22 (position GSE)
ScPot [–V]
Te [MK]
UT 11:30 12:00 12:30 13:00 13:30
X [Re] 4.38 3.72 3.05 2.37 1.68
Y [Re] –3.34 –3.38 –3.4 –3.41 –3.4
Z [Re] –9.74 –9.49 –9.21 –8.88 –8.5
R [Re] 11.2 10.7 10.3 9.8 9.31

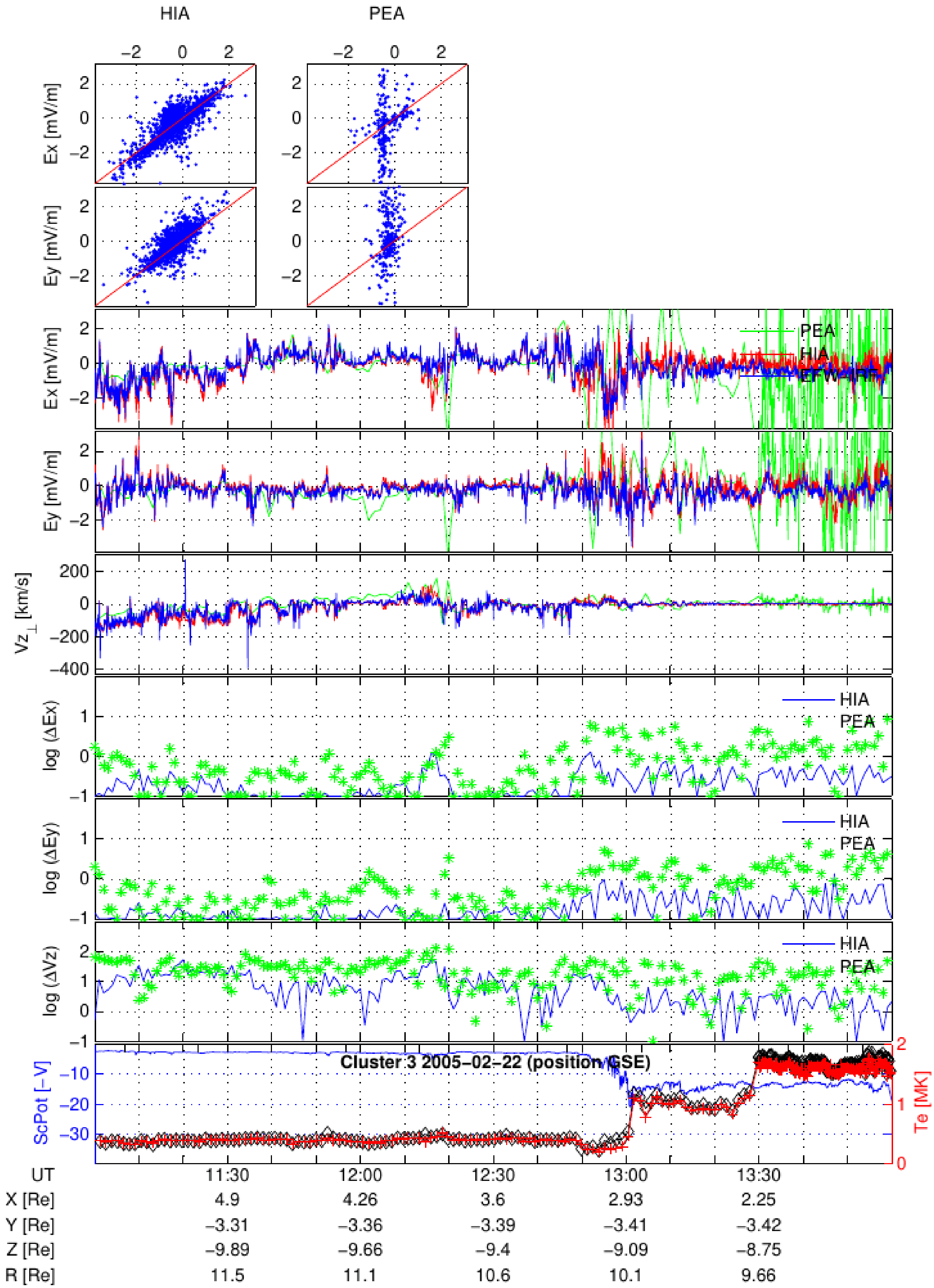
HIA
PEA
Ex [mV/m]
Ey [mV/m]
PEA
HIA
EFW-ARF
Vz⊥ [km/s]
log (ΔEx)
log (ΔEy)
log (ΔVz)
HIA
PEA
Cluster 3 2005−02−22 (position GSE)
ScPot [−V]
Te [MK]
UT 11:30 12:00 12:30 13:00 13:30
X [Re] 4.9 4.26 3.6 2.93 2.25
Y [Re] −3.31 −3.36 −3.39 −3.41 −3.42
Z [Re] −9.89 −9.66 −9.4 −9.09 −8.75
R [Re] 11.5 11.1 10.6 10.1 9.66

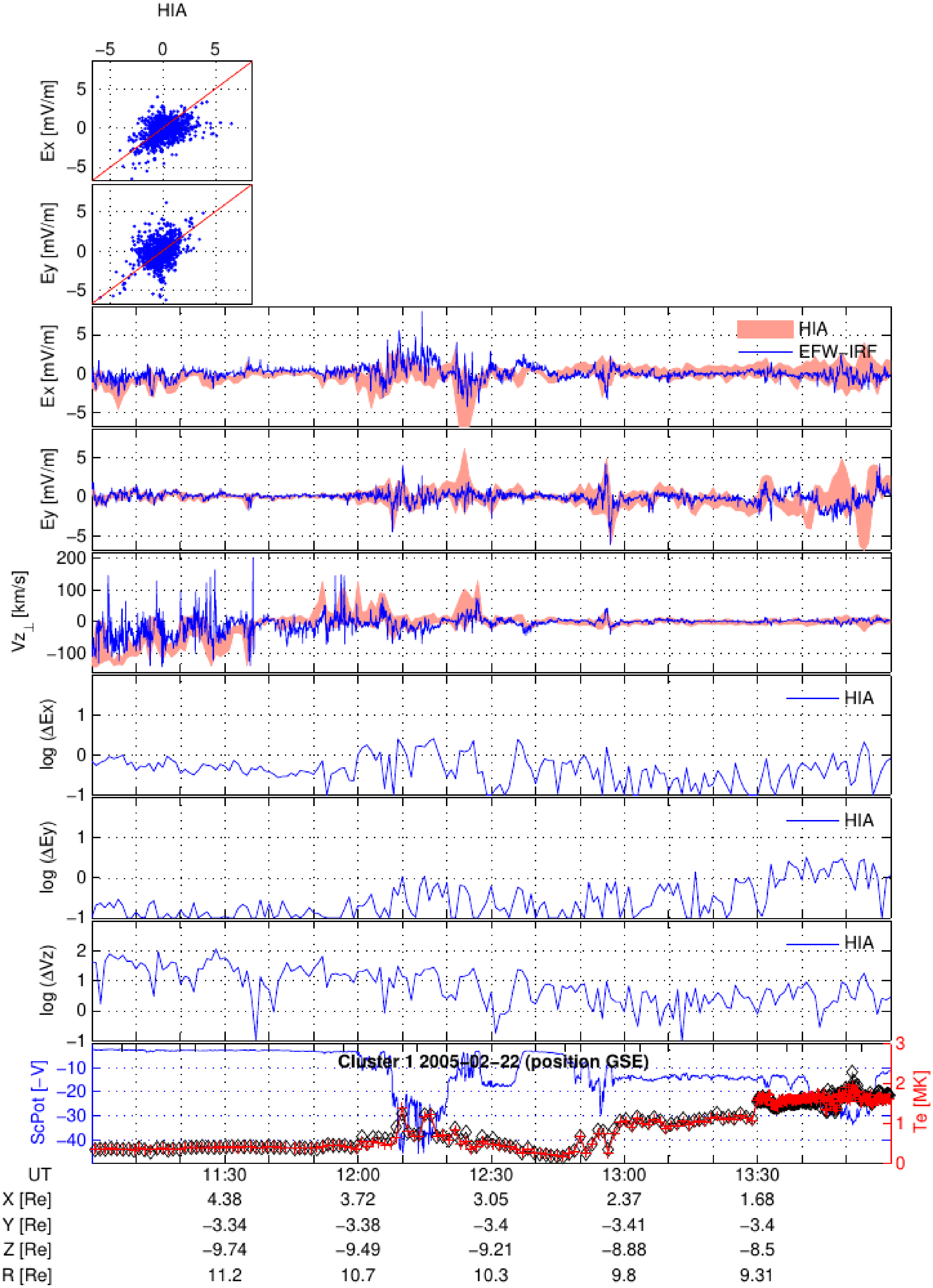
HIA
Ex [mV/m]
Ey [mV/m]
HIA
EFW-IRF
Vz⊥ [km/s]
log (ΔEx)
log (ΔEy)
log (ΔVz)
ScPot [–V]
Te [MK]
Cluster 1 2005–02–22 (position GSE)
UT
X [Re]
Y [Re]
Z [Re]
R [Re]
11:30
12:00
12:30
13:00
13:30
4.38
3.72
3.05
2.37
1.68
–3.34
–3.38
–3.4
–3.41
–3.4
–9.74
–9.49
–9.21
–8.88
–8.5
11.2
10.7
10.3
9.8
9.31

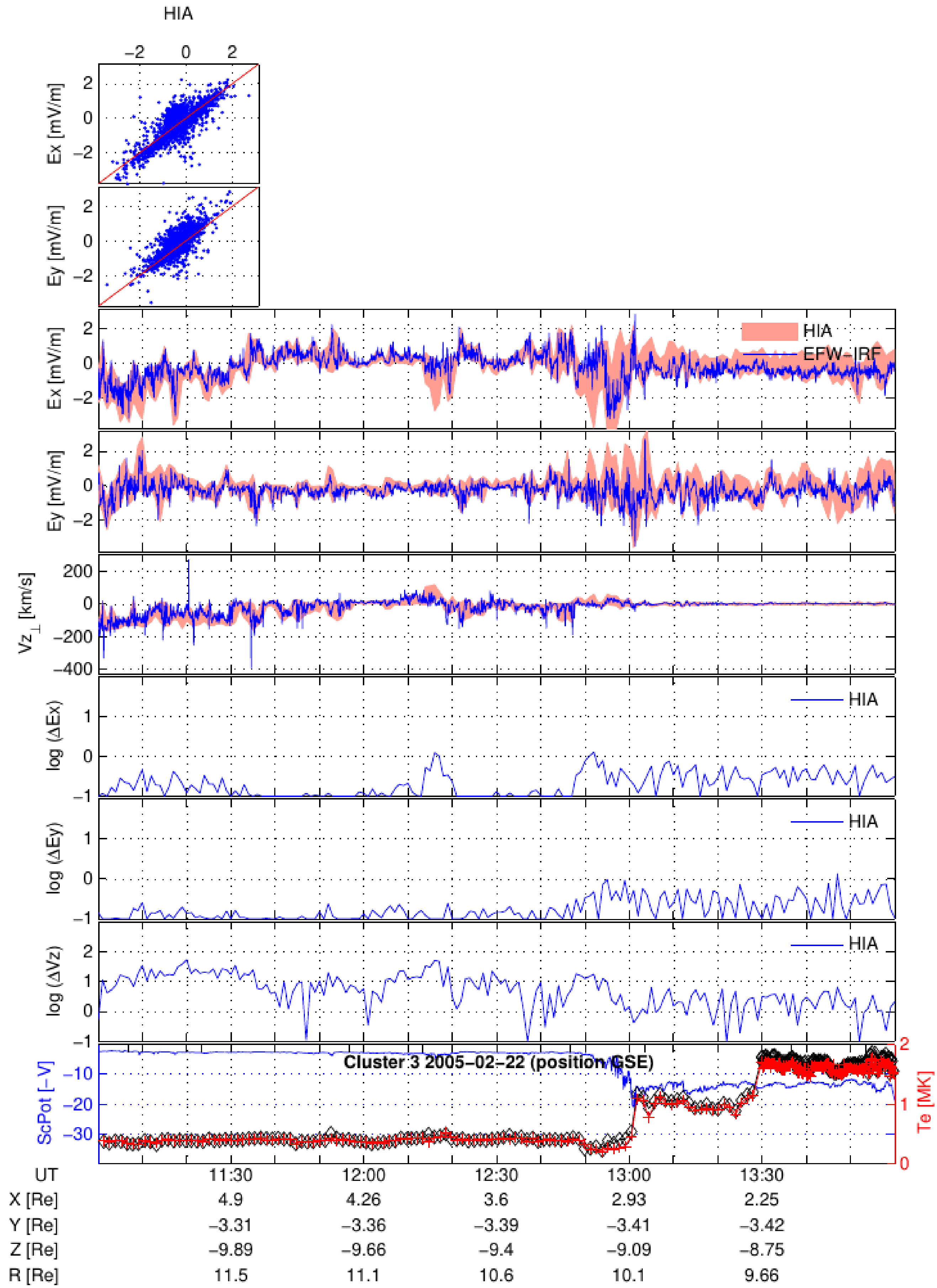
HIA
−2
0
2
Ex [mV/m]
Ey [mV/m]
HIA
EFW−IRF
Vz⊥ [km/s]
200
0
−200
−400
log (ΔEx)
log (ΔEy)
log (ΔVz)
ScPot [−V]
−10
−20
−30
Te [MK]
Cluster 3 2005−02−22 (position GSE)
UT
11:30
12:00
12:30
13:00
13:30
X [Re]
4.9
4.26
3.6
2.93
2.25
Y [Re]
−3.31
−3.36
−3.39
−3.41
−3.42
Z [Re]
−9.89
−9.66
−9.4
−9.09
−8.75
R [Re]
11.5
11.1
10.6
10.1
9.66

## Outer magnetosphere

## Event 6: Flank magnetosphere

2003-10-25 21:00 - 24:00 | CAA quicklook

**Standard plots:**

`031025_C1_Flank.pdf`

`031025_C3_Flank.pdf`

These show generally good agreement between EFW and HIA. CODIF on SC3 shows very high offsets and is not meaningful to compare to. PEACE is not particularly useful either, with high noise levels. CODIF on SC1 is still noisy, but here the average difference EFW-CODIF is not much higher than EFW-HIA, showing that while CODIF SC1 spin resolution data are noisy, the average moment is reasonable.

In the fine plots, we have removed the less useful PEACE data, showing EFW data with CODIF and HIA envelopes. On SC3, the CODIF envelope does not enclose the EFW and HIA data, illustrating the problem with CODIF moments on this s/c. On SC1, the CODIF envelope is much larger than the HIA envelope, showing its higher noise level, but the CODIF envelope encloses HIA and EFW, indicating a meaningful average. It is clear that the EFW data lies within the smaller envelope of the HIA data, showing a general agreement that is not meaningful to compare at detailed time resolution because of higher HIA noise levels. The EFW data reach outside the HIA envelope only in intervals of rapid variations, which HIA cannot properly follow.

The average difference between EFW and HIA is below 1 mV/m over all the interval, mostly a few tenths of mV/m.

This event thus demonstrates good agreement between HIA and EFW, to the extent allowed by higher HIA noise levels. CODIF and PEACE are so noisy as to not be useful for comparison. The high noise levels in the moments from the particle instruments are not surprising in this very low-density environment.

**Fine plots:**

`031025_C1_Flank_fine.pdf`

`031025_C3_Flank_fine.pdf`

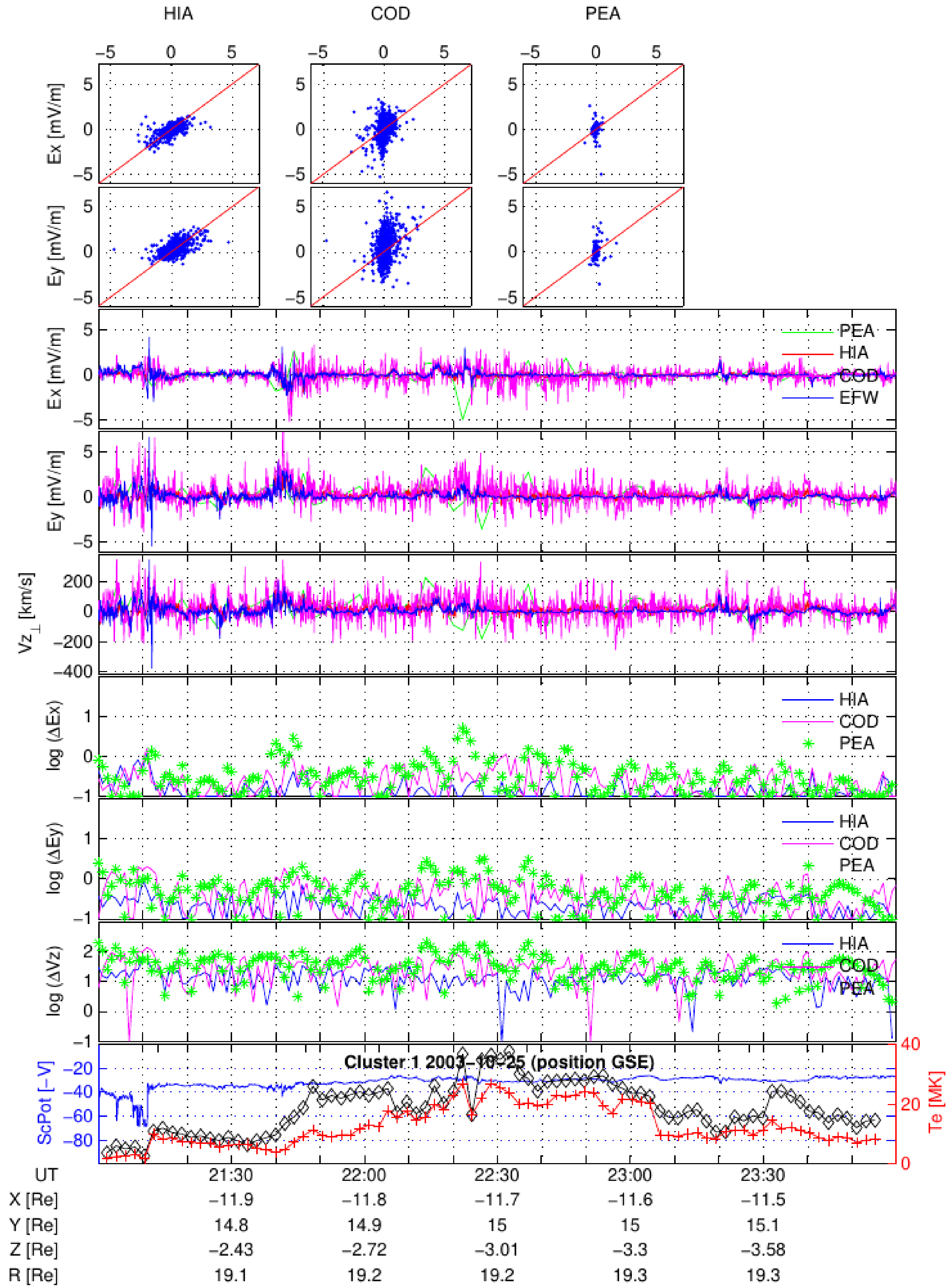
HIA
COD
PEA
Ex [mV/m]
Ey [mV/m]
PEA
HIA
COD
EFW
Ex [mV/m]
Ey [mV/m]
Vz⊥ [km/s]
log (ΔEx)
log (ΔEy)
log (ΔVz)
Cluster 1 2003-10-25 (position GSE)
ScPot [−V]
Te [MK]
UT 21:30 22:00 22:30 23:00 23:30
X [Re] −11.9 −11.8 −11.7 −11.6 −11.5
Y [Re] 14.8 14.9 15 15 15.1
Z [Re] −2.43 −2.72 −3.01 −3.3 −3.58
R [Re] 19.1 19.2 19.2 19.3 19.3

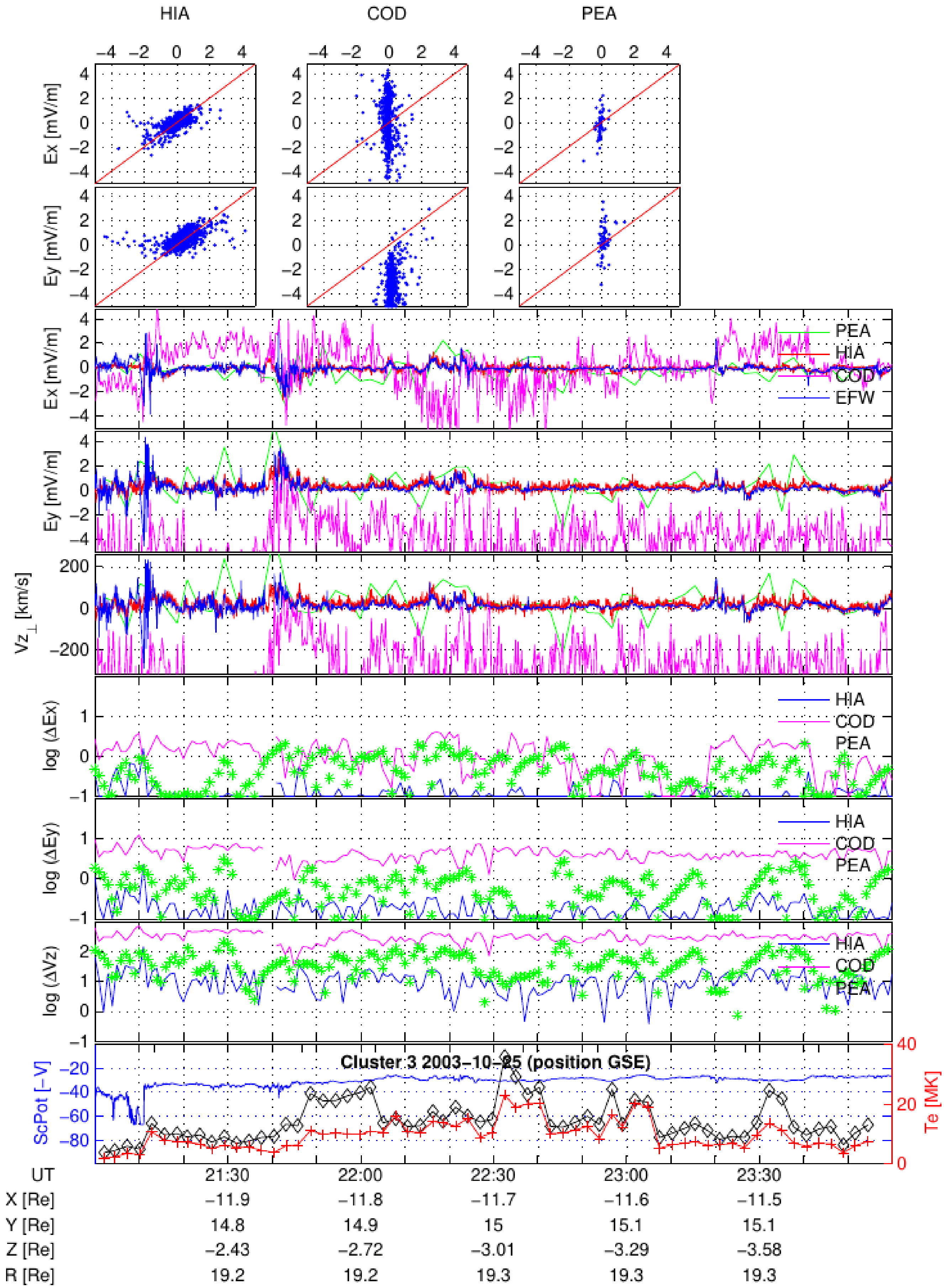
HIA
COD
PEA
Ex [mV/m]
Ey [mV/m]
PEA
HIA
COD
EFW
Vz⊥ [km/s]
log (ΔEx)
log (ΔEy)
log (ΔVz)
Cluster 3 2003–10–25 (position GSE)
ScPot [–V]
Te [MK]
UT
21:30
22:00
22:30
23:00
23:30
X [Re]
–11.9
–11.8
–11.7
–11.6
–11.5
Y [Re]
14.8
14.9
15
15.1
15.1
Z [Re]
–2.43
–2.72
–3.01
–3.29
–3.58
R [Re]
19.2
19.2
19.3
19.3
19.3

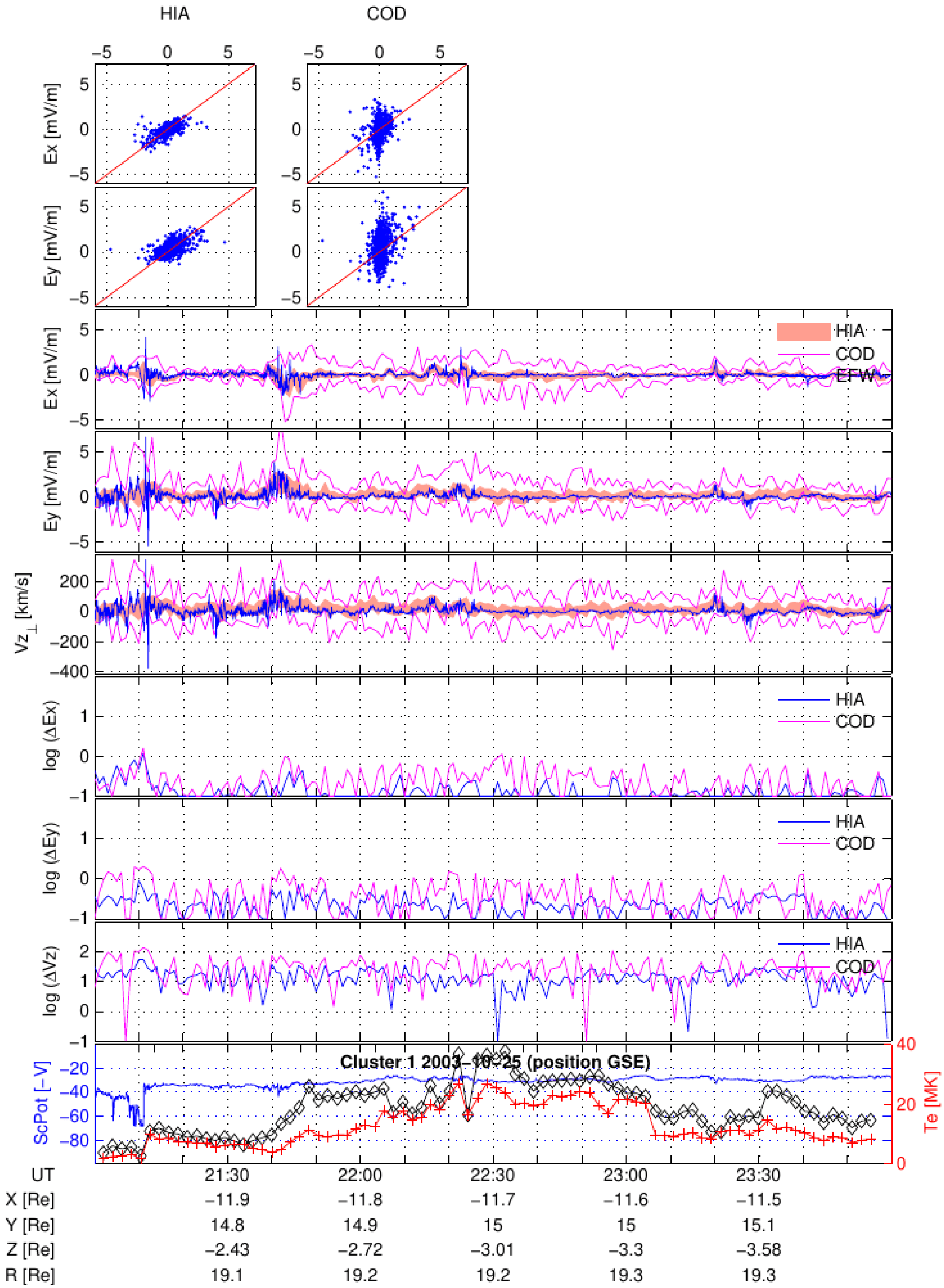
HIA
COD
Ex [mV/m]
Ey [mV/m]
HIA
COD
EFW
Vz⊥ [km/s]
log (ΔEx)
log (ΔEy)
log (ΔVz)
Cluster 1 2003-10-25 (position GSE)
ScPot [−V]
Te [MK]
UT 21:30 22:00 22:30 23:00 23:30
X [Re] −11.9 −11.8 −11.7 −11.6 −11.5
Y [Re] 14.8 14.9 15 15 15.1
Z [Re] −2.43 −2.72 −3.01 −3.3 −3.58
R [Re] 19.1 19.2 19.2 19.3 19.3

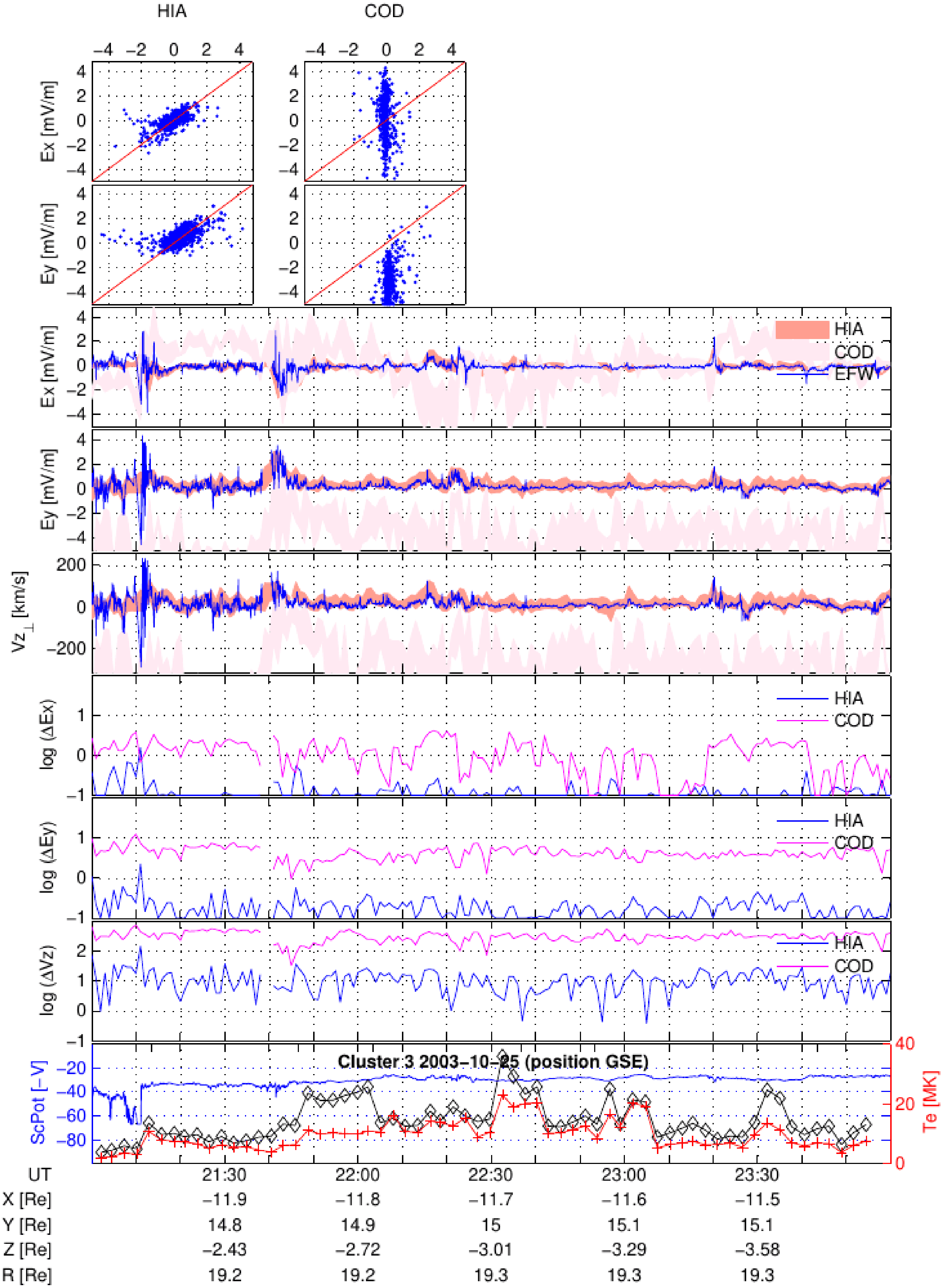

HIA
COD
Ex [mV/m]
Ey [mV/m]
Vz⊥ [km/s]
EFW
log (ΔEx)
log (ΔEy)
log (ΔVz)
Cluster 3 2003–10–25 (position GSE)
ScPot [–V]
Te [MK]
UT
21:30
22:00
22:30
23:00
23:30
X [Re]
–11.9
–11.8
–11.7
–11.6
–11.5
Y [Re]
14.8
14.9
15
15.1
15.1
Z [Re]
–2.43
–2.72
–3.01
–3.29
–3.58
R [Re]
19.2
19.2
19.3
19.3
19.3

## Event 7: Polar Cap

2005-05-17 03:00 - 06:00 | CAA quicklook

**Standard plots:**

`050517_C1_PC.pdf`

`050517_C3_PC.pdf`

For this event only HIA and PEACE data are available. The PEACE data show very large random fluctuations. The HIA data are somewhat better, in the sense that there are also large statistical fluctuations, but the average of the HIA data agree fairly well with the EFW data, to within about 1 mV/m. EFW appears to be the only instrument that can measure the electric field well in this region of cold, low-density plasma. The fine plots really only show that the HIA data have a very large scatter and in general surround the EFW data, which have a much better quality.

This event demonstrates the problems associates with particle measurements of the electric field in the low-density polar cap.

**Fine plots:**

`050517_C1_PC_fine.pdf`

`050517_C3_PC_fine.pdf`

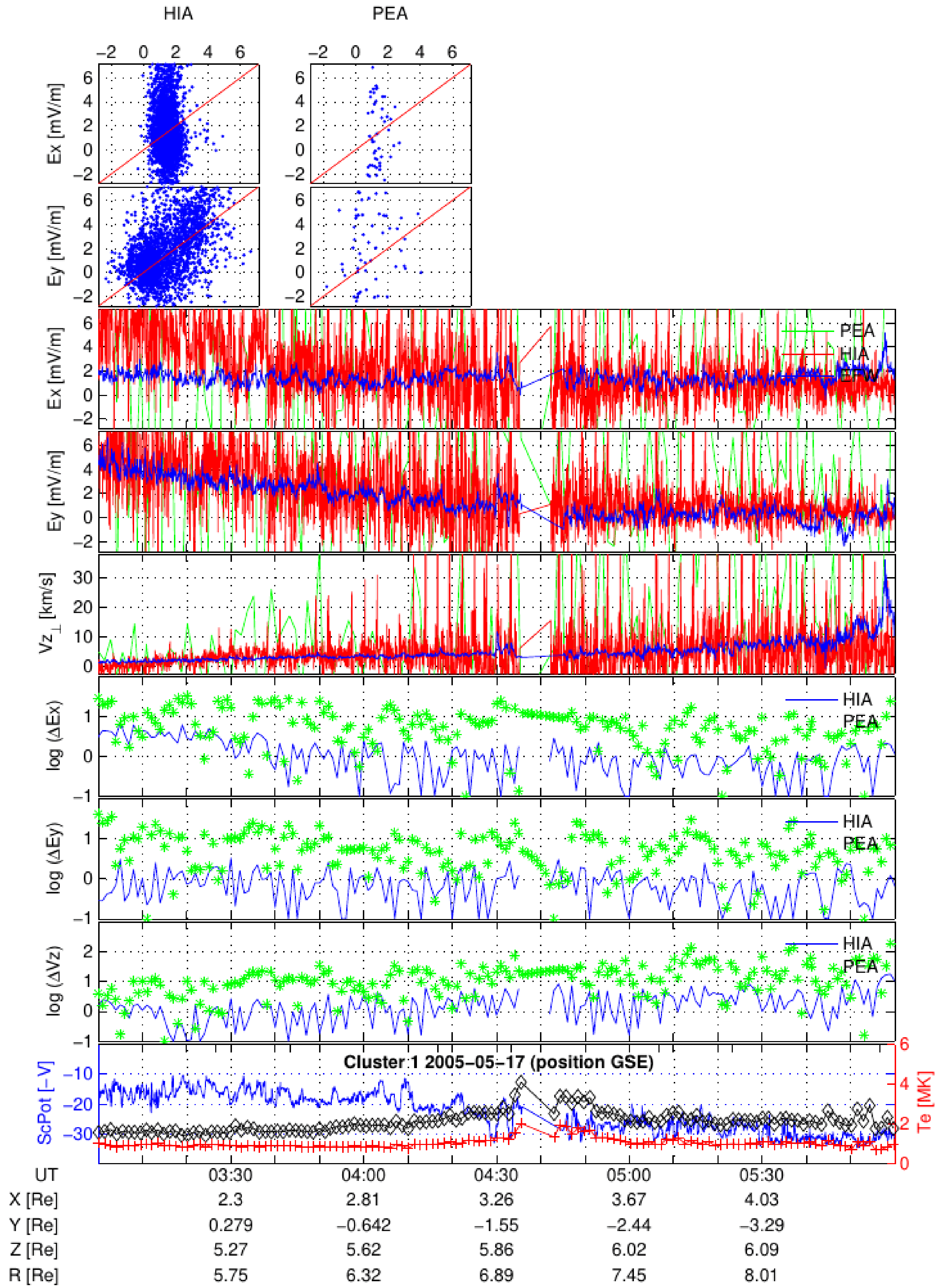
HIA
PEA
Ex [mV/m]
Ey [mV/m]
PEA
HIA
EFW
Vz⊥ [km/s]
log (ΔEx)
log (ΔEy)
log (ΔVz)
Cluster 1 2005−05−17 (position GSE)
ScPot [−V]
Te [MK]
UT 03:30 04:00 04:30 05:00 05:30
X [Re] 2.3 2.81 3.26 3.67 4.03
Y [Re] 0.279 −0.642 −1.55 −2.44 −3.29
Z [Re] 5.27 5.62 5.86 6.02 6.09
R [Re] 5.75 6.32 6.89 7.45 8.01

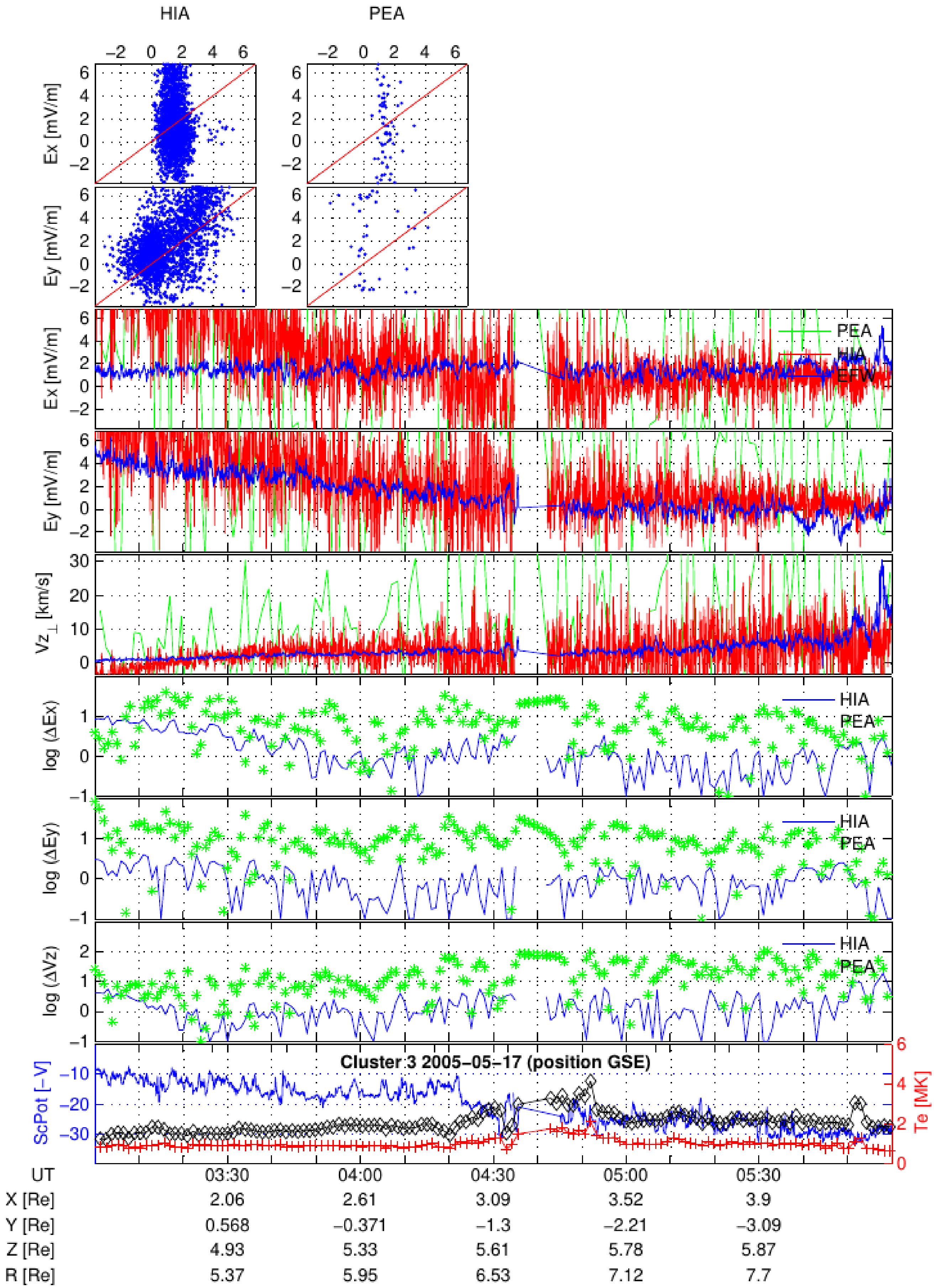
HIA
PEA
Ex [mV/m]
Ey [mV/m]
PEA
HIA
EFW
Vz⊥ [km/s]
log (ΔEx)
log (ΔEy)
log (ΔVz)
Cluster 3 2005−05−17 (position GSE)
ScPot [−V]
Te [MK]
UT
03:30
04:00
04:30
05:00
05:30
X [Re] 2.06 2.61 3.09 3.52 3.9
Y [Re] 0.568 −0.371 −1.3 −2.21 −3.09
Z [Re] 4.93 5.33 5.61 5.78 5.87
R [Re] 5.37 5.95 6.53 7.12 7.7

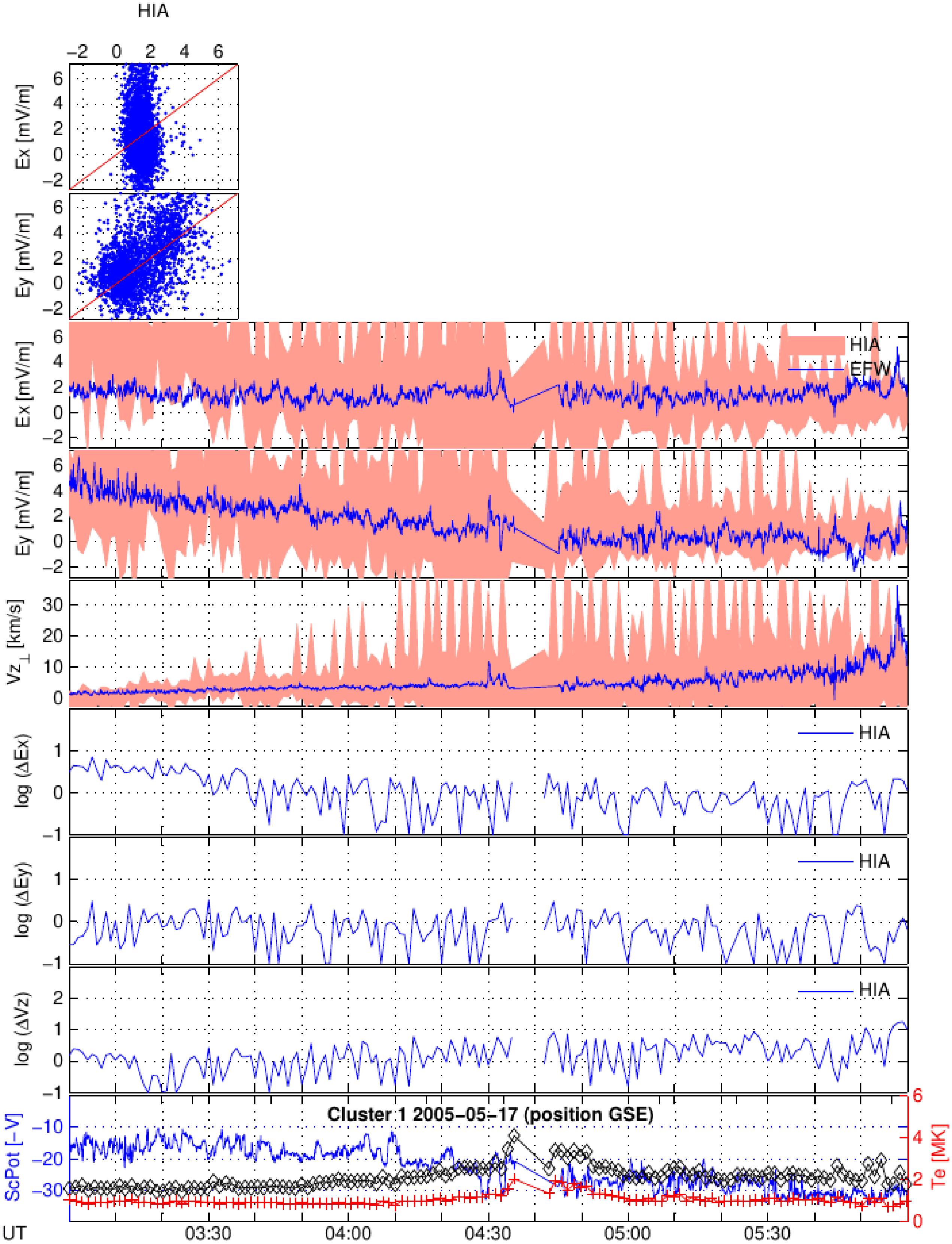


| UT | 03:30 | 04:00 | 04:30 | 05:00 | 05:30 |
|---|---|---|---|---|---|
| X [Re] | 2.3 | 2.81 | 3.26 | 3.67 | 4.03 |
| Y [Re] | 0.279 | −0.642 | −1.55 | −2.44 | −3.29 |
| Z [Re] | 5.27 | 5.62 | 5.86 | 6.02 | 6.09 |
| R [Re] | 5.75 | 6.32 | 6.89 | 7.45 | 8.01 |

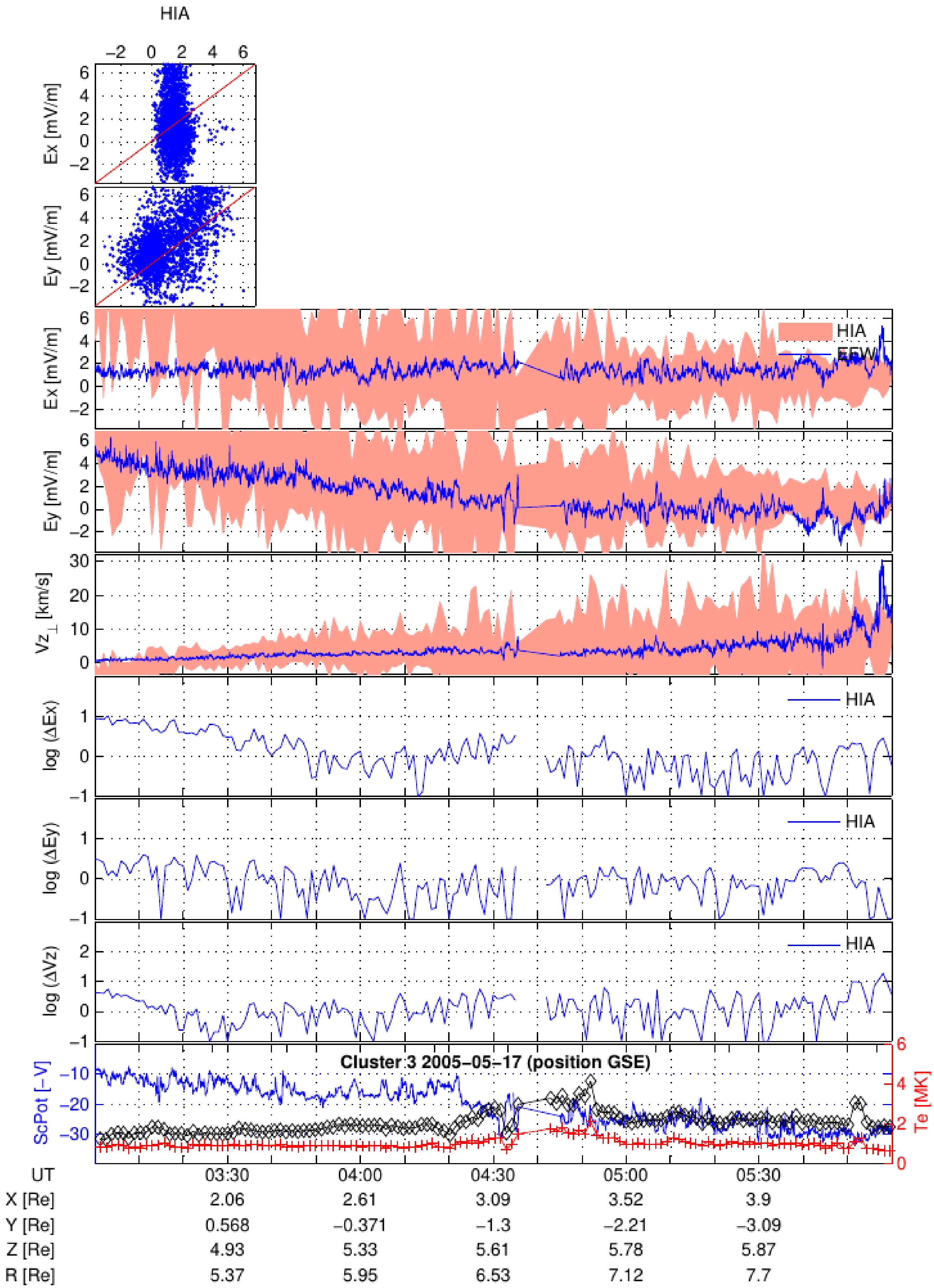
HIA
Ex [mV/m]
Ey [mV/m]
HIA
EFW
Ex [mV/m]
Ey [mV/m]
Vz⊥ [km/s]
log (ΔEx)
HIA
log (ΔEy)
HIA
log (ΔVz)
HIA
Cluster 3 2005−05−17 (position GSE)
ScPot [−V]
Te [MK]
UT
03:30
04:00
04:30
05:00
05:30
X [Re]
2.06
2.61
3.09
3.52
3.9
Y [Re]
0.568
−0.371
−1.3
−2.21
−3.09
Z [Re]
4.93
5.33
5.61
5.78
5.87
R [Re]
5.37
5.95
6.53
7.12
7.7

## Event 8: Plasma Sheet

2002-12-12 12:00 - 13:30 | CAA quicklook

**Standard plots:**

`021212_C1_CPS.pdf`

`021212_C3_CPS.pdf`

SC1 data show nice agreement between EFW and HIA and CODIF, to the limit allowed by the higher noise levels in HIA and CODIF (as usual higher in CODIF). On SC3, CODIF noise is very high, and HIA data are apparently bad, so no CIS data are useful here. PEACE moments are not useful on any of the satellites. EDI has data on SC3, showing good average agreement with EFW but a higher noise level with a lot of outliers.

The fine plot for SC1 shows EFW, HIA and CODIF only, showing a nice general agreement. Some EFW data are lacking, removed by the wake detection algorithms. Where data from all sensor exist, they agree well, and the EFW-HIA Ex difference stays below 1 mV/m except just before 12:20, though it should be noted that EFW and CODIF agrees to well within 1 mV/m here, indicating that the problem may lay with the HIA moment. One should note that Ex is not easily determined by particle instruments in the tail, as Bx usually is the dominating magnetic field component.

For SC3, the fine plot shows EDI and EFW generally agreeing, with EDI missing some rapid variations and producing a number of outliers. Despite the EDI outliers, the average EFW-EDI difference stays around 1 mV/m. The comment on Ex determination by particle instruments in the tail goes also for EDI.

This interval demonstrates good agreement between most instruments, to the extent allowed by the higher noise levels in EDI and CODIF.

**Fine plots:**

`021212_C1_CPS_fine.pdf`

`021212_C3_CPS_fine.pdf`

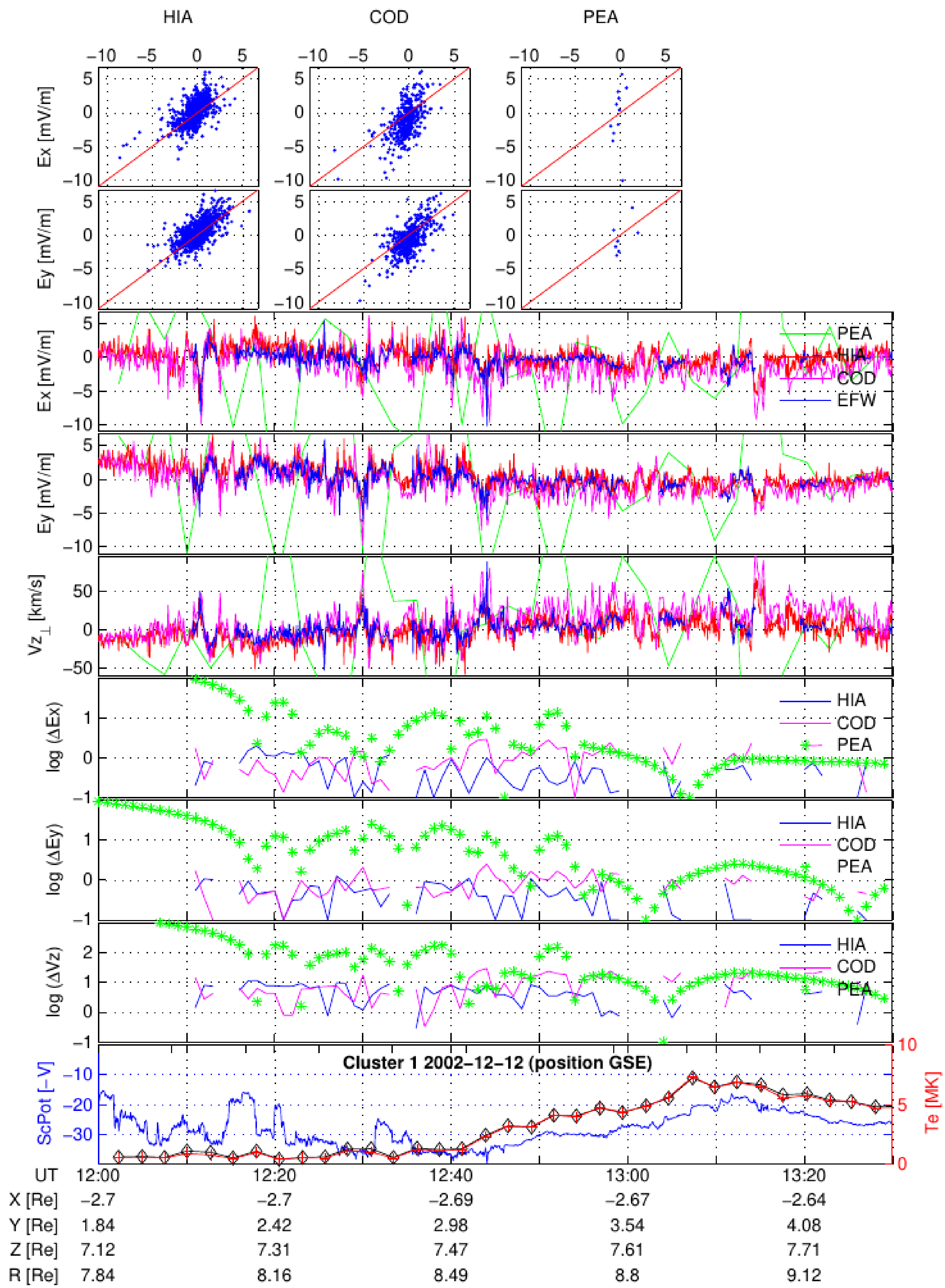
HIA
COD
PEA
Ex [mV/m]
Ey [mV/m]
PEA
HIA
COD
EFW
Vz⊥ [km/s]
log (ΔEx)
log (ΔEy)
log (ΔVz)
Cluster 1 2002−12−12 (position GSE)
ScPot [−V]
Te [MK]
UT 12:00 12:20 12:40 13:00 13:20
X [Re] −2.7 −2.7 −2.69 −2.67 −2.64
Y [Re] 1.84 2.42 2.98 3.54 4.08
Z [Re] 7.12 7.31 7.47 7.61 7.71
R [Re] 7.84 8.16 8.49 8.8 9.12

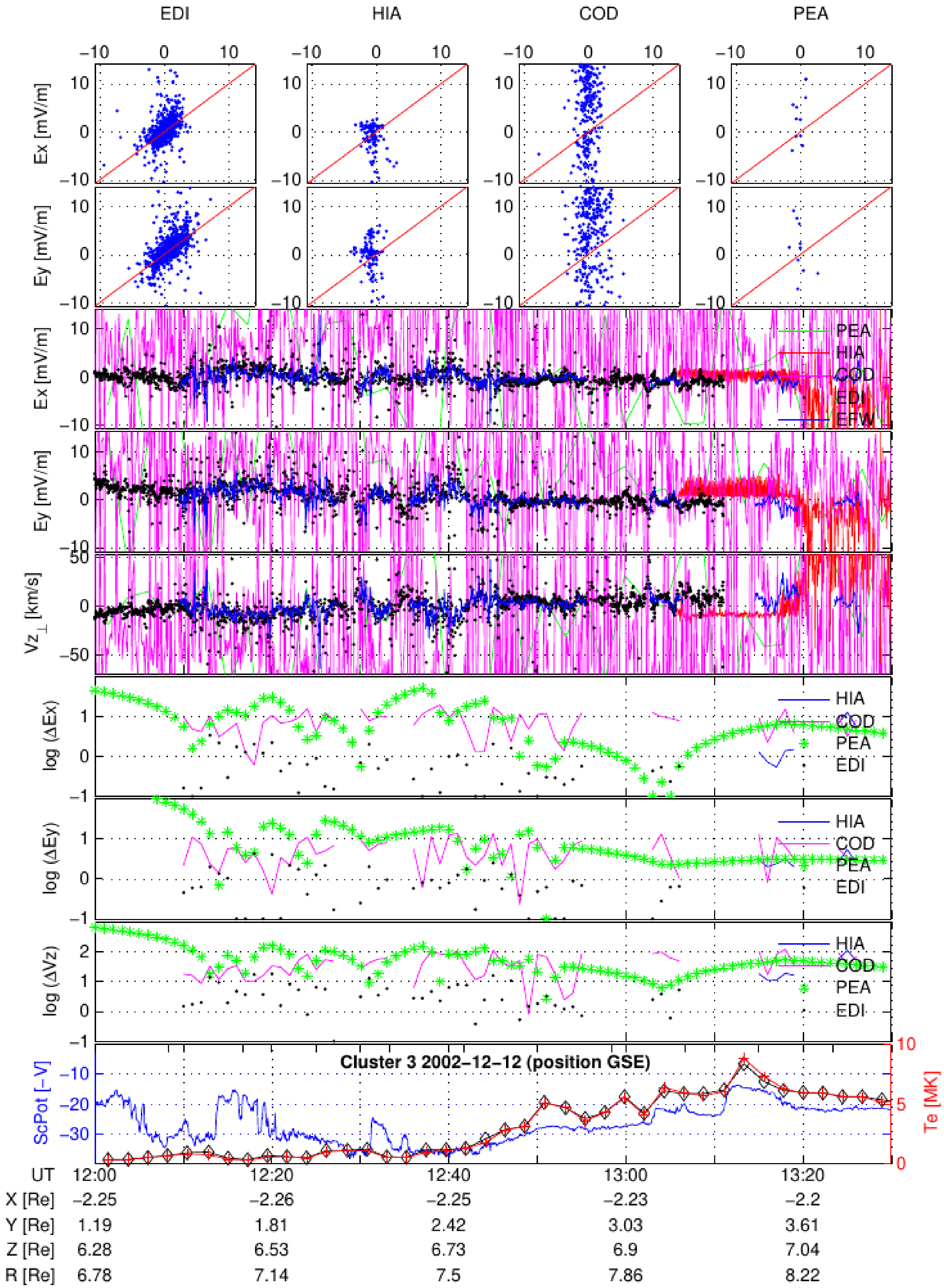
EDI
HIA
COD
PEA
Ex [mV/m]
Ey [mV/m]
Vz⊥ [km/s]
PEA
HIA
COD
EDI
EFW
log (ΔEx)
log (ΔEy)
log (ΔVz)
Cluster 3 2002−12−12 (position GSE)
ScPot [−V]
Te [MK]
UT 12:00 12:20 12:40 13:00 13:20
X [Re] −2.25 −2.26 −2.25 −2.23 −2.2
Y [Re] 1.19 1.81 2.42 3.03 3.61
Z [Re] 6.28 6.53 6.73 6.9 7.04
R [Re] 6.78 7.14 7.5 7.86 8.22

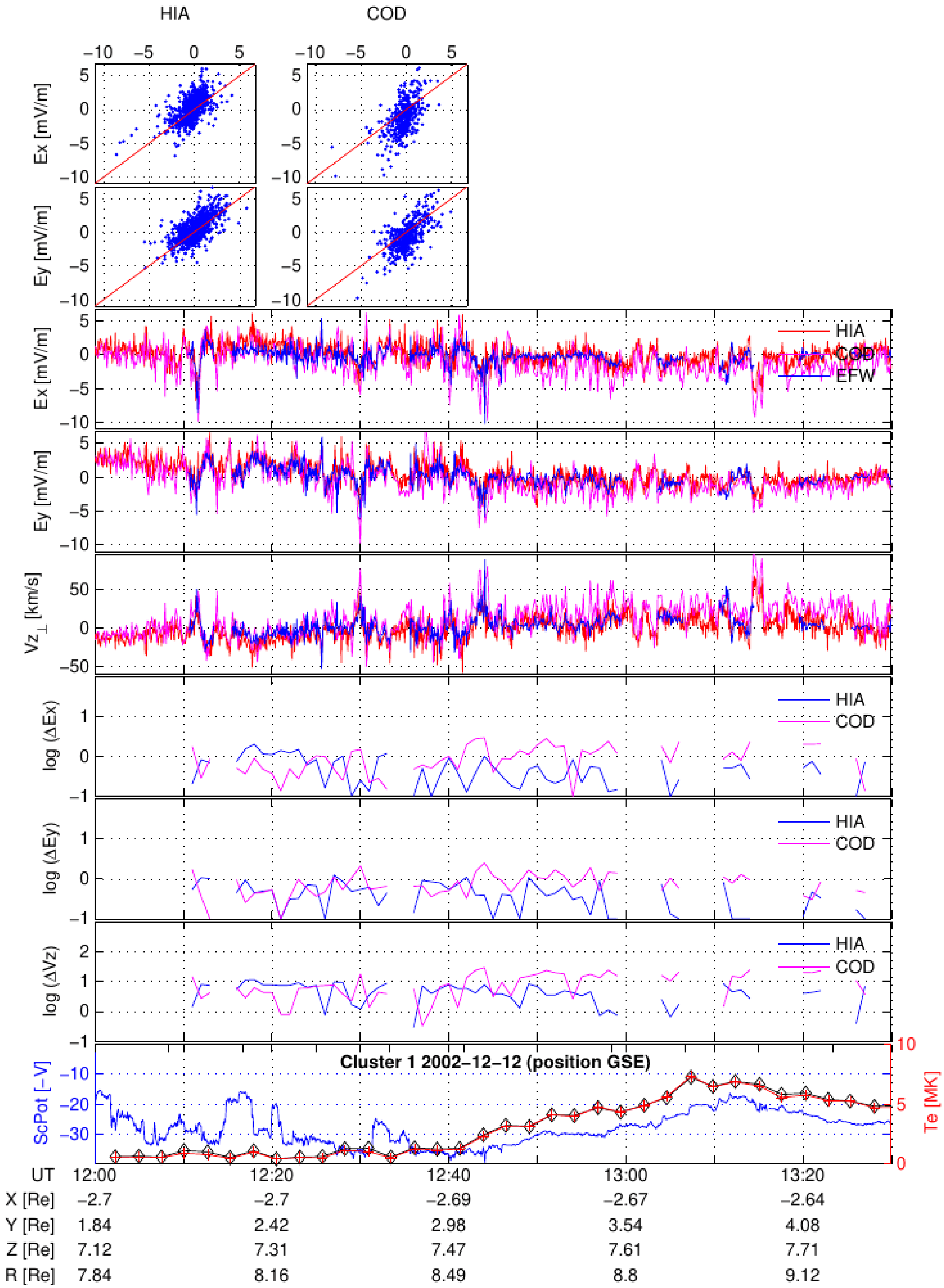
HIA
COD
Ex [mV/m]
Ey [mV/m]
HIA
COD
EFW
Vz⊥ [km/s]
log (ΔEx)
log (ΔEy)
log (ΔVz)
Cluster 1 2002−12−12 (position GSE)
ScPot [−V]
Te [MK]
UT 12:00 12:20 12:40 13:00 13:20
X [Re] −2.7 −2.7 −2.69 −2.67 −2.64
Y [Re] 1.84 2.42 2.98 3.54 4.08
Z [Re] 7.12 7.31 7.47 7.61 7.71
R [Re] 7.84 8.16 8.49 8.8 9.12

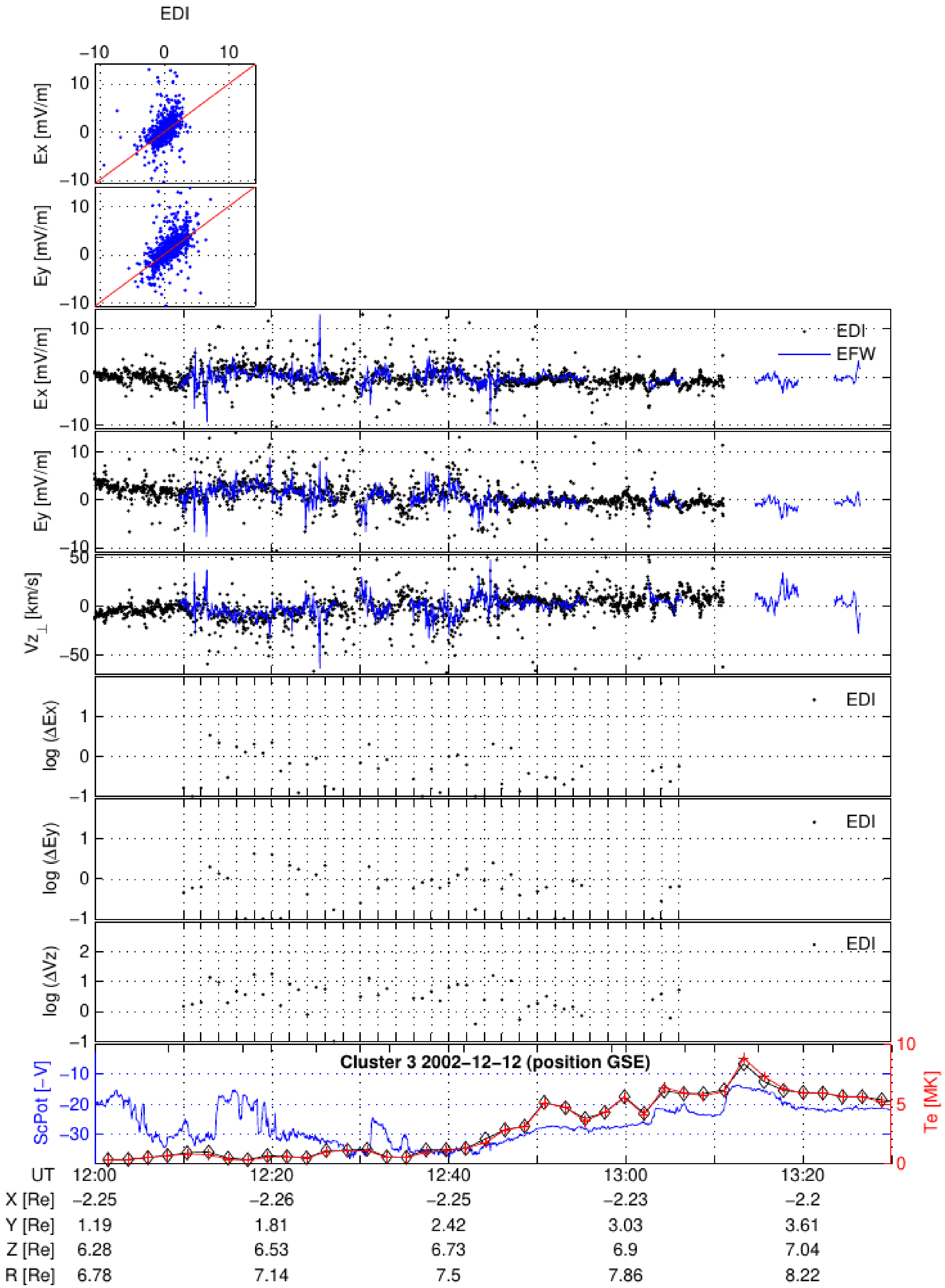
EDI
Ex [mV/m]
Ey [mV/m]
EDI
EFW
Vz⊥ [km/s]
log (ΔEx)
log (ΔEy)
log (ΔVz)
Cluster 3 2002−12−12 (position GSE)
ScPot [−V]
Te [MK]
UT 12:00 12:20 12:40 13:00 13:20
X [Re] −2.25 −2.26 −2.25 −2.23 −2.2
Y [Re] 1.19 1.81 2.42 3.03 3.61
Z [Re] 6.28 6.53 6.73 6.9 7.04
R [Re] 6.78 7.14 7.5 7.86 8.22

## Event 9: Lobes and CPS

2003-11-01 09:00 - 12:00 | CAA quicklook

**Standard plots:**

031101_C1_Lobe_CPS.pdf

031101_C3_Lobe_CPS.pdf

Here we find the usual high noise level for CODIF, for SC3 combined with an offset. PEACE data are slightly more useful, while HIA provides the best comparison data set. However, variations are rapid and cannot be caught in detail by HIA moment intergration, resulting in larger variability in EFW than in HIA data for this event. This shows up as a slope in the EFW-HIA scatter plots, despite the average HIA-EFW difference satying well within 1 mV/m except in the very most active regions.

These data shows the same results though with less clutter of less significant data.

This event demonstrates that the E-field in active regions cannot readily be caught by the particle instruments.

**Fine plots:**

031101_C1_Lobe_CPS_fine.pdf

031101_C3_Lobe_CPS_fine.pdf

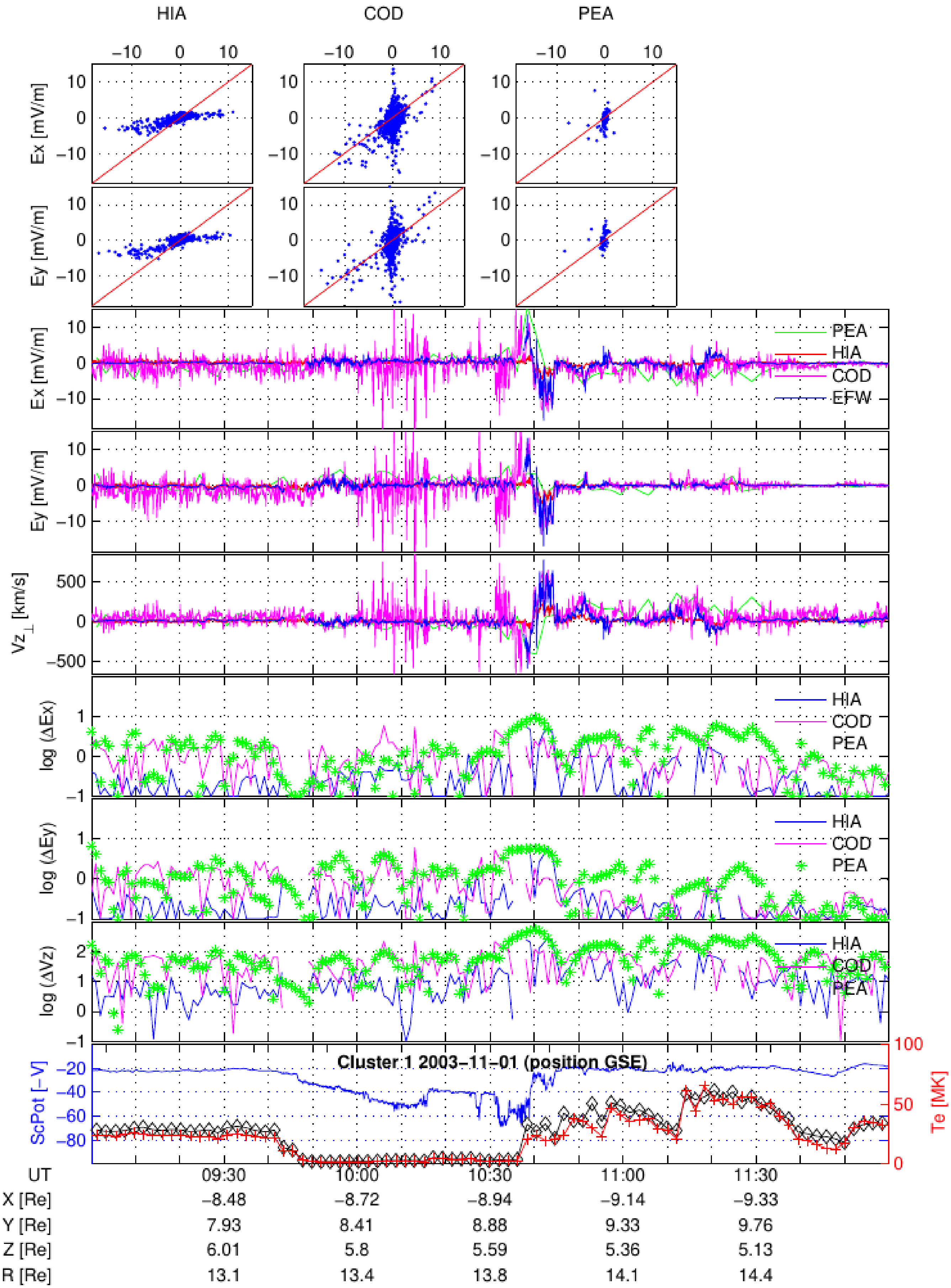
HIA
COD
PEA
Ex [mV/m]
Ey [mV/m]
PEA
HIA
COD
EFW
Vz⊥ [km/s]
log (ΔEx)
log (ΔEy)
log (ΔVz)
Cluster 1 2003–11–01 (position GSE)
ScPot [–V]
Te [MK]
UT
09:30
10:00
10:30
11:00
11:30
X [Re]
–8.48
–8.72
–8.94
–9.14
–9.33
Y [Re]
7.93
8.41
8.88
9.33
9.76
Z [Re]
6.01
5.8
5.59
5.36
5.13
R [Re]
13.1
13.4
13.8
14.1
14.4

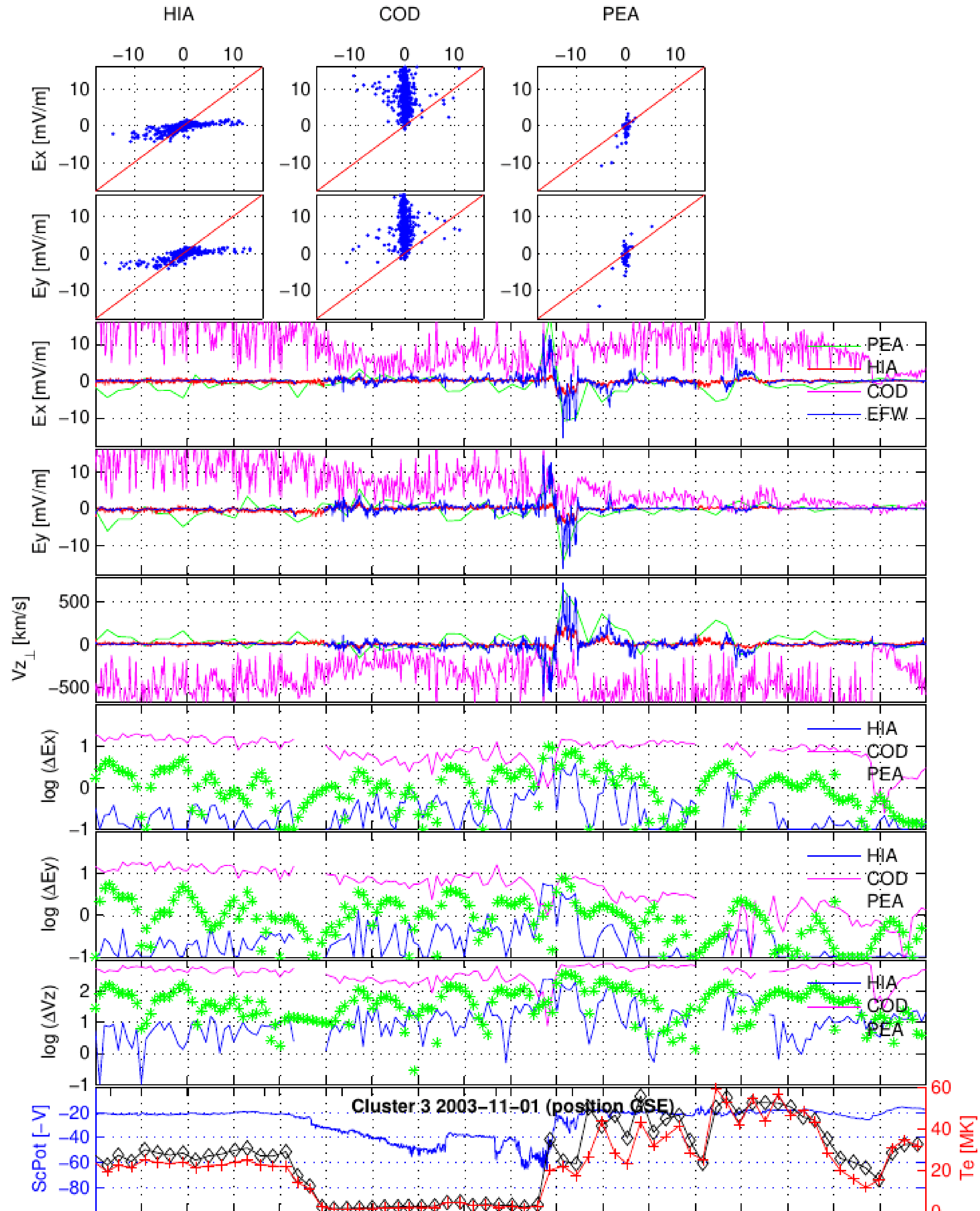


| UT | 09:30 | 10:00 | 10:30 | 11:00 | 11:30 |
|---|---|---|---|---|---|
| X [Re] | –8.45 | –8.69 | –8.91 | –9.12 | –9.3 |
| Y [Re] | 7.96 | 8.44 | 8.91 | 9.36 | 9.79 |
| Z [Re] | 6 | 5.79 | 5.58 | 5.35 | 5.12 |
| R [Re] | 13.1 | 13.4 | 13.8 | 14.1 | 14.4 |

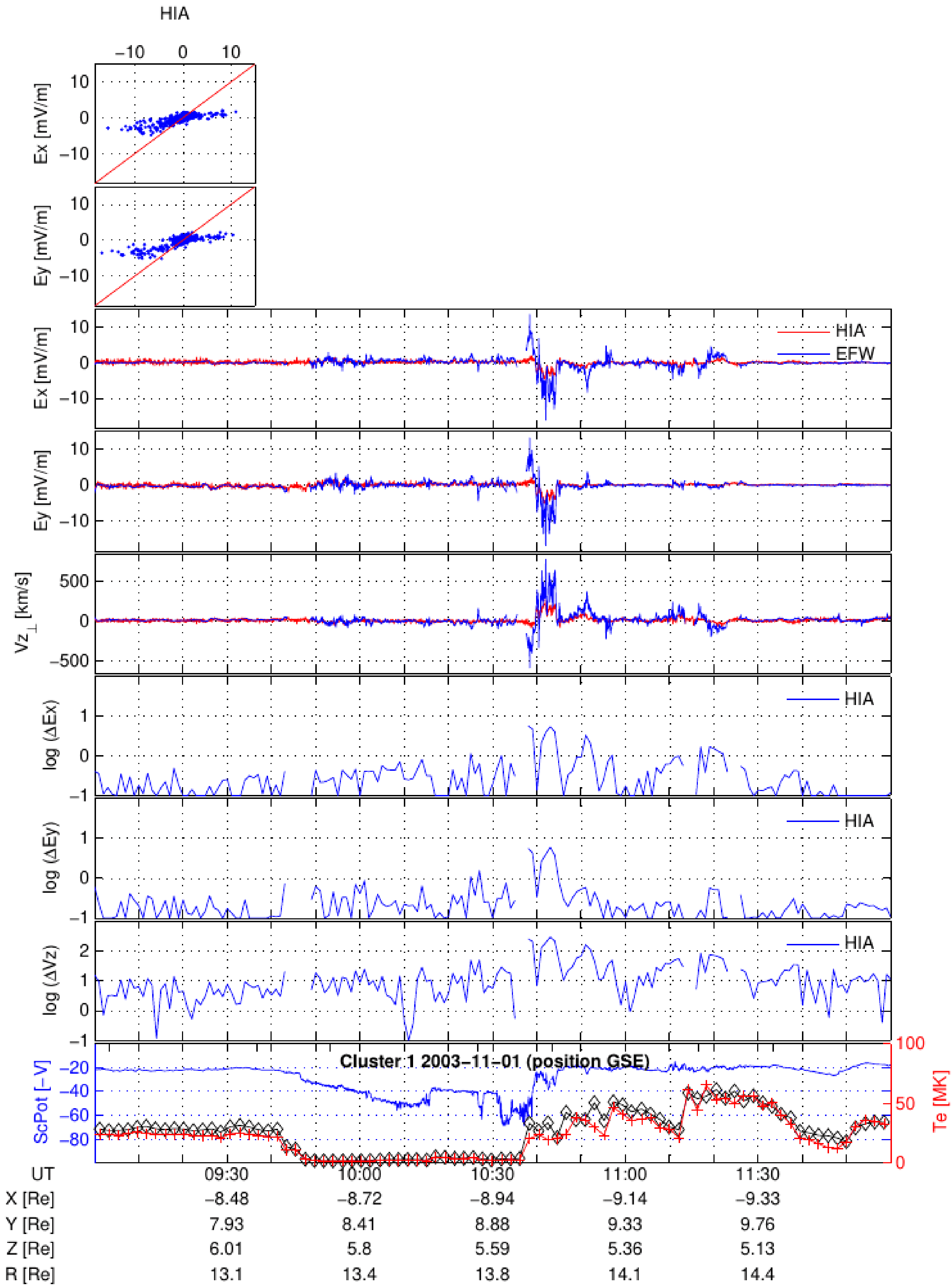
HIA
−10 0 10
Ex [mV/m]
Ey [mV/m]
HIA
EFW
Vz⊥ [km/s]
log (ΔEx)
log (ΔEy)
log (ΔVz)
Cluster 1 2003−11−01 (position GSE)
ScPot [−V]
Te [MK]
UT 09:30 10:00 10:30 11:00 11:30
X [Re] −8.48 −8.72 −8.94 −9.14 −9.33
Y [Re] 7.93 8.41 8.88 9.33 9.76
Z [Re] 6.01 5.8 5.59 5.36 5.13
R [Re] 13.1 13.4 13.8 14.1 14.4

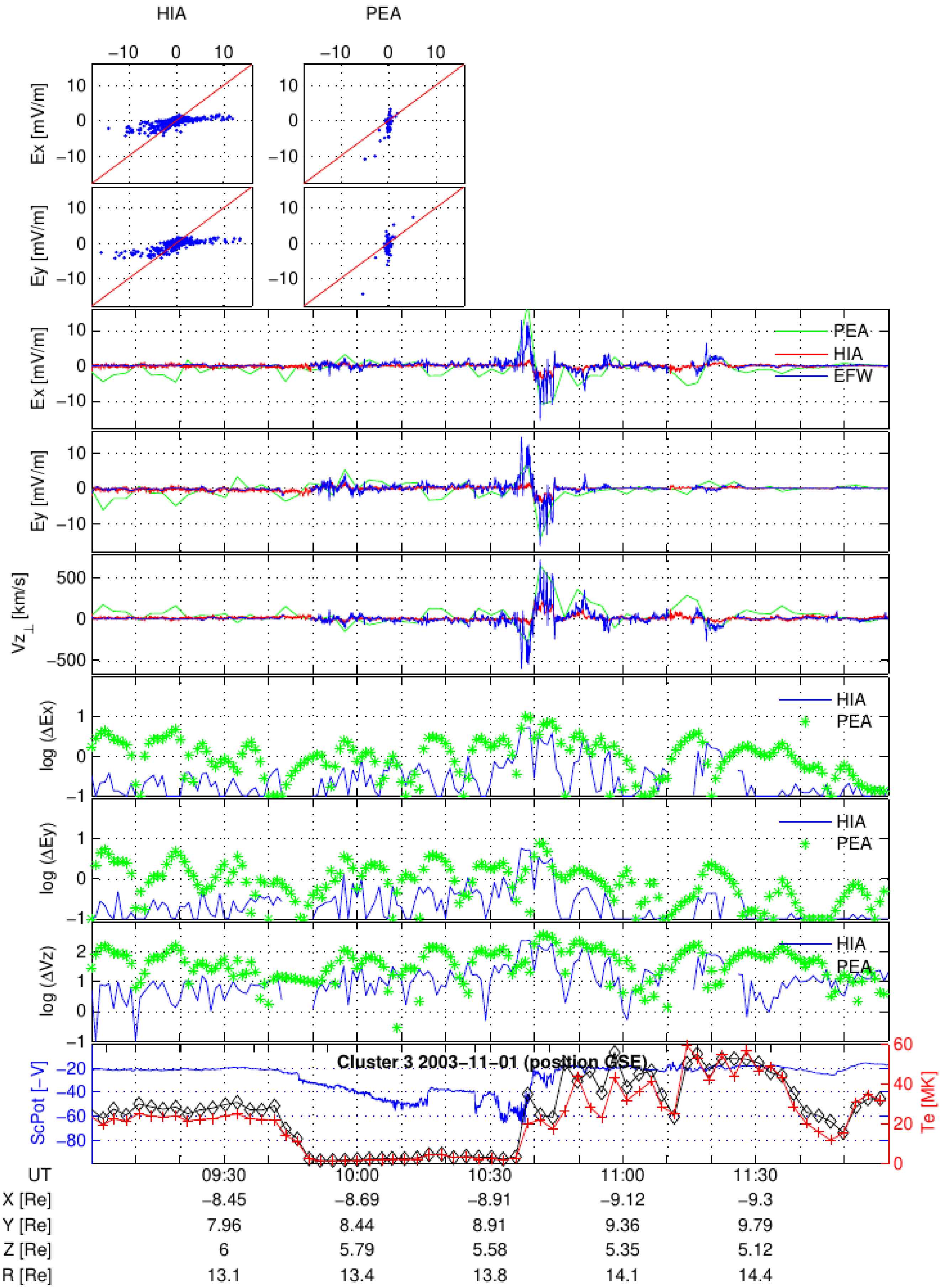
HIA
PEA
Ex [mV/m]
Ey [mV/m]
PEA
HIA
EFW
Vz⊥ [km/s]
log (ΔEx)
log (ΔEy)
log (ΔVz)
Cluster 3 2003−11−01 (position GSE)
ScPot [−V]
Te [MK]
UT 09:30 10:00 10:30 11:00 11:30
X [Re] −8.45 −8.69 −8.91 −9.12 −9.3
Y [Re] 7.96 8.44 8.91 9.36 9.79
Z [Re] 6 5.79 5.58 5.35 5.12
R [Re] 13.1 13.4 13.8 14.1 14.4

## Event 10: Plasma Sheet

2003-11-02 00:00 - 03:00 | CAA quicklook

**Standard plots:**

031102_C1_CPS.pdf

031102_C3_CPS.pdf

The time series show good agreement between EFW and HIA on both s/c, though for SC1, this is best seen in the fine plot because of the noise from the CODIF data. On SC3, the CODIF moment has such a large offset as to not hide the HIA and EFW data, and no fine plot is therefore needed. On SC1, the CODIF envelope in the fine plot still contains HIA and EFW, though some offset to positive Ex and Ey is evident in CODIF data here as well. In the SC3 plot, it is clear that HIA has higher noise level than EFW, but the agreement between the two instruments is still impressive. The SC1 fine plot shows the same, with EFW staying inside the HIA noise envelope. PEACE noise is too high to make detailed comparison meaningful, but the average difference EFW-PEACE still stays within a few mV/m. The average EFW-HIA difference is a few tenths of mV/m, reaching close to 1 mV/m only where the data shows rapid variations HIA cannot reliably catch.

This event demonstrates as good an agreement between EFW and HIA as can ever be expected.

**Fine plots:**

031102_C1_CPS_fine.pdf

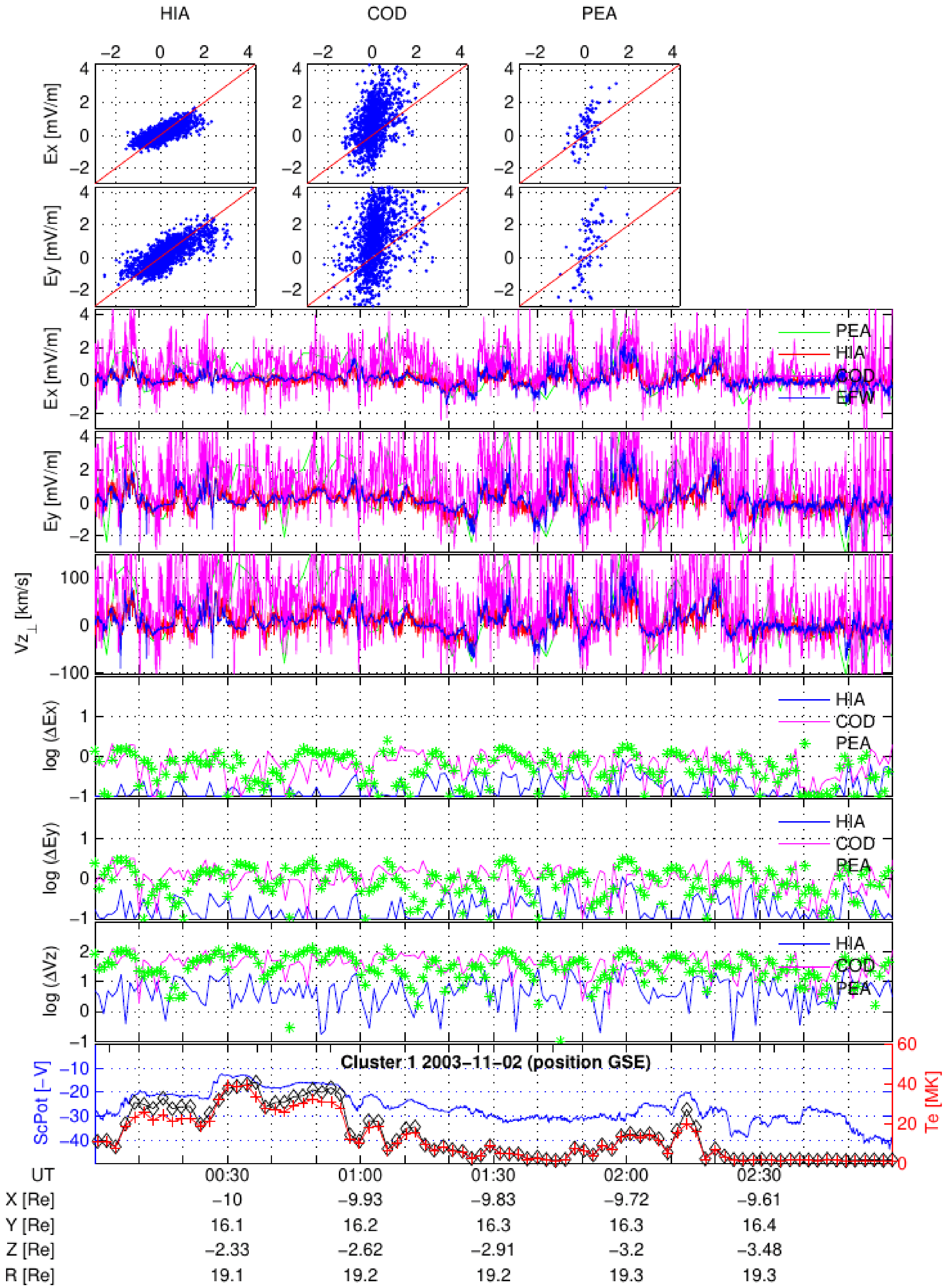
HIA
COD
PEA
Ex [mV/m]
Ey [mV/m]
PEA
HIA
COD
EFW
Vz⊥ [km/s]
log (ΔEx)
log (ΔEy)
log (ΔVz)
Cluster 1 2003–11–02 (position GSE)
ScPot [–V]
Te [MK]
UT
00:30
01:00
01:30
02:00
02:30
X [Re]
–10
–9.93
–9.83
–9.72
–9.61
Y [Re]
16.1
16.2
16.3
16.3
16.4
Z [Re]
–2.33
–2.62
–2.91
–3.2
–3.48
R [Re]
19.1
19.2
19.2
19.3
19.3

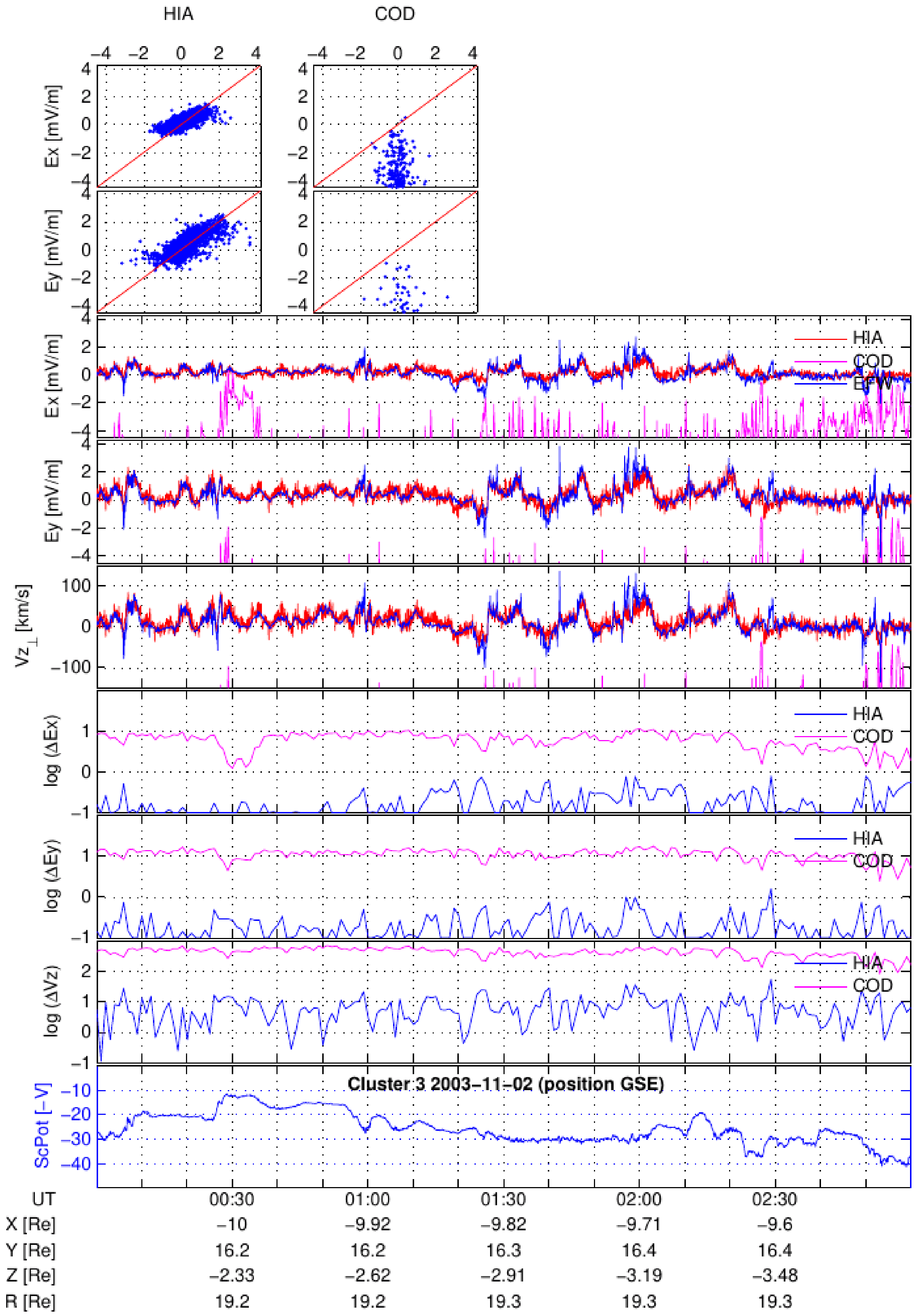
HIA
COD
Ex [mV/m]
Ey [mV/m]
HIA
COD
EFW
Vz⊥ [km/s]
log (ΔEx)
log (ΔEy)
log (ΔVz)
ScPot [−V]
Cluster 3 2003−11−02 (position GSE)
UT 00:30 01:00 01:30 02:00 02:30
X [Re] −10 −9.92 −9.82 −9.71 −9.6
Y [Re] 16.2 16.2 16.3 16.4 16.4
Z [Re] −2.33 −2.62 −2.91 −3.19 −3.48
R [Re] 19.2 19.2 19.3 19.3 19.3

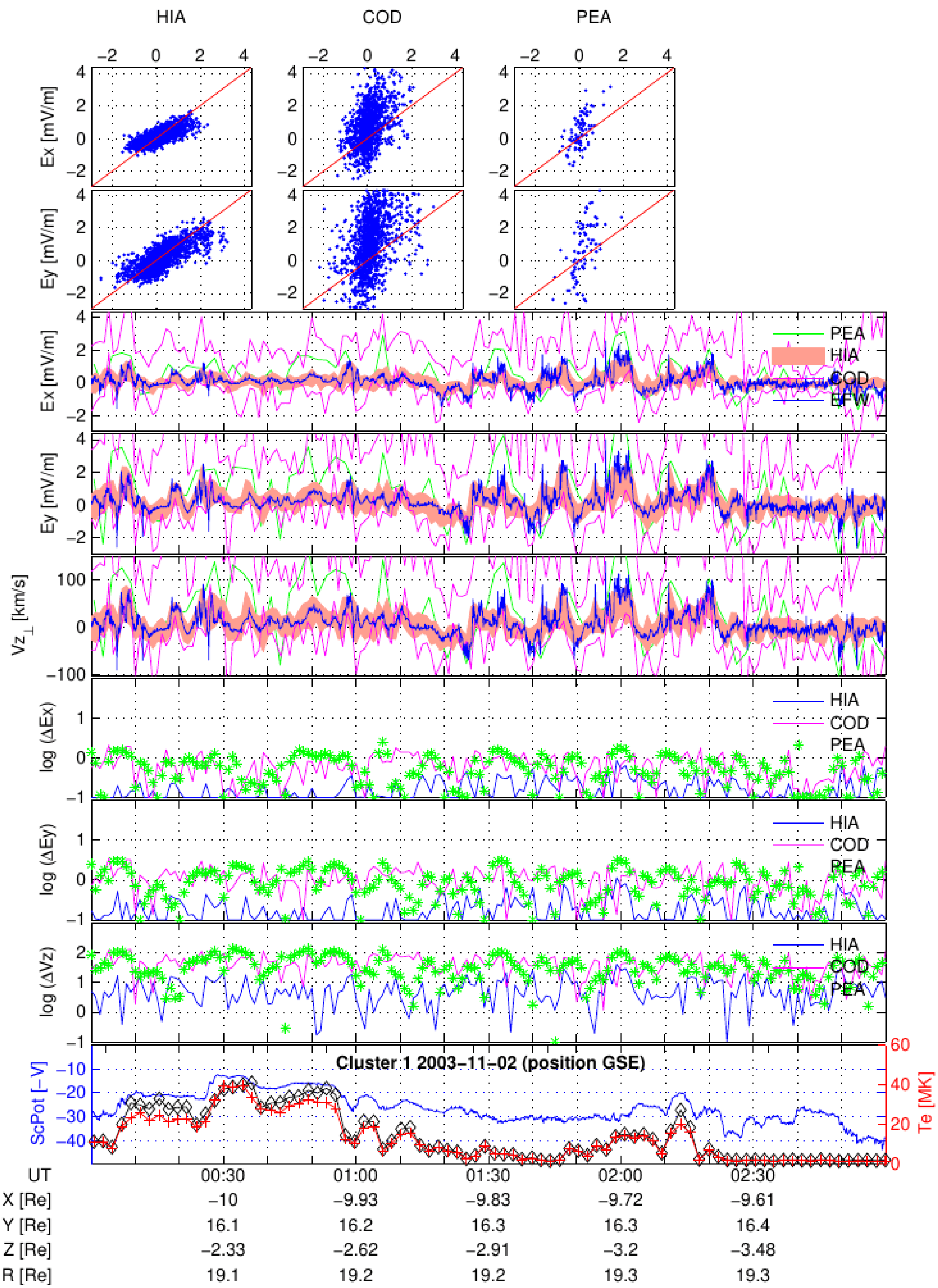
HIA
COD
PEA
Ex [mV/m]
Ey [mV/m]
PEA
HIA
COD
EFW
Vz⊥ [km/s]
log (ΔEx)
log (ΔEy)
log (ΔVz)
Cluster 1 2003−11−02 (position GSE)
ScPot [−V]
Te [MK]
UT
00:30
01:00
01:30
02:00
02:30
X [Re]
−10
−9.93
−9.83
−9.72
−9.61
Y [Re]
16.1
16.2
16.3
16.3
16.4
Z [Re]
−2.33
−2.62
−2.91
−3.2
−3.48
R [Re]
19.1
19.2
19.2
19.3
19.3

## Event 11: Plasma Sheet

2003-11-03 21:00 - 22:30 | CAA quicklook

**Standard plots:**

`031103_C1_CPS.pdf`

`031103_C3_CPS.pdf`

While in a noisy region, the data all show a general agreement, except CD3 CODIF which has a large offset. It is interesting to note that HIA does not capture the larger excursions in the field, neither the small-scale variations nor the slower variation around 21:30-21:40. For this particular variation, even PEACE shows reasonable agreement. EFW generally agrees best with HIA and EDI with differences of well below 1 mV/m throughout the interval.

This event demonstrates excellent agreement between EFW, EDI and HIA data.

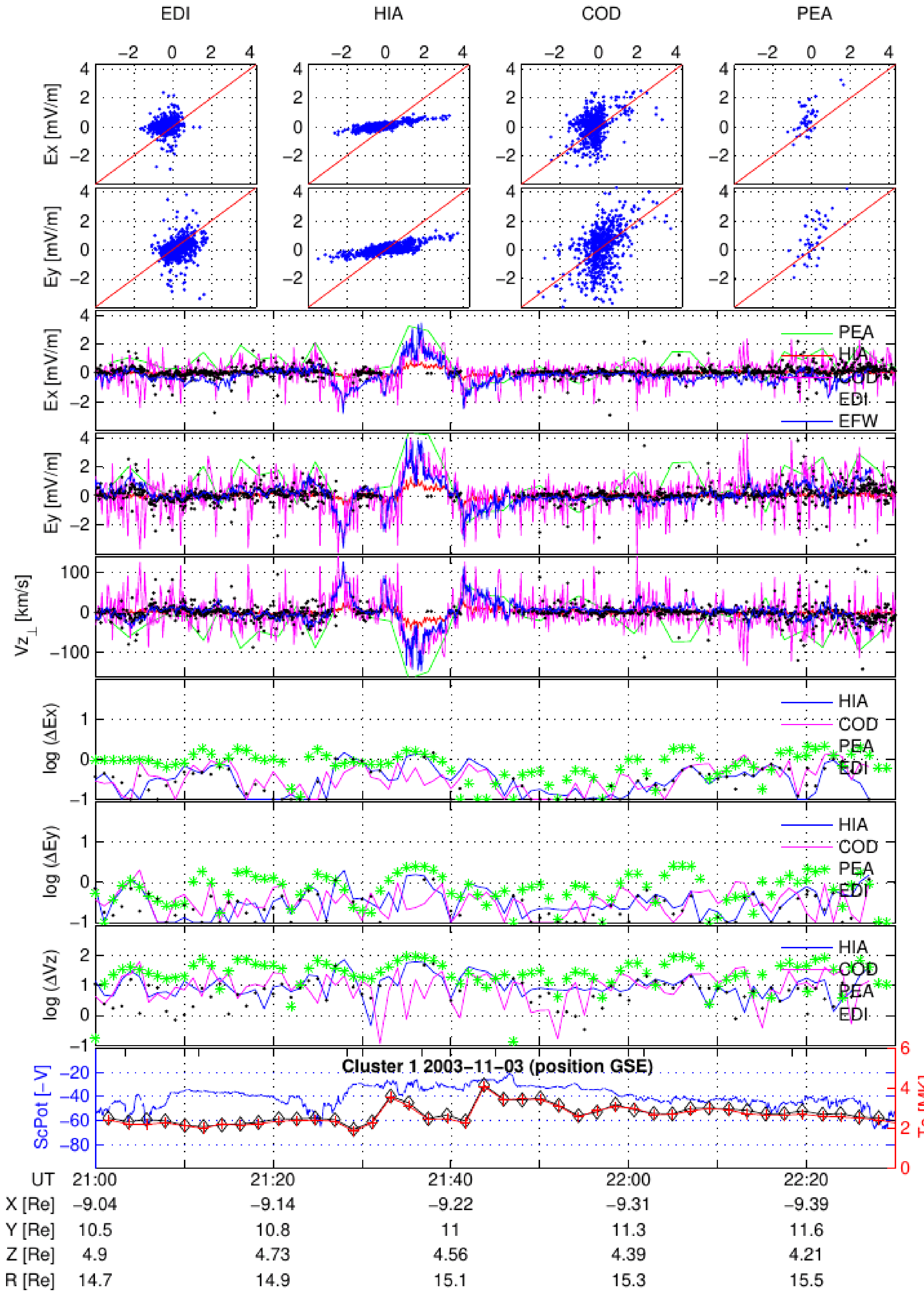
EDI
HIA
COD
PEA
Ex [mV/m]
Ey [mV/m]
PEA
HIA
COD
EDI
EFW
Vz⊥ [km/s]
log (ΔEx)
log (ΔEy)
log (ΔVz)
HIA
COD
PEA
EDI
Cluster 1 2003−11−03 (position GSE)
ScPot [−V]
Te [MK]
UT 21:00 21:20 21:40 22:00 22:20
X [Re] −9.04 −9.14 −9.22 −9.31 −9.39
Y [Re] 10.5 10.8 11 11.3 11.6
Z [Re] 4.9 4.73 4.56 4.39 4.21
R [Re] 14.7 14.9 15.1 15.3 15.5

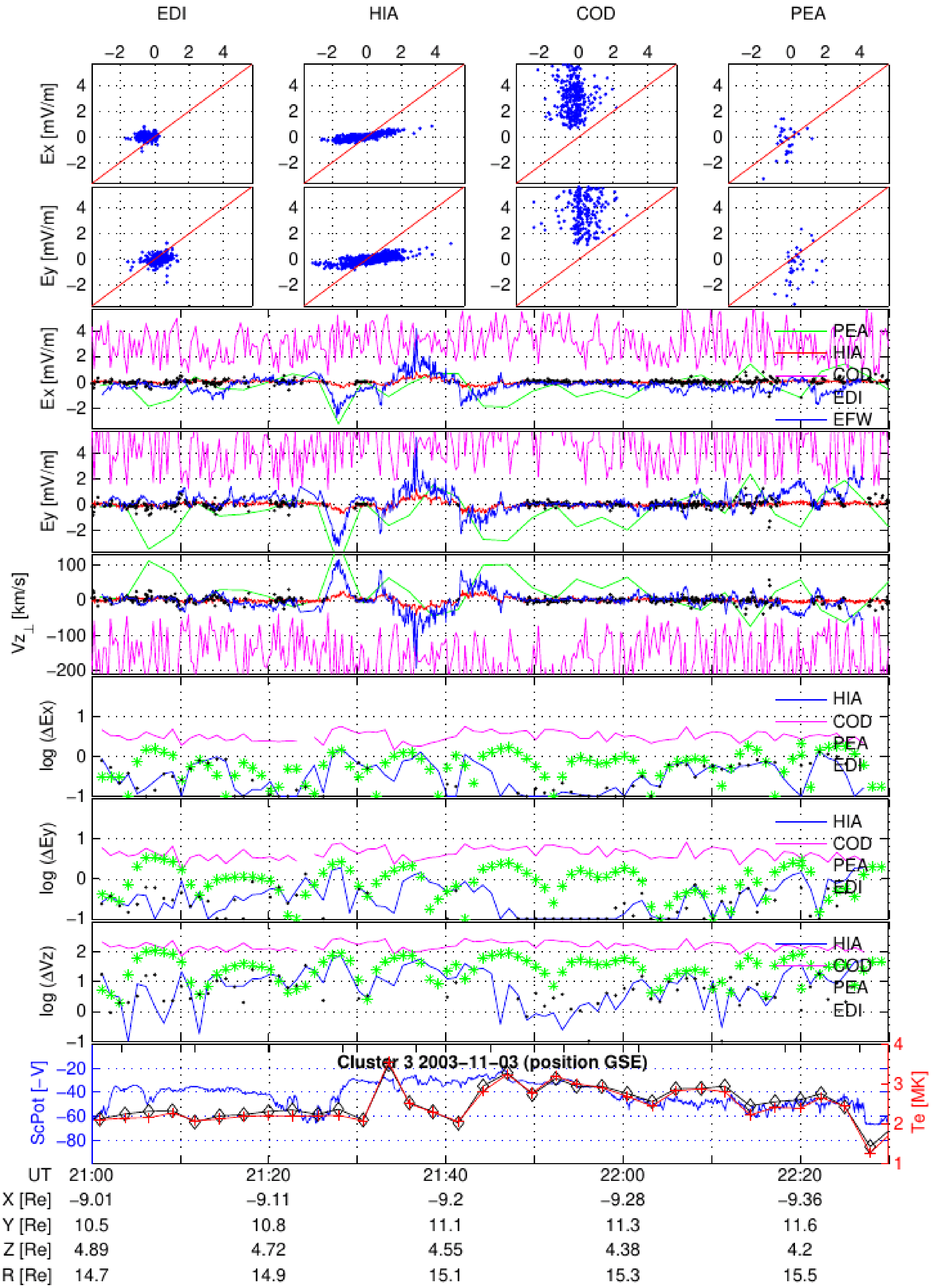
EDI
HIA
COD
PEA
Ex [mV/m]
Ey [mV/m]
PEA
HIA
COD
EDI
EFW
Vz⊥ [km/s]
log (ΔEx)
log (ΔEy)
log (ΔVz)
Cluster 3 2003−11−03 (position GSE)
ScPot [−V]
Te [MK]
UT 21:00 21:20 21:40 22:00 22:20
X [Re] −9.01 −9.11 −9.2 −9.28 −9.36
Y [Re] 10.5 10.8 11.1 11.3 11.6
Z [Re] 4.89 4.72 4.55 4.38 4.2
R [Re] 14.7 14.9 15.1 15.3 15.5

## Event 12: Plasma Sheet

2004-09-19 15:00 - 18:00 | CAA quicklook

**Standard plots:**

040919_C3_CPS.pdf

EFW shows a very good agreement with HIA, as seen both in the standard plot and in the fine plot. EFW lies well within the envelope of the HIA variations, except for a few cases where HIA does not respond to the larger field spikes. CODIF has the same problem as for other cases with a large offset on SC3. PEACE has a lower time resolution but generally also agrees with the EFW and HIA variations, although it often measures somewhat larger values. The difference between EFW and HIA is well below 1 mV/m and often as low as 0.1 mV/m. No EDI data are available.

This event demonstrates very good agreement between EFW and HIA.

**Fine plots:**

040919_C3_CPS_fine.pdf

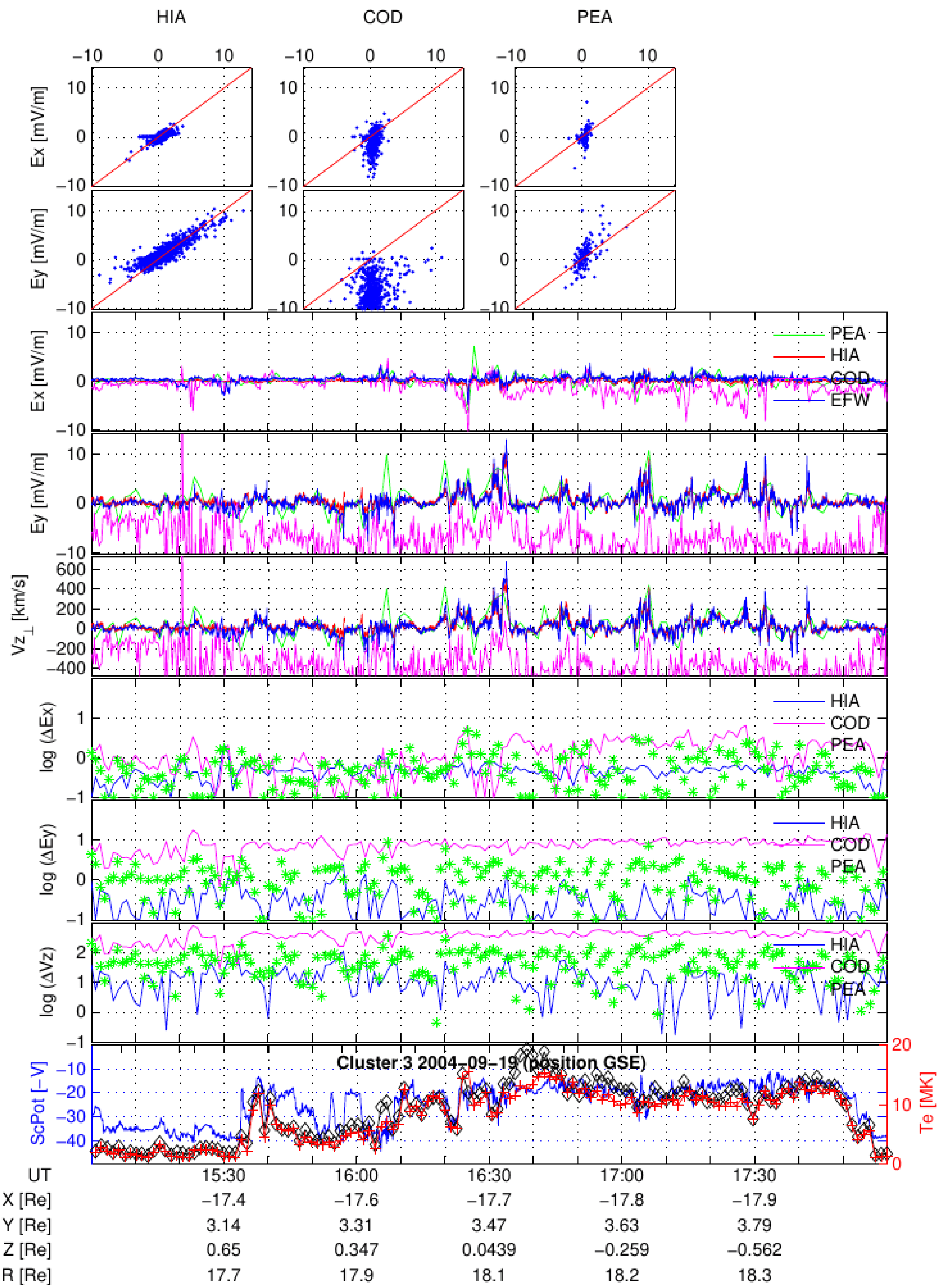
HIA
COD
PEA
Ex [mV/m]
Ey [mV/m]
PEA
HIA
COD
EFW
Vz⊥ [km/s]
log (ΔEx)
log (ΔEy)
log (ΔVz)
Cluster 3 2004–09–19 (position GSE)
ScPot [–V]
Te [MK]
UT
15:30
16:00
16:30
17:00
17:30
X [Re]
–17.4
–17.6
–17.7
–17.8
–17.9
Y [Re]
3.14
3.31
3.47
3.63
3.79
Z [Re]
0.65
0.347
0.0439
–0.259
–0.562
R [Re]
17.7
17.9
18.1
18.2
18.3

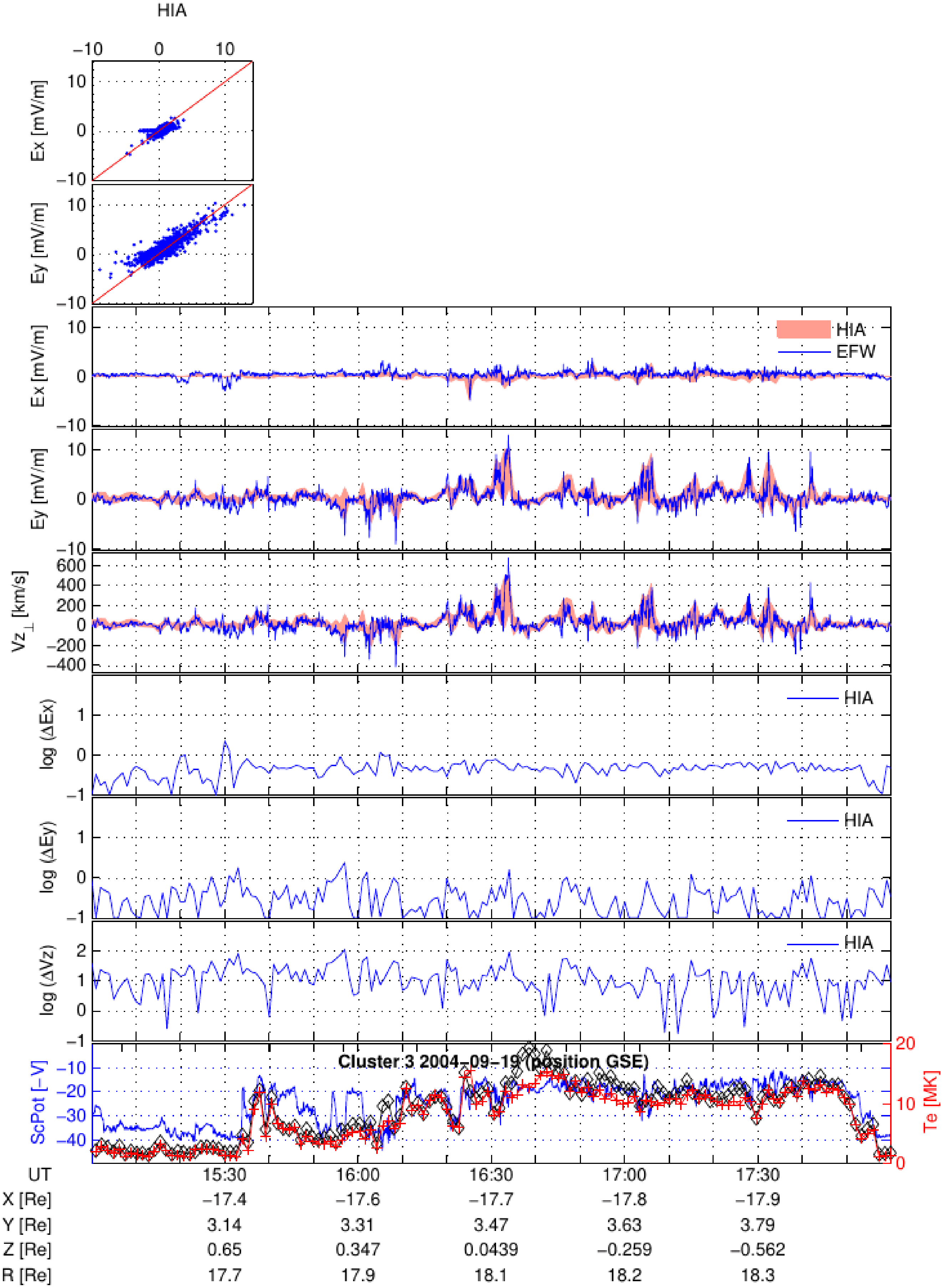
HIA
Ex [mV/m]
Ey [mV/m]
HIA
EFW
Vz⊥ [km/s]
log (ΔEx)
log (ΔEy)
log (ΔVz)
Cluster 3 2004–09–19 (position GSE)
ScPot [–V]
Te [MK]
UT 15:30 16:00 16:30 17:00 17:30
X [Re] –17.4 –17.6 –17.7 –17.8 –17.9
Y [Re] 3.14 3.31 3.47 3.63 3.79
Z [Re] 0.65 0.347 0.0439 –0.259 –0.562
R [Re] 17.7 17.9 18.1 18.2 18.3

## Auroral zone

## Event 13: Auroral zone

2003-11-01 00:00 - 01:10 | CAA quicklook

**Standard plots:**

`031101_C1_AZ.pdf`

`031101_C3_AZ.pdf`

These plots show PEACE moments too noisy for useful comparison. Noise levels are high also in HIA and CODIF, and the rapid variations present cannot be caught by the particle instruments. EDI produces useful data at the start of the interval, agreeing with EFW to within 1 mV/m, but produces outliers and loses signal when the plasma activity increases. The C3 CODIF data are subject to a very large offset.

This compares EFW to HIA and CODIF on SC1 and to HIA only on SC3, by producing envelopes of the noisy ion data. It can be seen that HIA and EFW comfortably stays within the CODIF noise envelope, and that EFW stays within the HIA envelope. Exceptions are points of very rapidly varying and impulsive electric fields, which cannot be accurately determined by moments from a particle instrument. The disagreement between EFW and HIA can therefore at times reach 10 mV/m, particularly on SC1.

This event demonstrates as good an agreement as can be expected between EFW and HIA in a noisy environment.

**Fine plots:**

`031101_C1_AZ_fine.pdf`

`031101_C3_AZ_fine.pdf`

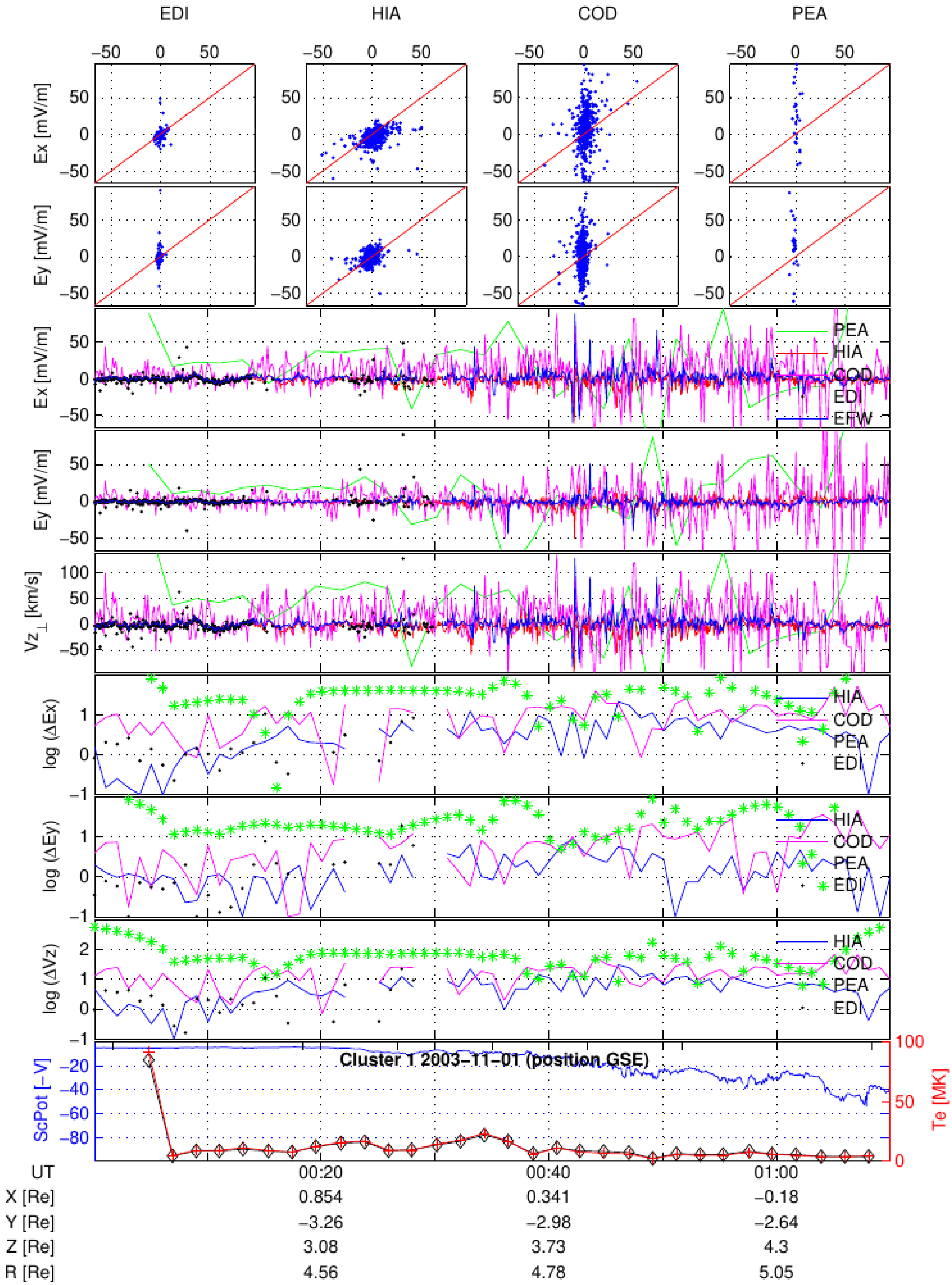
EDI
HIA
COD
PEA
Ex [mV/m]
Ey [mV/m]
PEA
HIA
COD
EDI
EFW
Vz⊥ [km/s]
log (ΔEx)
log (ΔEy)
log (ΔVz)
Cluster 1 2003–11–01 (position GSE)
ScPot [–V]
Te [MK]
UT
00:20
00:40
01:00
X [Re]
0.854
0.341
–0.18
Y [Re]
–3.26
–2.98
–2.64
Z [Re]
3.08
3.73
4.3
R [Re]
4.56
4.78
5.05

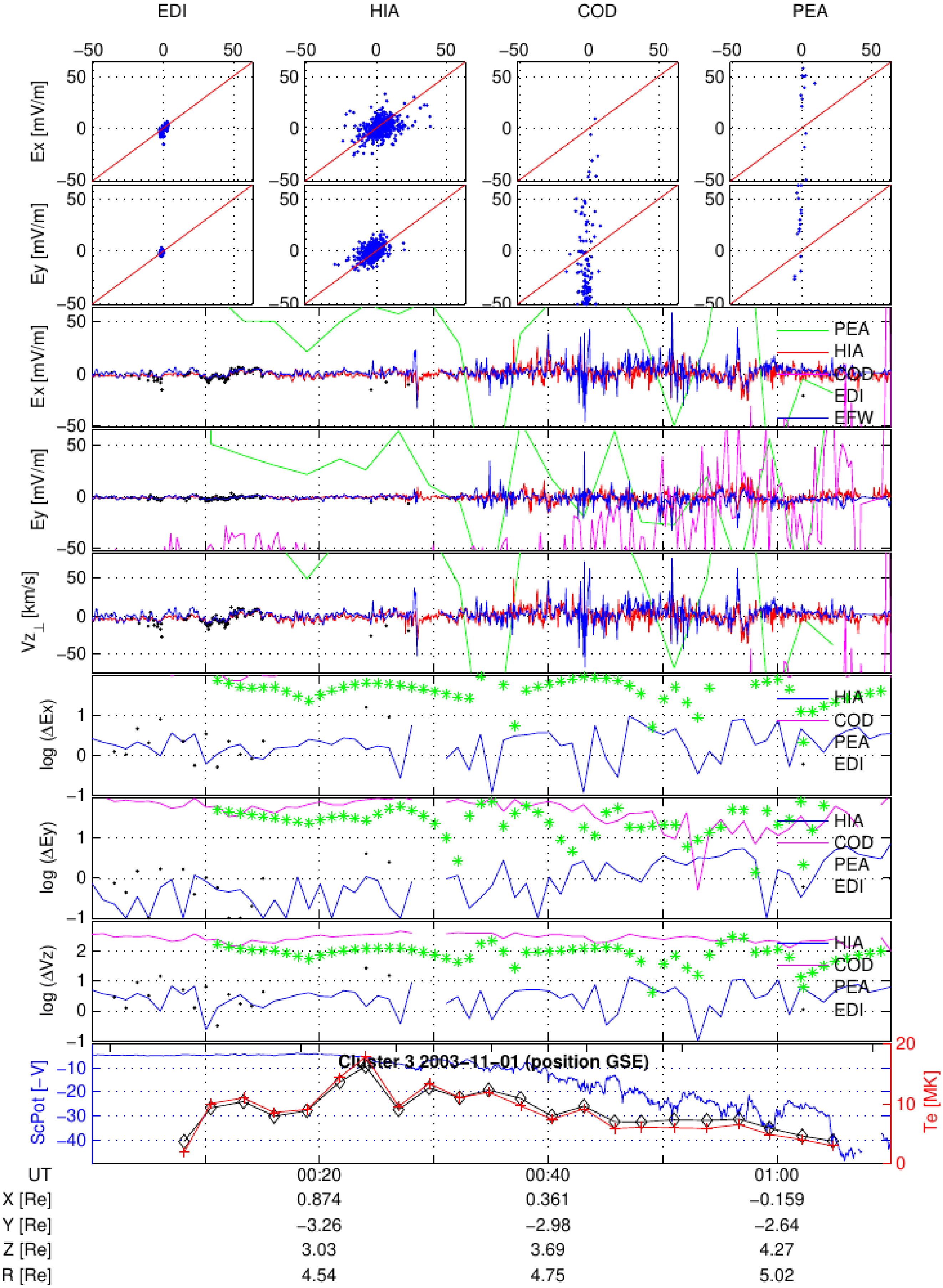
EDI
HIA
COD
PEA
Ex [mV/m]
Ey [mV/m]
PEA
HIA
COD
EDI
EFW
Vz⊥ [km/s]
log (ΔEx)
log (ΔEy)
log (ΔVz)
Cluster 3 2003−11−01 (position GSE)
ScPot [−V]
Te [MK]
UT
00:20
00:40
01:00
X [Re]
0.874
0.361
−0.159
Y [Re]
−3.26
−2.98
−2.64
Z [Re]
3.03
3.69
4.27
R [Re]
4.54
4.75
5.02

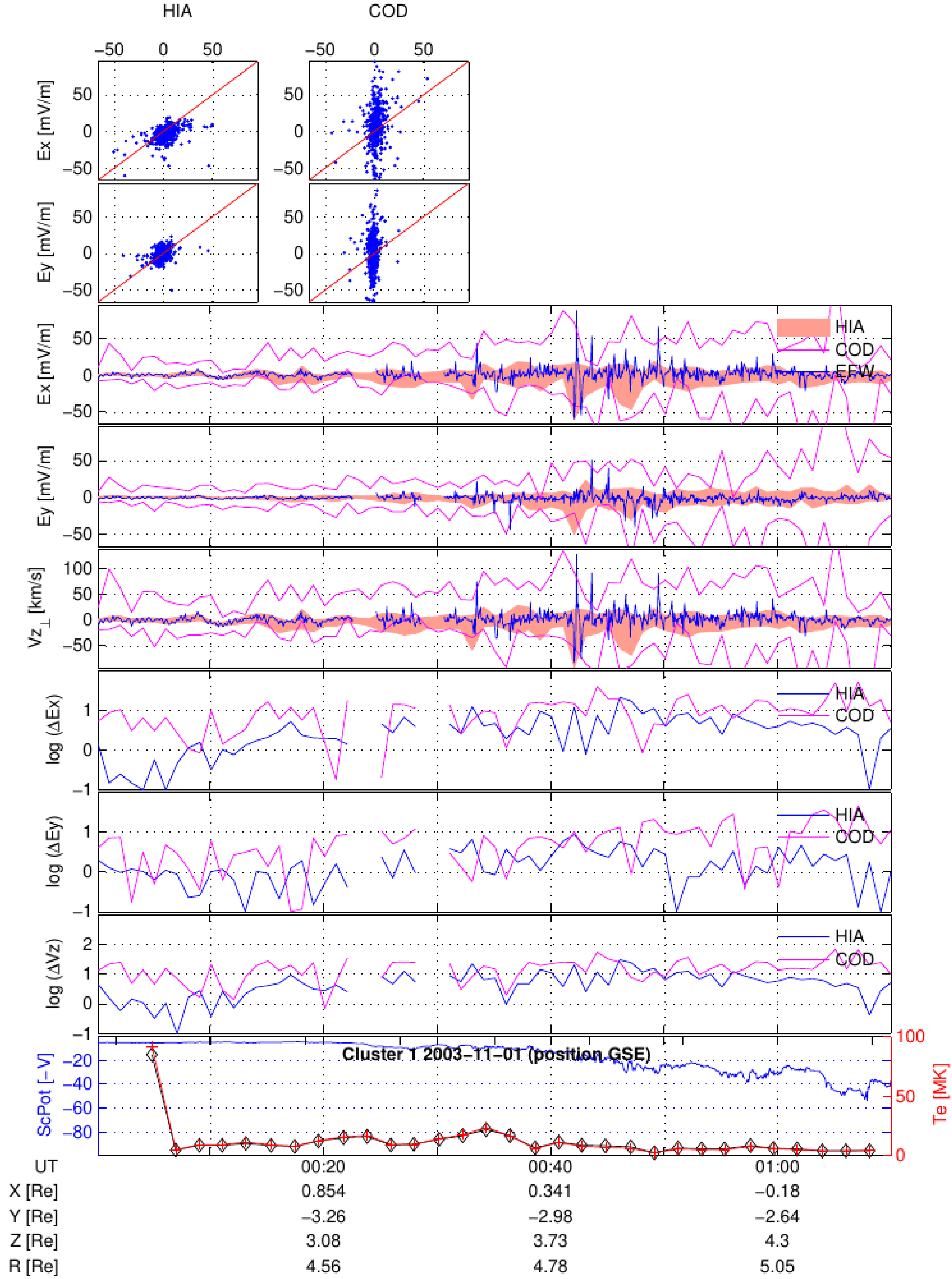
HIA
COD
Ex [mV/m]
Ey [mV/m]
HIA
COD
EFW
Vz⊥ [km/s]
log (ΔEx)
log (ΔEy)
log (ΔVz)
Cluster 1 2003−11−01 (position GSE)
ScPot [−V]
Te [MK]
UT
00:20
00:40
01:00
X [Re]
0.854
0.341
−0.18
Y [Re]
−3.26
−2.98
−2.64
Z [Re]
3.08
3.73
4.3
R [Re]
4.56
4.78
5.05

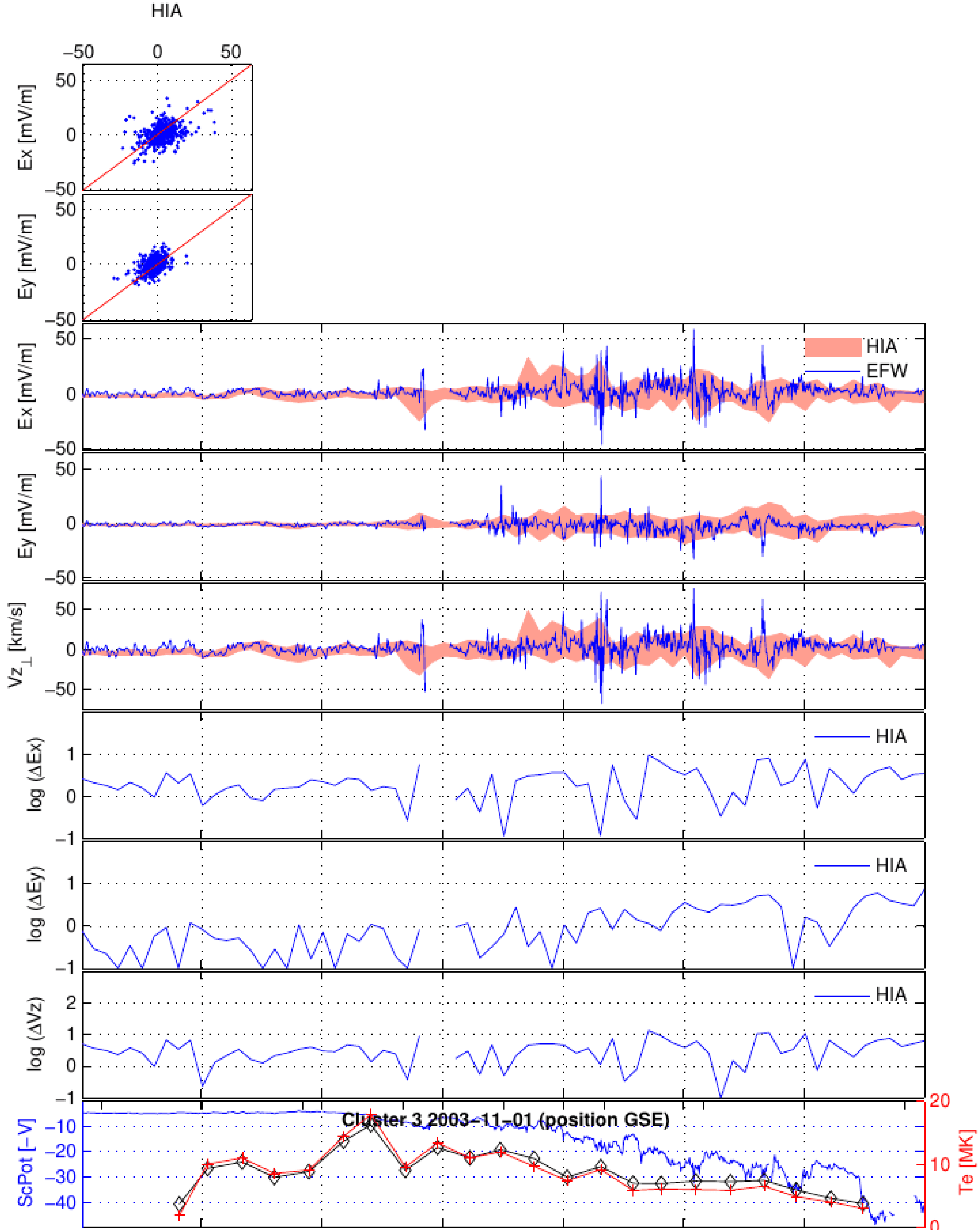


| UT | 00:20 | 00:40 | 01:00 |
|---|---|---|---|
| X [Re] | 0.874 | 0.361 | −0.159 |
| Y [Re] | −3.26 | −2.98 | −2.64 |
| Z [Re] | 3.03 | 3.69 | 4.27 |
| R [Re] | 4.54 | 4.75 | 5.02 |

## Event 14: Auroral zone

2003-11-05 12:00 - 15:00 | CAA quicklook

**Standard plots:**

`031105_C1_AZ.pdf`

EFW shows good general agreement to EDI and HIA, while CODIF and PEACE velocity moments have too much noise and/or offsets to make a comparison meaningful. The averaged EFW-HIA difference is around 1 mV/m and is increases with the variations in the field, reaching several mV/m in the very dynamic interval (auroral zone) 14:00-14:30. In this region, there is little EDI data, and EDI also shows a lot of outliers in the interval 13:00-14:00, where the activity is somewhat lower but still high. Despite the EDI outliers, the EFW-EDI difference stays around 1 mV/m.

These plots show EFW staying inside the EDI and HIA noise level envelopes, except when rapid variations occur that cannot be caught by the other instruments. For some variations, HIA shows a consistent difference to EDI and EFW: an example is in SC3 at 12:42, where EDI and EFW catch a rapid variation not seen in the HIA velocity moment. As the activity level increases, neither EDI nor HIA can track it: an example is 14:40-14:50, where only EFW catches the full variations.

This event demonstrates EFW-EDI-CIS agreement to the extent allowed by the activity level of the data and the noise in EDI and CIS data.

**Fine plots:**

`031105_C1_AZ_fine.pdf`

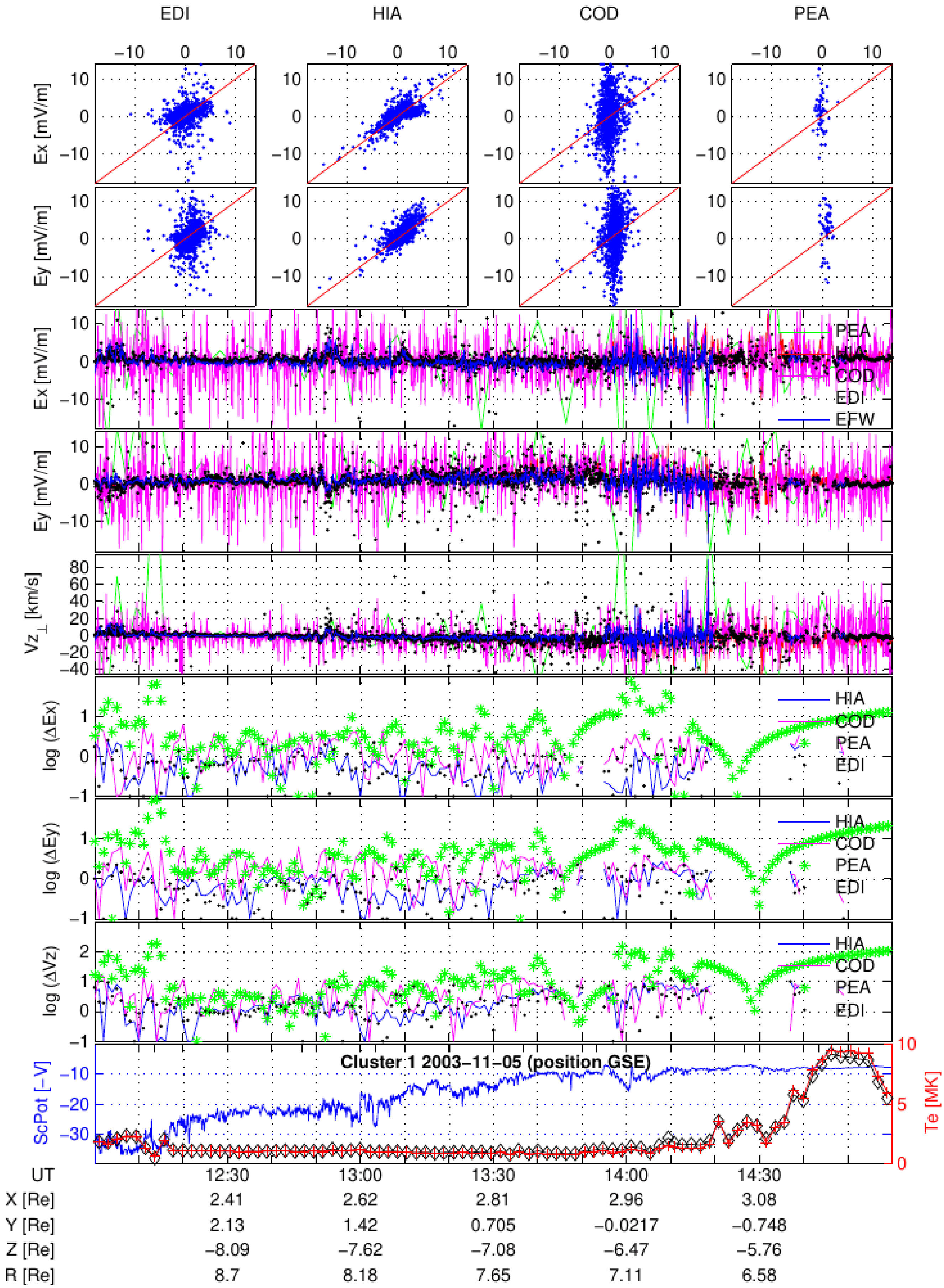
EDI
HIA
COD
PEA
Ex [mV/m]
Ey [mV/m]
Vz⊥ [km/s]
log (ΔEx)
log (ΔEy)
log (ΔVz)
PEA
HIA
COD
EDI
EFW
Cluster 1 2003–11–05 (position GSE)
ScPot [–V]
Te [MK]
UT
12:30
13:00
13:30
14:00
14:30
X [Re]
2.41
2.62
2.81
2.96
3.08
Y [Re]
2.13
1.42
0.705
–0.0217
–0.748
Z [Re]
–8.09
–7.62
–7.08
–6.47
–5.76
R [Re]
8.7
8.18
7.65
7.11
6.58

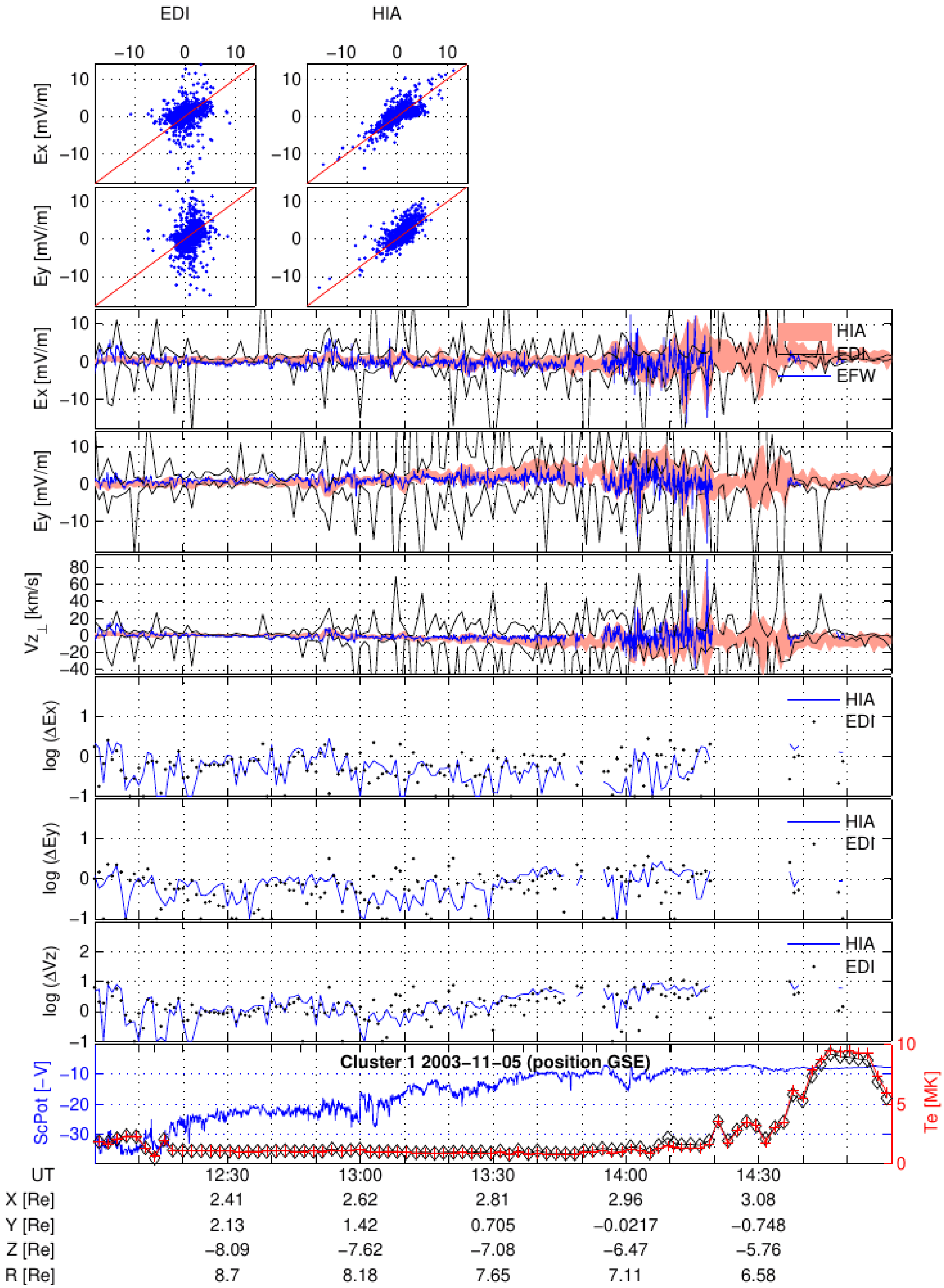
EDI
HIA
Ex [mV/m]
Ey [mV/m]
HIA
EDI
EFW
Vz⊥ [km/s]
log (ΔEx)
log (ΔEy)
log (ΔVz)
Cluster 1 2003−11−05 (position GSE)
ScPot [−V]
Te [MK]
UT 12:30 13:00 13:30 14:00 14:30
X [Re] 2.41 2.62 2.81 2.96 3.08
Y [Re] 2.13 1.42 0.705 −0.0217 −0.748
Z [Re] −8.09 −7.62 −7.08 −6.47 −5.76
R [Re] 8.7 8.18 7.65 7.11 6.58

## Inner magnetosphere

## Event 15: Plasmasphere

2003-10-12 21:00 - 24:00 | CAA quicklook

**Standard plots:**

`031012_C1_PS.pdf`

`031012_C3_PS.pdf`

For this event, all particle instruments provide very noisy data, though their averages appear to be useful, as the deltas are ususally below 1 mV/m. EFW and EDI show more consistent behaviour. A lot of EFW data is lacking, removed by the corotation algorithm. The remaining data are within 1 mV/m from EDI, though the increasing trend in SC3 EFW Ex from 21:40 to 21:50 is clearly not physical and could have been removed.

These show only EFW and EDI. The nice agreement on the wave signatures around 23:30 is particularly apparent.

This events demonstrates agreement between EFW and EDI to within 1 mV/m, and shows that the EFW routines for cold plasma wake detection efficiently removes unreliable data.

**Fine plots:**

`031012_C1_PS_fine.pdf`

`031012_C3_PS_fine.pdf`

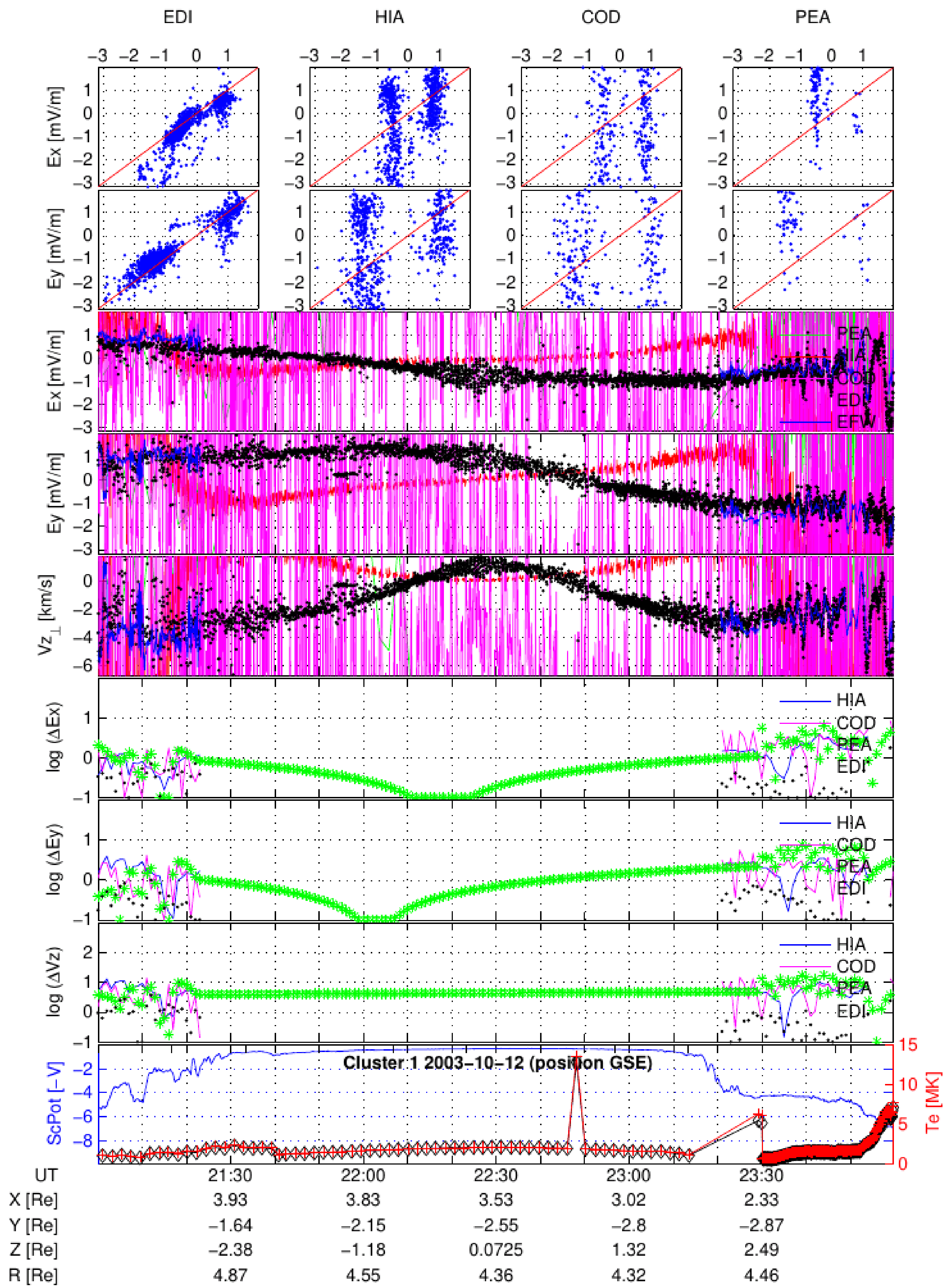
EDI
HIA
COD
PEA
Ex [mV/m]
Ey [mV/m]
Vz⊥ [km/s]
PEA
HIA
COD
EDI
EFW
log (ΔEx)
log (ΔEy)
log (ΔVz)
Cluster 1 2003–10–12 (position GSE)
ScPot [–V]
Te [MK]
UT
21:30
22:00
22:30
23:00
23:30
X [Re]
3.93
3.83
3.53
3.02
2.33
Y [Re]
–1.64
–2.15
–2.55
–2.8
–2.87
Z [Re]
–2.38
–1.18
0.0725
1.32
2.49
R [Re]
4.87
4.55
4.36
4.32
4.46

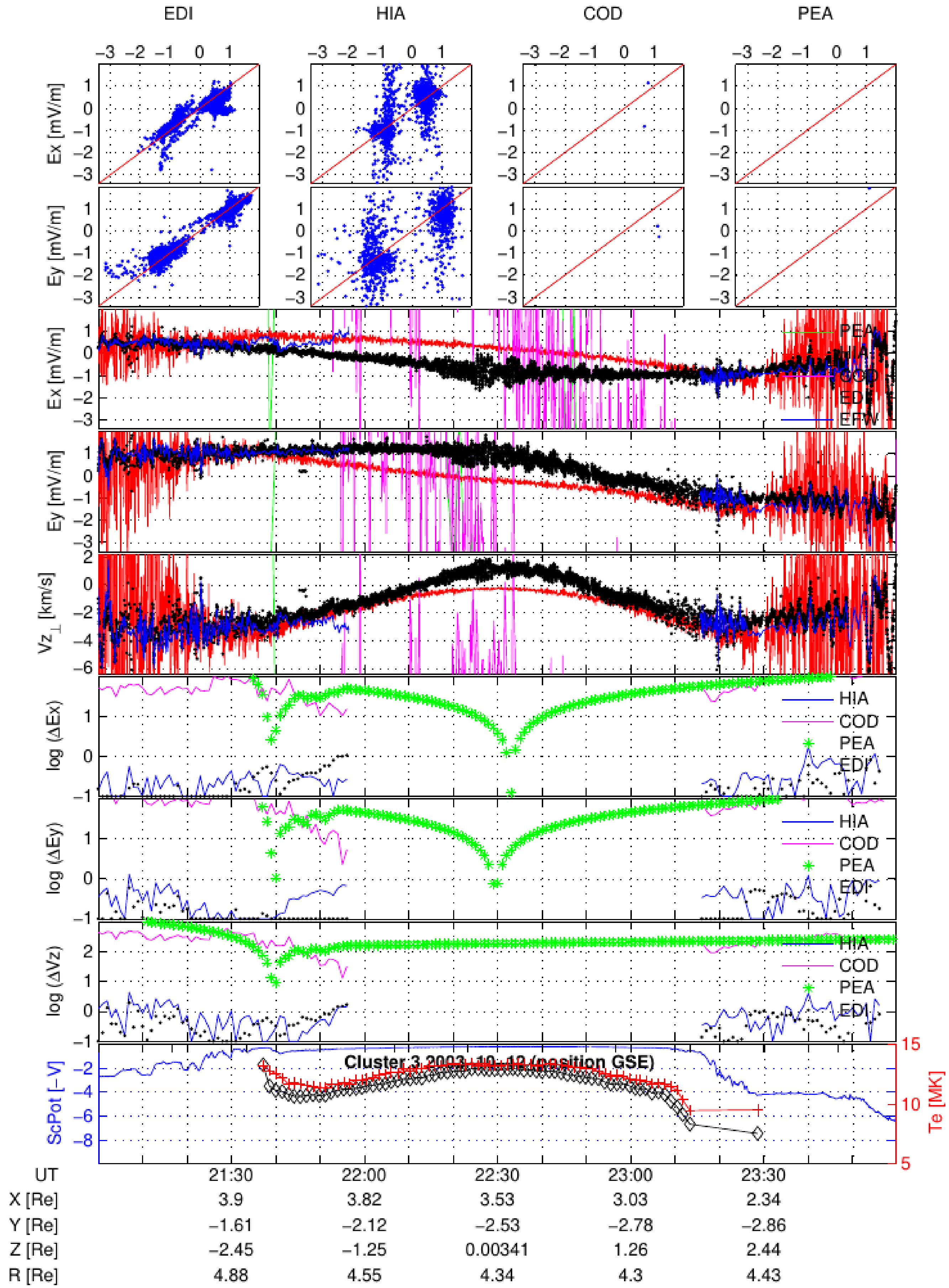
EDI
HIA
COD
PEA
Ex [mV/m]
Ey [mV/m]
Vz⊥ [km/s]
log (ΔEx)
log (ΔEy)
log (ΔVz)
PEA
HIA
COD
EDI
EFW
ScPot [−V]
Te [MK]
Cluster 3 2003−10−12 (position GSE)
UT 21:30 22:00 22:30 23:00 23:30
X [Re] 3.9 3.82 3.53 3.03 2.34
Y [Re] −1.61 −2.12 −2.53 −2.78 −2.86
Z [Re] −2.45 −1.25 0.00341 1.26 2.44
R [Re] 4.88 4.55 4.34 4.3 4.43

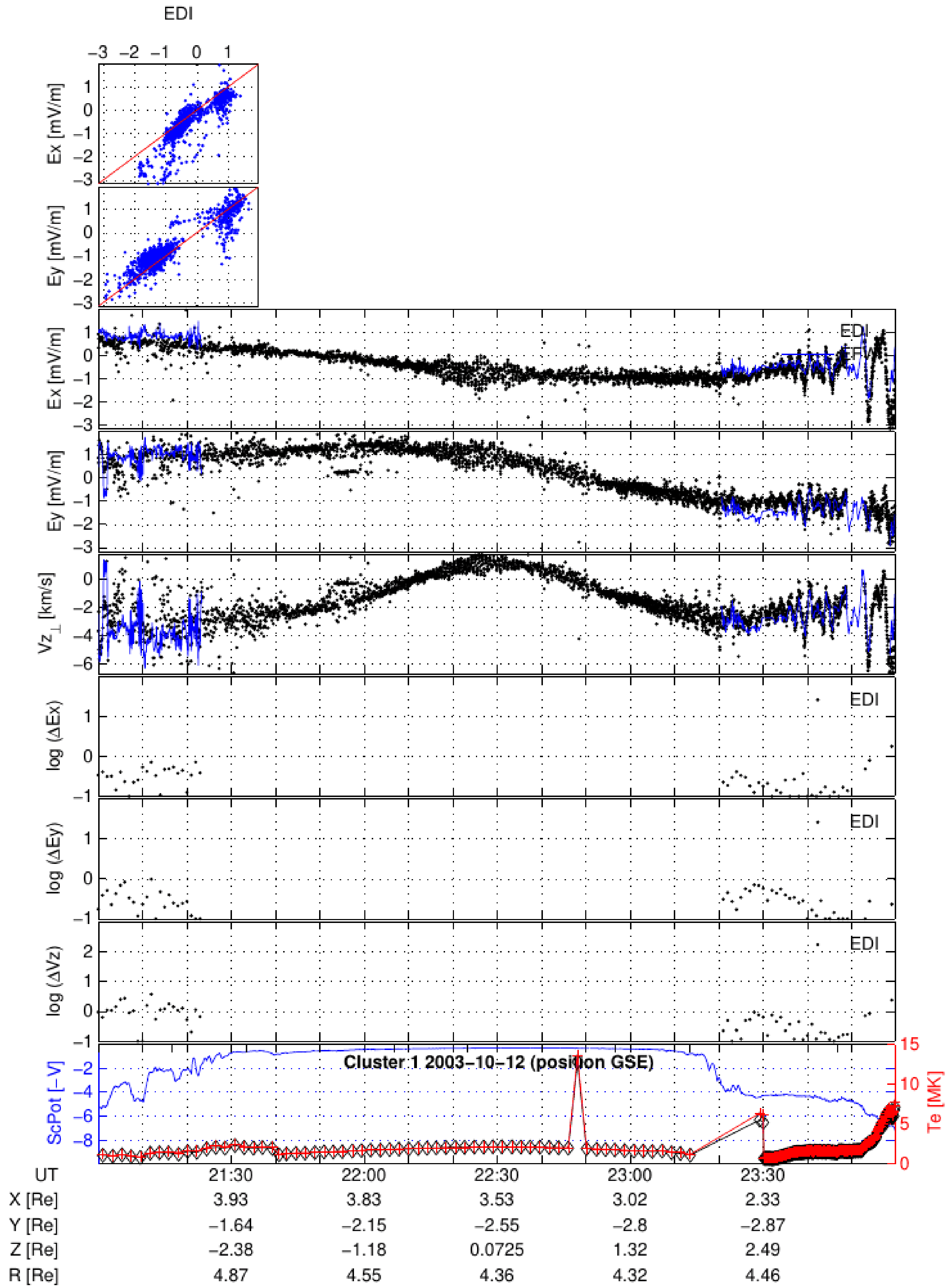
EDI
−3 −2 −1 0 1
Ex [mV/m]
Ey [mV/m]
EDI
EFW
Ex [mV/m]
Ey [mV/m]
Vz⊥ [km/s]
log (ΔEx)
log (ΔEy)
log (ΔVz)
ScPot [−V]
Te [MK]
Cluster 1 2003−10−12 (position GSE)
UT 21:30 22:00 22:30 23:00 23:30
X [Re] 3.93 3.83 3.53 3.02 2.33
Y [Re] −1.64 −2.15 −2.55 −2.8 −2.87
Z [Re] −2.38 −1.18 0.0725 1.32 2.49
R [Re] 4.87 4.55 4.36 4.32 4.46

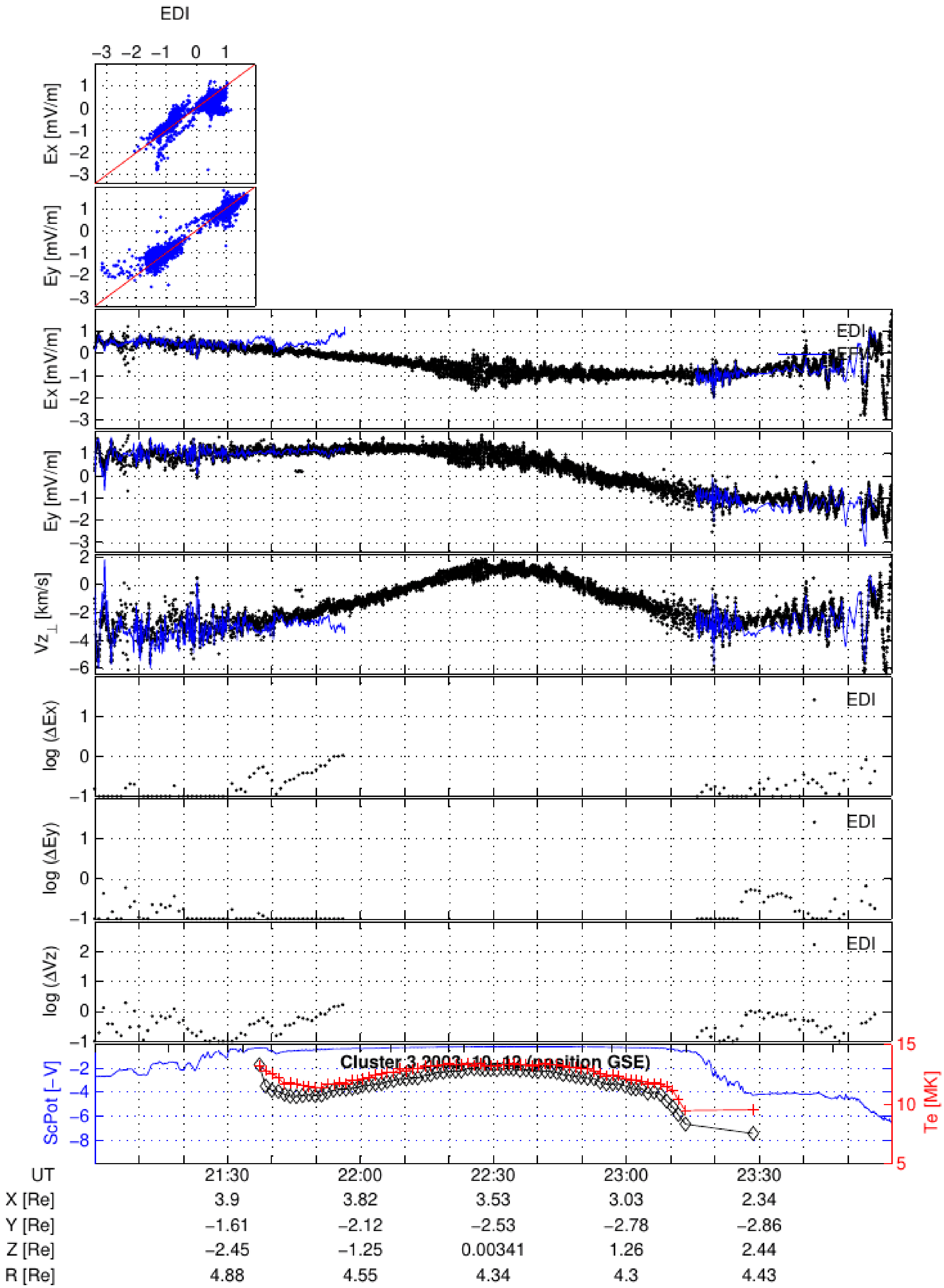
EDI
−3 −2 −1 0 1
Ex [mV/m]
Ey [mV/m]
EDI
EFW
Vz⊥ [km/s]
log (ΔEx)
log (ΔEy)
log (ΔVz)
Cluster 3 2003−10−12 (position GSE)
ScPot [−V]
Te [MK]
UT 21:30 22:00 22:30 23:00 23:30
X [Re] 3.9 3.82 3.53 3.03 2.34
Y [Re] −1.61 −2.12 −2.53 −2.78 −2.86
Z [Re] −2.45 −1.25 0.00341 1.26 2.44
R [Re] 4.88 4.55 4.34 4.3 4.43

## Event 16: Waves in the inner magnetosphere

2003-10-24 18:00 - 21:00 | CAA quicklook

**Standard plots:**

`031024_C3_Waves.pdf`

This plot shows very nice agreement (within 1 mV/m) between EFW, EDI and HIA. CODIF and PEACE moments are not useful. EDI and EFW generally differ by a few tenths of mV/m, with occasional points with higher differences mainly due to EDI outliers. HIA cannot catch wave amplitudes correctly, missing the peaks, while EDI instead tends to get the peaks but not the data between (probably because the field is locally constant in time at wave crests and troughs).

This event demonstrates excellent agreement between EFW, EDI and HIA data.

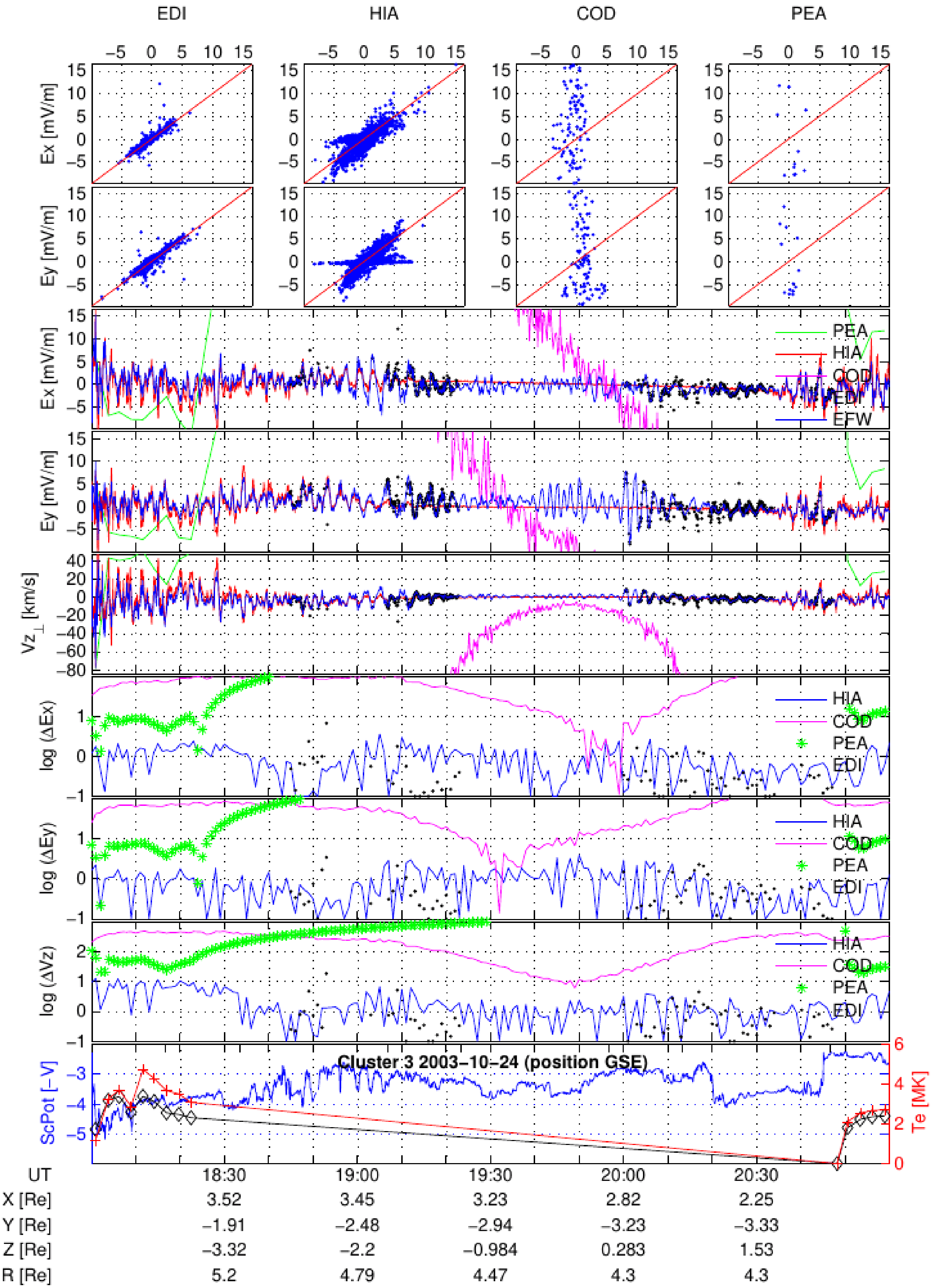
EDI
HIA
COD
PEA
Ex [mV/m]
Ey [mV/m]
PEA
HIA
COD
EDI
EFW
Vz⊥ [km/s]
log (ΔEx)
log (ΔEy)
log (ΔVz)
HIA
COD
PEA
EDI
Cluster:3 2003−10−24 (position GSE)
ScPot [−V]
Te [MK]
UT 18:30 19:00 19:30 20:00 20:30
X [Re] 3.52 3.45 3.23 2.82 2.25
Y [Re] −1.91 −2.48 −2.94 −3.23 −3.33
Z [Re] −3.32 −2.2 −0.984 0.283 1.53
R [Re] 5.2 4.79 4.47 4.3 4.3

## Event 17: Plasmasphere

2003-11-05 15:00-18:00 | CAA quicklook

**Standard plots:**

`031105_C1_PS.pdf`

`031105_C3_PS.pdf`

We here find excellent agreement between EFW and EDI, with the averaged difference on SC3 below 0.1 mV/m for a large part of the interval (15:40-16:50) and on within 1 mV/m all the time on both s/c. HIA differs from EDI and EFW during a large part of the interval. The CODIF and PEACE velocity moments are to noisy to be useful for comparison.

These plots highlight the EFW-EDI agreement, and illustrates that HIA differs not because of high noise level but by some systematic problem, as EFW and EDI both are outside the HIA noise envelope. EDI shows more outliers and noise on SC1 than on SC3, but the averaged EFW-EDI difference is below 1 mV/m despite this.

This event demonstrates excellent EFW-EDI agreement, to within 1 mV/m all the time and within 0.1 mV/m for a substantial interval.

**Fine plots:**

`031105_C1_PS_fine.pdf`

`031105_C3_PS_fine.pdf`

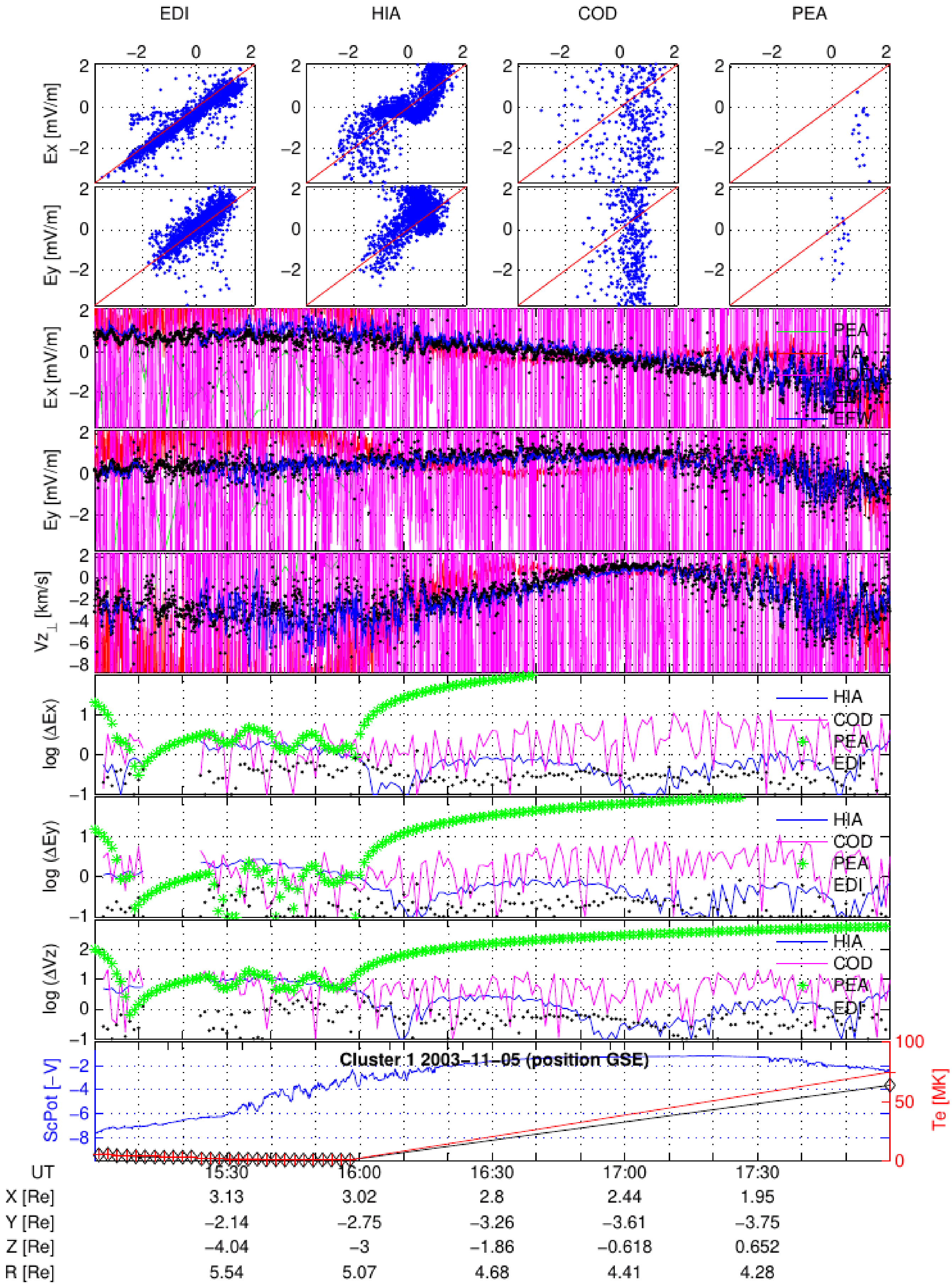
EDI
HIA
COD
PEA
Ex [mV/m]
Ey [mV/m]
PEA
HIA
COD
EDI
EFW
Vz⊥ [km/s]
log (ΔEx)
log (ΔEy)
log (ΔVz)
HIA
COD
PEA
EDI
Cluster 1 2003–11–05 (position GSE)
ScPot [–V]
Te [MK]
UT
15:30
16:00
16:30
17:00
17:30
X [Re] 3.13 3.02 2.8 2.44 1.95
Y [Re] –2.14 –2.75 –3.26 –3.61 –3.75
Z [Re] –4.04 –3 –1.86 –0.618 0.652
R [Re] 5.54 5.07 4.68 4.41 4.28

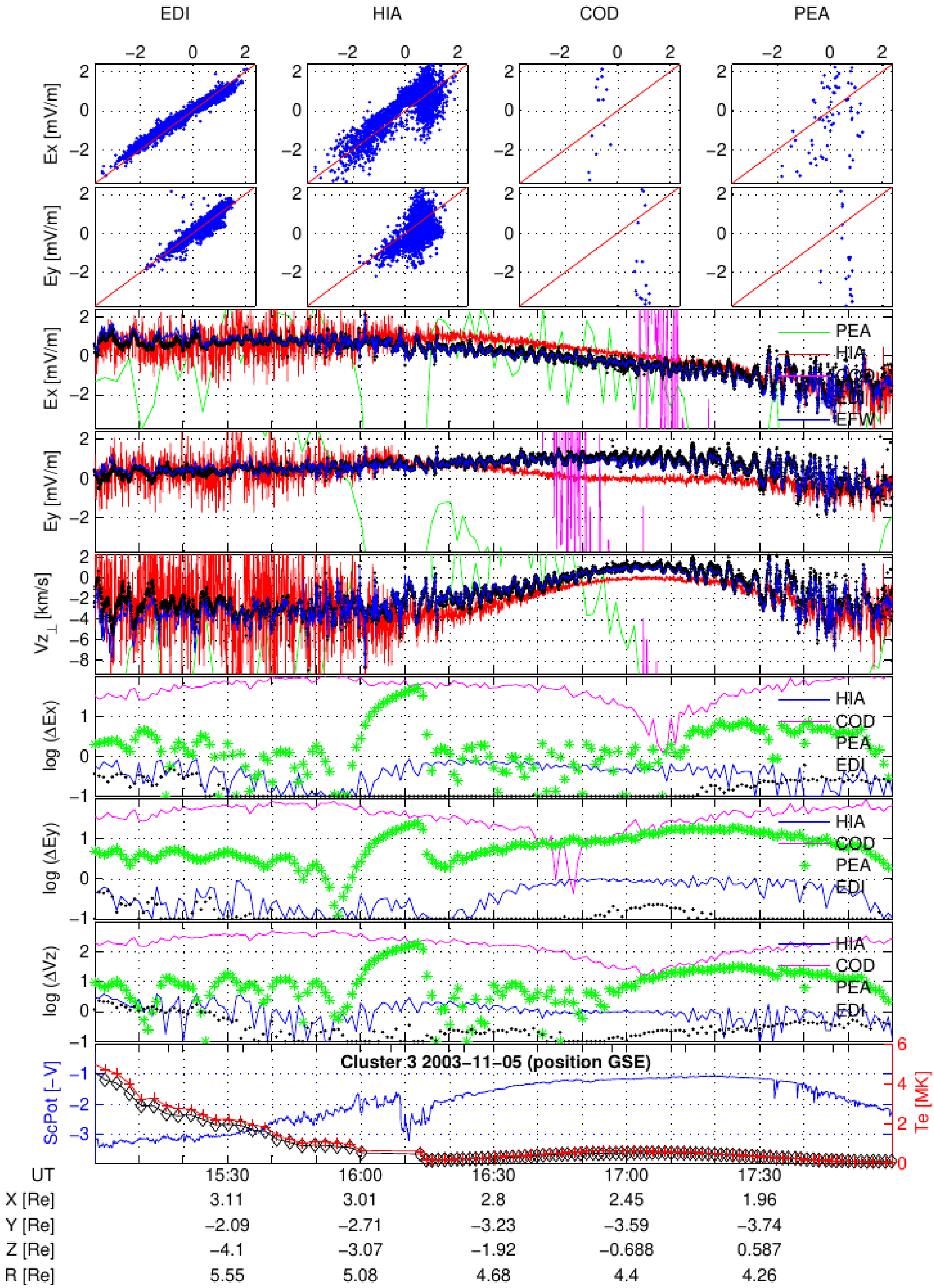
EDI
HIA
COD
PEA
Ex [mV/m]
Ey [mV/m]
PEA
HIA
COD
EDI
EFW
Vz⊥ [km/s]
log (ΔEx)
log (ΔEy)
log (ΔVz)
Cluster 3 2003–11–05 (position GSE)
ScPot [–V]
Te [MK]
UT 15:30 16:00 16:30 17:00 17:30
X [Re] 3.11 3.01 2.8 2.45 1.96
Y [Re] –2.09 –2.71 –3.23 –3.59 –3.74
Z [Re] –4.1 –3.07 –1.92 –0.688 0.587
R [Re] 5.55 5.08 4.68 4.4 4.26

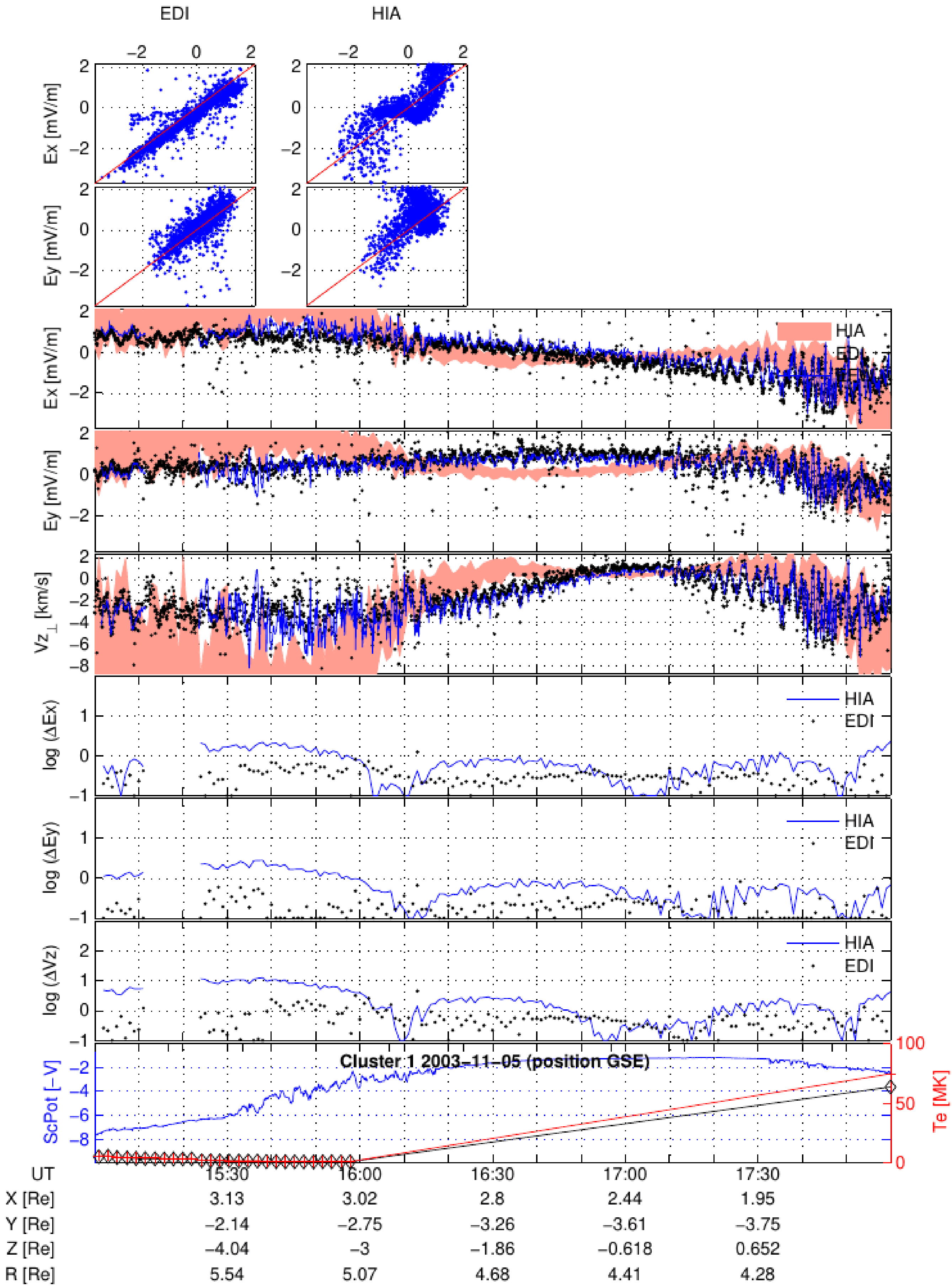
EDI
HIA
Ex [mV/m]
Ey [mV/m]
Vz⊥ [km/s]
log (ΔEx)
log (ΔEy)
log (ΔVz)
HIA
EDI
Cluster 1 2003–11–05 (position GSE)
ScPot [–V]
Te [MK]
UT 15:30 16:00 16:30 17:00 17:30
X [Re] 3.13 3.02 2.8 2.44 1.95
Y [Re] –2.14 –2.75 –3.26 –3.61 –3.75
Z [Re] –4.04 –3 –1.86 –0.618 0.652
R [Re] 5.54 5.07 4.68 4.41 4.28

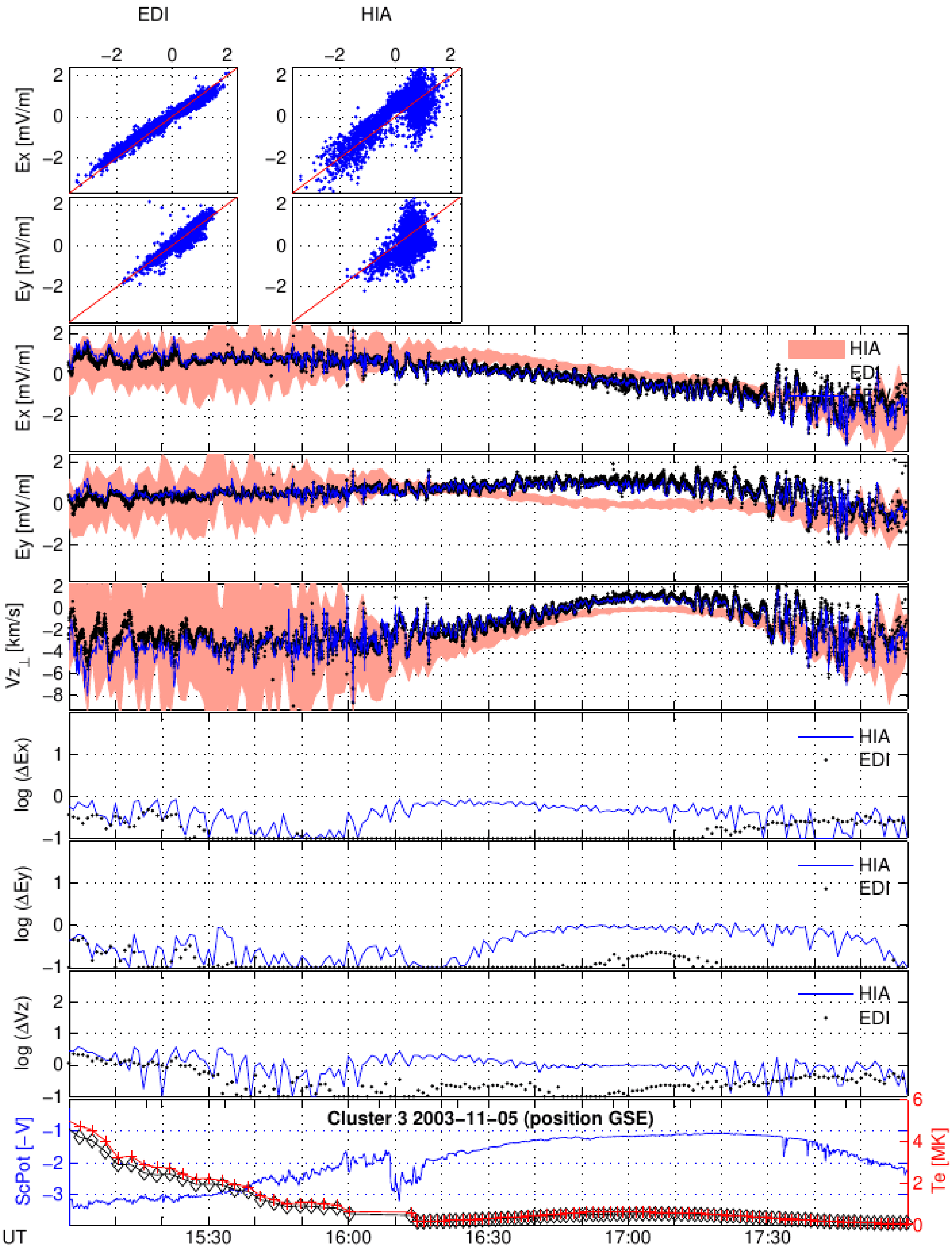


| UT | 15:30 | 16:00 | 16:30 | 17:00 | 17:30 |
|---|---|---|---|---|---|
| X [Re] | 3.11 | 3.01 | 2.8 | 2.45 | 1.96 |
| Y [Re] | –2.09 | –2.71 | –3.23 | –3.59 | –3.74 |
| Z [Re] | –4.1 | –3.07 | –1.92 | –0.688 | 0.587 |
| R [Re] | 5.55 | 5.08 | 4.68 | 4.4 | 4.26 |

## Event 18: Sub-Auroral Ion Drift event

2004-04-08 06:30 - 08:00 | CAA quicklook

**Standard plots:**

`040408_C1_SAID.pdf`

`040408_C3_SAID.pdf`

EFW agrees very well with EDI, while CODIF and PEACE have difficulty to measure the electric field in this region. HIA data are unavailable. The spacecraft cross the equatorial plane at low altitude and enter the plasmasphere between about 07:00 and 07:30. Both SC1 and SC3 contain two nice examples of a Sub-Auroral Ion Drift event, captured perfectly with both EFW and EDI. In addition, there are waves in the southern hemisphere (between 06:30 and 07:00) where EFW and EDI also agree very well. The difference plot shows agreement to within a few times 0.1 mV/m.

This event demonstrates excellent agreement between EFW and EDI for SAID events and waves, while CODIF and PEACE can not measure the electric field.

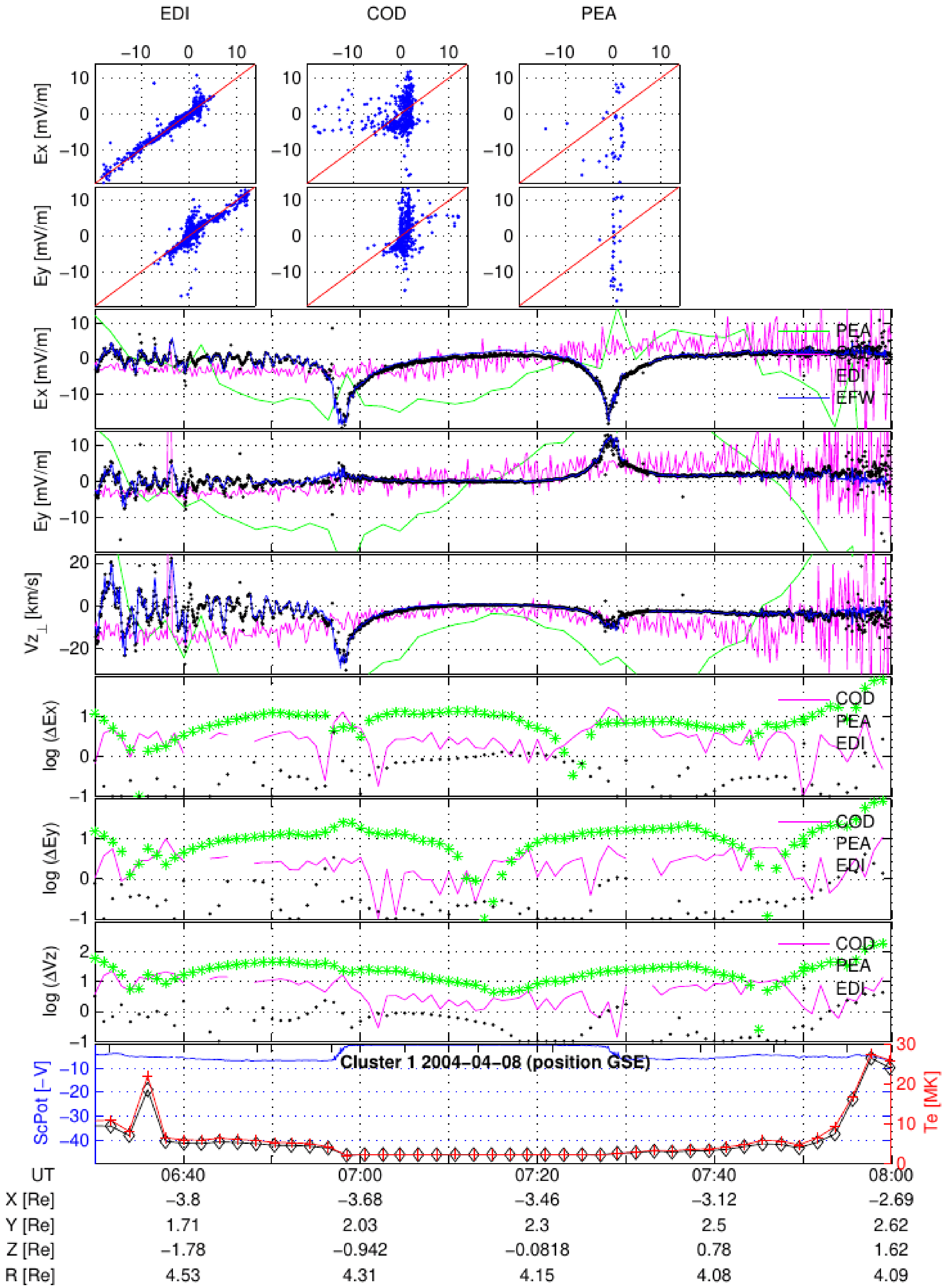
EDI
COD
PEA
Ex [mV/m]
Ey [mV/m]
PEA
COD
EDI
EFW
Vz⊥ [km/s]
log (ΔEx)
log (ΔEy)
log (ΔVz)
Cluster 1 2004−04−08 (position GSE)
ScPot [−V]
Te [MK]
UT 06:40 07:00 07:20 07:40 08:00
X [Re] −3.8 −3.68 −3.46 −3.12 −2.69
Y [Re] 1.71 2.03 2.3 2.5 2.62
Z [Re] −1.78 −0.942 −0.0818 0.78 1.62
R [Re] 4.53 4.31 4.15 4.08 4.09

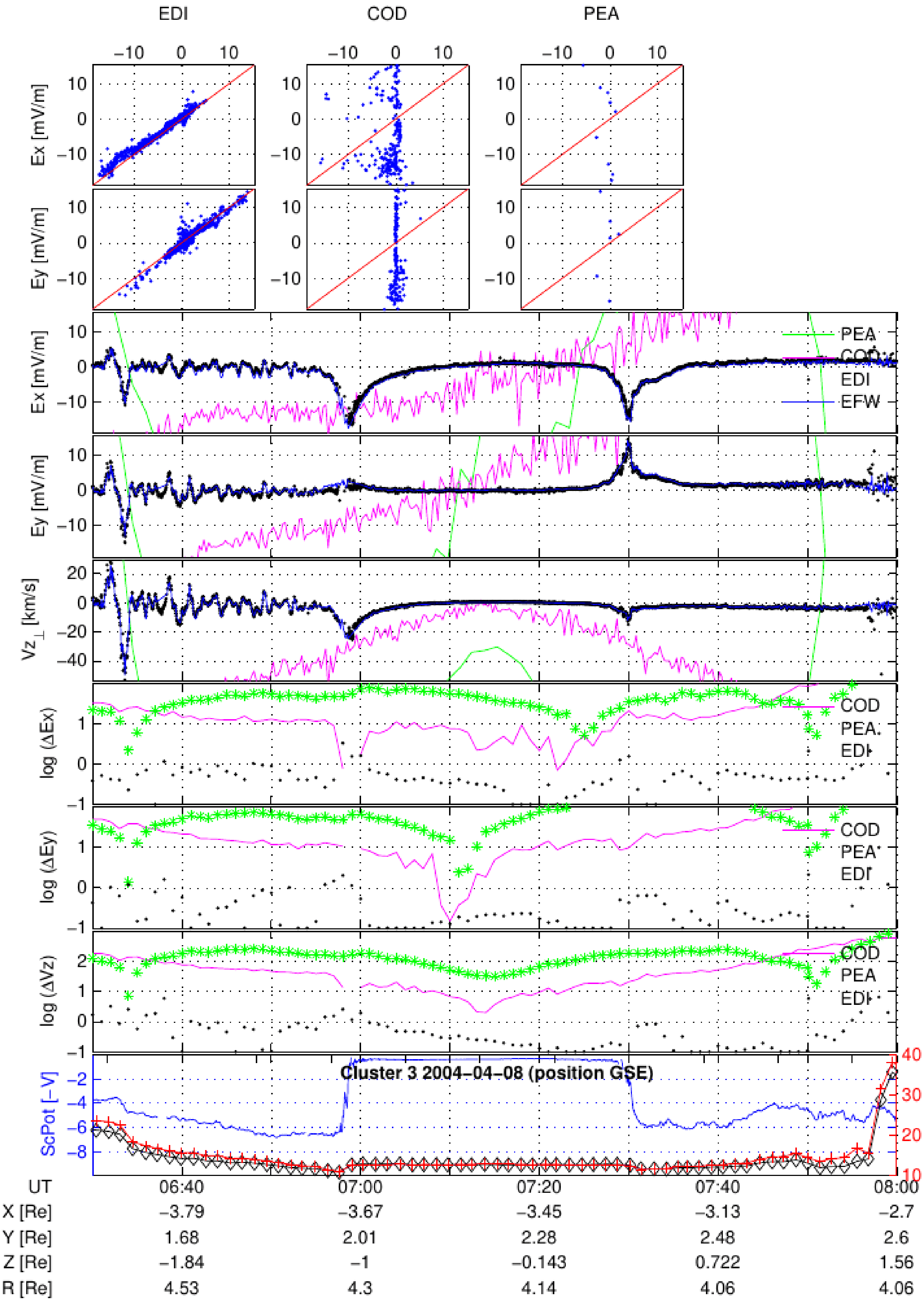
EDI
COD
PEA
Ex [mV/m]
Ey [mV/m]
Vz⊥ [km/s]
log (ΔEx)
log (ΔEy)
log (ΔVz)
PEA
COD
EDI
EFW
Cluster 3 2004−04−08 (position GSE)
ScPot [−V]
Te [MK]
UT 06:40 07:00 07:20 07:40 08:00
X [Re] −3.79 −3.67 −3.45 −3.13 −2.7
Y [Re] 1.68 2.01 2.28 2.48 2.6
Z [Re] −1.84 −1 −0.143 0.722 1.56
R [Re] 4.53 4.3 4.14 4.06 4.06

## Event 19: Plasmasphere

2004-04-13 00:00 - 02:20 | CAA quicklook

**Standard plots:**

`040413_C1_PS.pdf`

In this example only EDI and CODIF data are available for comparison. The agreement between EFW and EDI is exceptionally good, with differences of below 0.1 mV/m for a major part of the interval in the dense plasmasphere. At the very start and end of the interval (before 00:05 and after 02:00) EDI has difficulty to measure the rapid field variations. CODIF has a problem to measure the correct field throughout the interval.

This event demonstrates excellent agreement between EFW and EDI in the plasmasphere.

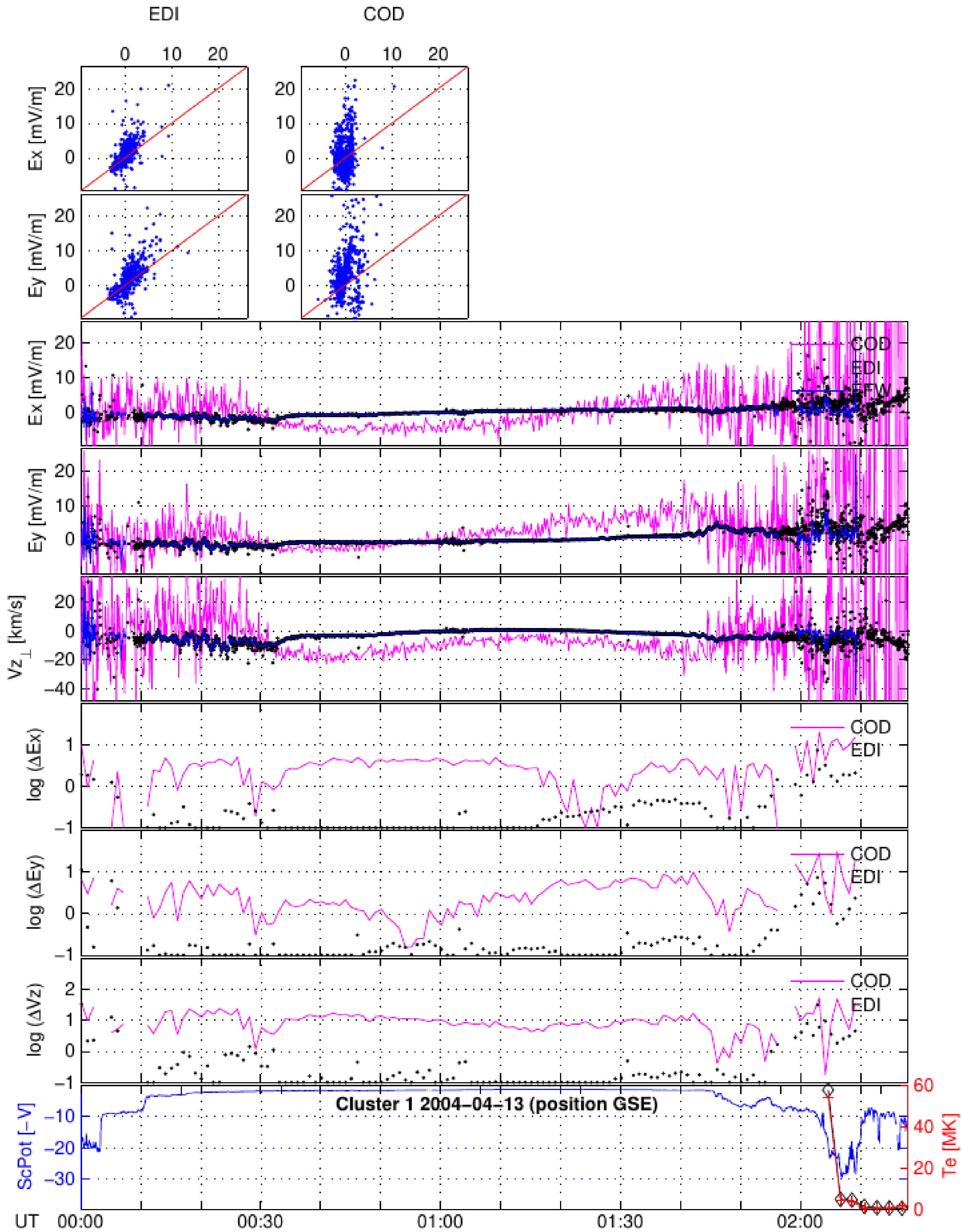


| UT | 00:00 | 00:30 | 01:00 | 01:30 | 02:00 |
|---|---|---|---|---|---|
| X [Re] | −3.68 | −3.71 | −3.56 | −3.21 | −2.63 |
| Y [Re] | 1.1 | 1.7 | 2.21 | 2.6 | 2.8 |
| Z [Re] | −3.56 | −2.46 | −1.24 | 0.0468 | 1.33 |
| R [Re] | 5.24 | 4.76 | 4.37 | 4.13 | 4.07 |

## Event 20: Dayside Plasmasphere

2004-09-23 12:00 - 15:00 | CAA quicklook

**Standard plots:**

040923_C1_PS_Dayside.pdf

The spacecraft is here in a relatively high density plasma in the dayside plasmasphere. Data from all instruments are available, but as the standard plot shows, the data from in particular CODIF and PEACE, but also HIA, are not good. PEACE has a data gap from 12:35 to 14:20. The EDI data show a large scatter for some shorter time periods, but generally agrees well with EFW. The fine plot includes only the EDI data (as shaded envelope plot) and HIA data (as line plot), and shows that the EFW data lie well within the envelope of the EDI variations. Between 14:05 and 14:20 there are some nice oscillations captured by both EFW and EDI. The oscillations between 12:45 and 13:00 which are seen clearly in EFW are probably too rapid to be seen by EDI. The fields are generally rather small, and the agreement with EDI is within a few times 0.1 mV/m. HIA is not a good reference in this event, as seen by its systematic error of about 1 mV/m.

This event demonstrates a good agreement between EFW and EDI with problems in the measurements of the other particle instruments.

**Fine plots:**

040923_C1_PS_Dayside_fine.pdf

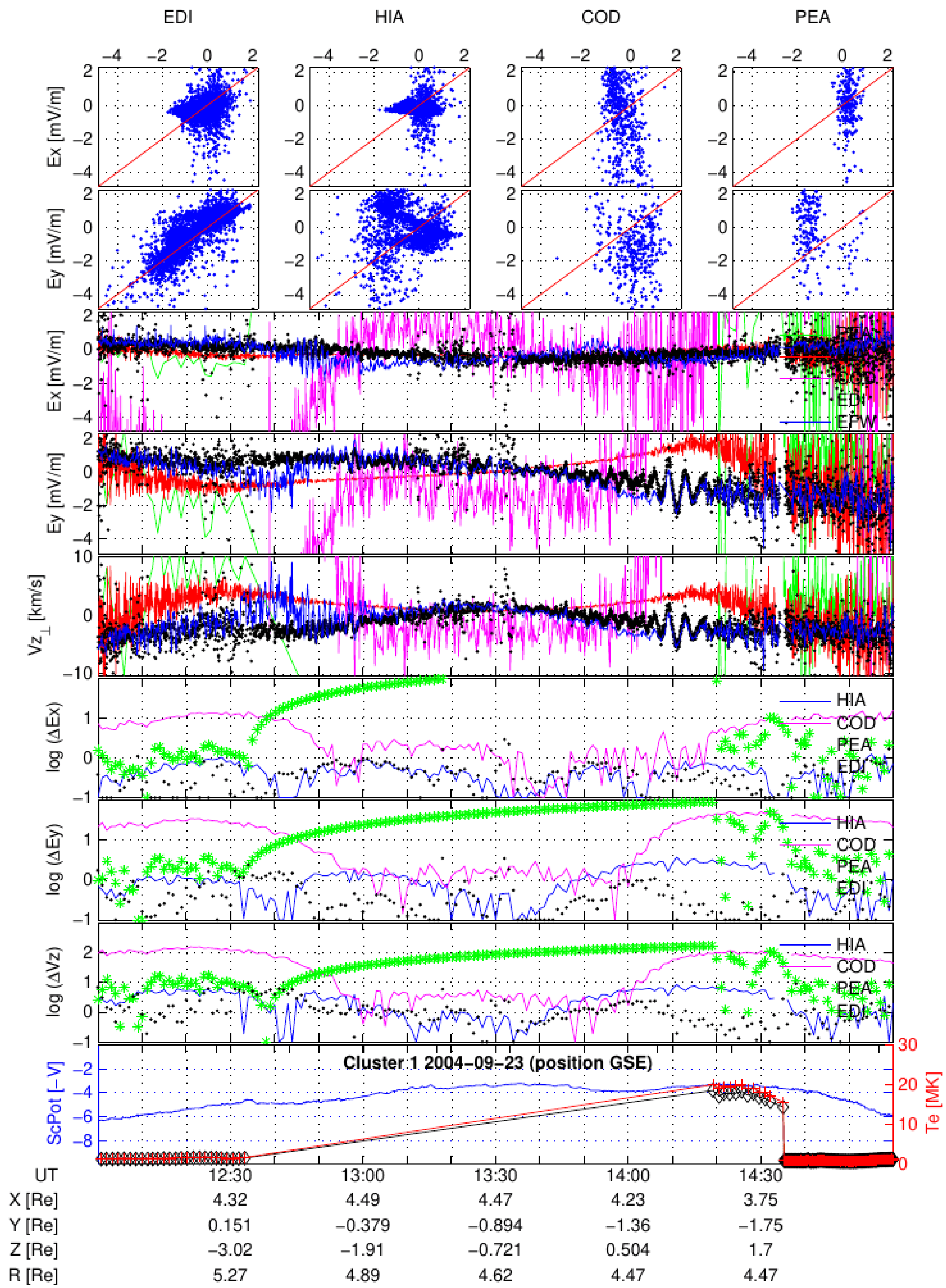
EDI
HIA
COD
PEA
Ex [mV/m]
Ey [mV/m]
Vz⊥ [km/s]
log (ΔEx)
log (ΔEy)
log (ΔVz)
HIA
COD
PEA
EDI
EFW
Cluster 1 2004–09–23 (position GSE)
ScPot [–V]
Te [MK]
UT
12:30
13:00
13:30
14:00
14:30
X [Re]
4.32
4.49
4.47
4.23
3.75
Y [Re]
0.151
–0.379
–0.894
–1.36
–1.75
Z [Re]
–3.02
–1.91
–0.721
0.504
1.7
R [Re]
5.27
4.89
4.62
4.47
4.47

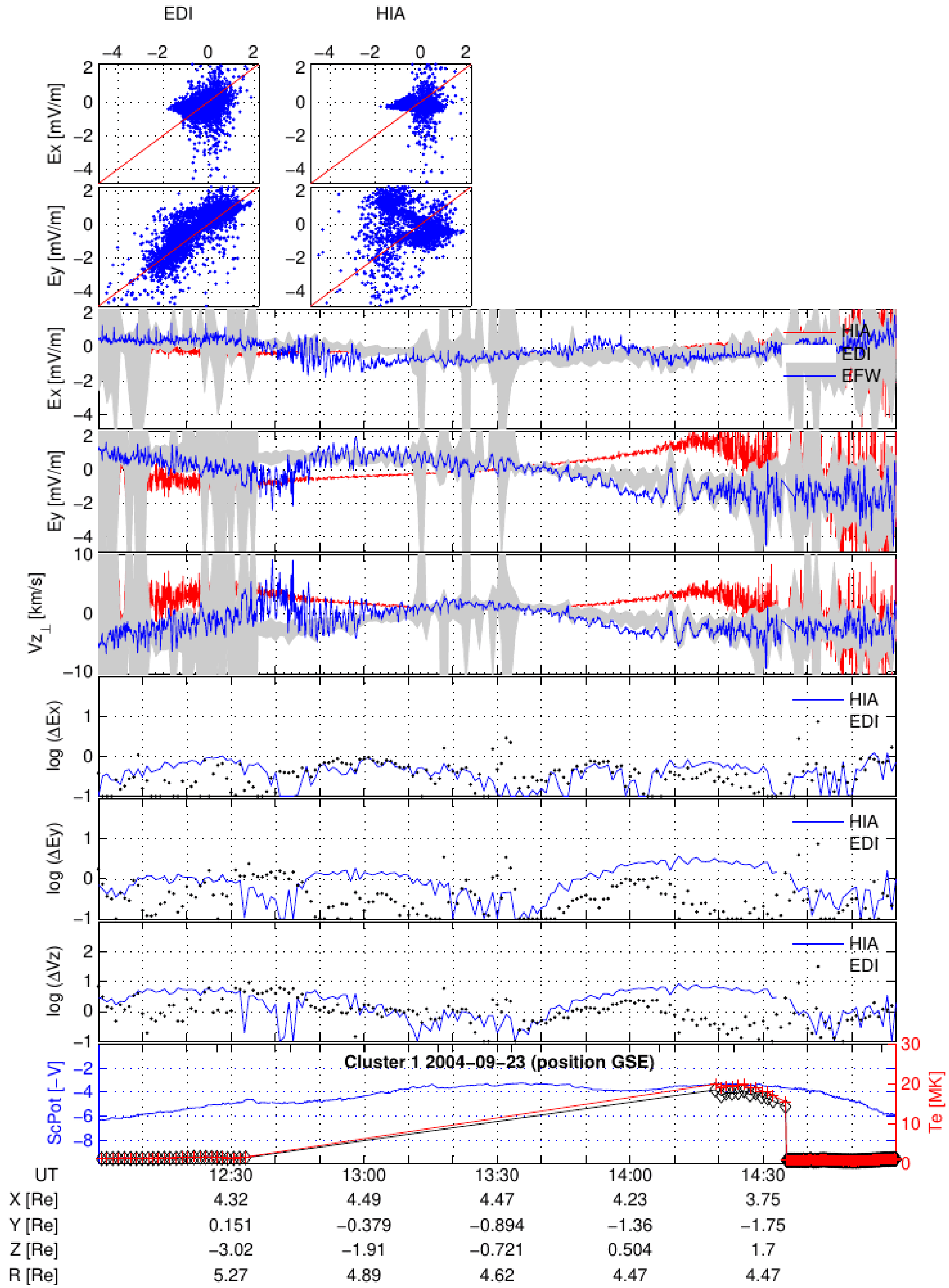
EDI
HIA
Ex [mV/m]
Ey [mV/m]
HIA
EDI
EFW
Vz⊥ [km/s]
log (ΔEx)
log (ΔEy)
log (ΔVz)
Cluster 1 2004−09−23 (position GSE)
ScPot [−V]
Te [MK]
UT
12:30
13:00
13:30
14:00
14:30
X [Re]
4.32
4.49
4.47
4.23
3.75
Y [Re]
0.151
−0.379
−0.894
−1.36
−1.75
Z [Re]
−3.02
−1.91
−0.721
0.504
1.7
R [Re]
5.27
4.89
4.62
4.47
4.47

# Conclusions

We have presented a comparison of the CAA EFW electric field to EDI, CIS-HIA, CIS-CODIF and PEACE. We conclude that generally EFW provides the best quality measurement of the electric field. Normally the statistical difference between the electric fields measured by EFW and other instruments lies within 1 mV/m, provided the measurements by other instruments are reasonable at all.

The observed differences between EFW and the other instruments are usually caused by higher noise and offsets in EDI and the particle instruments. However in some cases the difference may be caused by spurious fields measured by EFW, which cannot be corrected by applying offset corrections to the data.

We find that generally EFW best agrees with CIS-HIA. CIS-CODIF has much larger noise level and offset in the Z direction than CIS-HIA (especially CIS-CODIF on C3). On the other hand we find that in some cases CIS-HIA does not follow the large electric field variations which is seen by EFW, PEACE and CODIF. We also found cases when HIA and CODIF data differ by a constant factor.

We find that PEACE moments have very limited use inside the magnetosphere. However, there is a good agreement between EFW and PEACE in the magnetosheath, especially when the SC is in the burst mode.

EFW-EDI comparisons in some cases show a remarkable agreement down to 0.1 mV/m for quiet fields. However, in more active regions EDI has much more scatter, which is expected. In general the agreement between EFW and EDI is very good.

Finally, we conclude that we see the expected picture: the quality of the electric field measured by the different instruments strongly depends on the plasma environment. We usually find a statistical agreement between EFW and at least one of the other instruments within 1 mV/m. Provided that the measured field is real, EFW generally provides the best measurement of the electric field. The production procedure used by the EFW team results in high data quality.